INVESTIGATION OF THE EFFECTS OF KML29, A SELECTIVE INHIBITOR OF MONOACYLGLYCEROL LIPASE (MAGL) ON FEVER INDUCED BY LIPOPOLYSACCHARIDE (LPS) IN RATS

A THESIS SUBMITTED TO
THE GRADUATE SCHOOL OF NATURAL AND APPLIED SCIENCES
OF
MIDDLE EAST TECHNICAL UNIVERSITY

BY

FETHİYE ESİN GALİOĞLU

IN PARTIAL FULLFILLMENT OF THE REQUIREMENTS
FOR
THE DEGREE OF MASTER OF SCIENCE
IN
BIOCHEMISTRY

FEBRUARY 2015

Approval of the thesis:

INVESTIGATION OF THE EFFECTS OF KML-29, A SELECTIVE INHIBITOR OF MONOACYLGLYCEROL LIPASE (MAGL) ON FEVER INDUCED BY LIPOPOLYSACCHARIDE (LPS) IN RATS

submitted by **FETHİYE ESİN GALİOĞLU** in partial fulfillment of the requirements for the degree of **Master of Science in Biochemistry Department, Middle East Technical University** by,

Prof. Dr. Gülbin Dural Ünver _____
Dean, Graduate School of **Natural and Applied Sciences**

Prof. Dr. Orhan Adalı _____
Head of Department, **Biochemistry**

Prof. Dr. Mahinur S. Akkaya _____
Supervisor, **Chemistry Department, METU**

Prof. Dr. Eyüp S. Akarsu _____
Co-Supervisor, **Medical Pharmacology Dept., Ankara University**

Examining Committee Members:

Assoc. Prof. Dr. Çağdaş D. Son _____
Biology Department, METU

Prof. Dr. Mahinur S. Akkaya _____
Chemistry Department, METU

Prof. Dr. Eyüp S. Akarsu _____
Medical Pharmacology Dept., Ankara University

Assist. Prof. Dr. Mehmet Somel _____
Biology Department, METU

Assist. Prof. Dr. Zeynep I. Kalaylıoğlu _____
Statistics Department, METU

Date: 16.02.2015

I hereby declare that all information in this document has been obtained and presented in accordance with academic rules and ethical conduct. I also declare that, as required by these rules and conduct, I have fully cited and referenced all material and results that are not original to this work.

Name, Last Name: FETHİYE ESİN GALİOĞLU

Signature

ABSTRACT

INVESTIGATION OF THE EFFECTS OF KML29, A SELECTIVE INHIBITOR OF MONOACYLGLYCEROL LIPASE (MAGL) ON FEVER INDUCED BY LIPOPOLYSACCHARIDE (LPS) IN RATS

Galioğlu, Fethiye Esin

M.S., Department of Biochemistry

Supervisor: Prof. Dr. Mahinur S. Akkaya

Co-supervisor: Prof. Dr. Eyüp S. Akarsu

February 2015, 126 Pages

Endocannabinoid system has recently come into prominence as one of the primary neuromodulatory systems that plays vital roles in sustaining homeostasis. Monoacylglycerol lipase (MAGL) is the main degradation enzyme of the most abundant endocannabinoid found in the brain, 2-arachidonoyl glycerol (2-AG). MAGL is thought to have a potential to exert protective effects on inflammatory states. MAGL serves as a key metabolic node connecting the endocannabinoid and prostaglandin signaling networks and its inhibition causes increase in 2-AG levels and decrease in arachidonic acid levels, both of which may result in remission of inflammation through different mechanisms.

In the current study we utilized Lipopolysaccharide (LPS; *Escherichia coli* O111:B4 250 μg/kg, sc)-administered Wistar albino male rats in order to initiate fever, an

inflammatory state mainly generated by the brain and investigated whether injection of KML29 (20 mg/kg, sc), a selective and irreversible inhibitor of MAGL, simultaneously with LPS would alter the fever response by means of a biotelemetric technique.

Our results showed that KML29 has a modest but significant ameliorating effect on LPS-induced fever, specifically during the plateau phase. Statistical analysis revealed that the decline in overall temperature change (ΔT_{ab}) values of the group whose LPS injection was done simultaneously with KML29 was 1.7 fold less (between 250-600 minutes) compared to the group whose LPS injection was done simultaneously with saline.

These results indicate that MAGL activation is an important aspect of physiopathology of inflammation and endogenously increased 2-AG by MAGL inhibiton can lead to protection against fever.

Keywords: Monoacylglycerol lipase inhibition, KML29, Lipopolysaccharide, fever, rat

ÖZ

MONOAÇİLGLİSEROL LİPAZ (MAGL) ENZİMİNİN SELEKTİF İNHİBİTÖRÜ OLAN KML29'UN SIÇANLARDA LİPOPOLİSAKKARİD (LPS) İLE İNDÜKLENEN ATEŞ ÜZERİNE OLAN ETKİLERİNİN ARAŞTIRILMASI

Galioğlu, Fethiye Esin

Yüksek Lisans, Biyokimya Bölümü

Tez Yöneticisi: Prof. Dr. Mahinur S. Akkaya

Ortak Tez Yöneticisi: Prof. Dr. Eyüp S. Akarsu

Şubat 2015, 126 sayfa

Endokannabinoid sistem son zamanlarda homeostazisin sürdürülmesinde hayati rol oynayan primer nöromodülatör sistemlerden biri olarak önem kazanmıştır. Beyinde en çok bulunan endokannabinoid olan 2-Araşidonil gliserolün (2-AG) primer degredasyon enzimi olan Monoaçilgliserol lipazın (MAGL) inhibisyonunun inflamatuvar süreçler üzerinde koruyucu etki gösterme potansiyeline sahip olduğu düşünülmektedir.

MAGL, endokannabinoid ve prostaglandin sinyalizasyon sistemlerini birbirine bağlayan kilit noktalardan biri olarak görev yapar ve inhibisyonu, 2-AG seviyesini arttırıp araşidonik asit seviyesini düşürür ki her iki durum da farklı mekanizmalar aracılığıyla inflamasyonda hafiflemeye neden olabilir.

Bu çalışmada inflamatuvar bir süreç olan ve temelde beyin tarafından meydana getirilen ateşi tetikleyebilmek amacıyla Lipopolisakkarid (LPS; *Escherichia coli* O111:B4 250 µg/kg, sc) uygulaması yapılmış Wistar albino erkek sıçanlar kullanılmış ve biyotelemetrik bir teknik aracılığıyla, selektif ve geri dönüşümsüz bir MAGL inhibitörü olan KML29'un (20 mg/kg, sc) LPS ile eş zamanlı uygulanmasının ateş üzerinde düzeltici bir etki gösterip göstermeyeceği incelenmiştir.

Sonuçlarımız KML29'un LPS tarafından uyarılan ateş cevabının plato dönemi üzerinde etkili olduğunu göstermiştir. Etki farmakolojik anlamda çok belirgin olmamakla birlikte, istatistiksel analiz, bu azalmanın LPS ile birlikte KML29 enjekte edilen grupta belli bir zaman diliminden sonra (250-600 dakika arası) sıcaklık farkı (ΔT_{ab}) değerlerinin total olarak 1.7 kat daha düşük olduğunu göstermiştir. Bu sonuçlar MAGL aktivasyonunun inflamasyon fizyopatolojisinin önemli bir unsuru olduğuna ve MAGL inhibisyonuyla endojen olarak artan 2-AG'nin ateşe karşı koruyucu bir etki gösterebileceğine işaret etmektedir.

Anahtar Kelimeler: Monoaçilgliserol lipaz inhibisyonu, KML29, Lipopolisakkarid, ateş, sıçan

to Zeynep Gürerk Atbaşoğlu…

ACKNOWLEDGEMENTS

I would like to express my heartfelt gratitude and thanks to my supervisor Prof. Dr. Mahinur S. Akkaya for her valuable supervision, support and encouragement during my study. I appreciate everything she has done for me.

I wish to express my sincerest gratitude and thanks to my co-supervisor Prof. Dr. Eyüp S. Akarsu for his valuable guidance, suggestions and support. I am grateful to him for his help in creating solutions even in the most stressful times and providing me a comfortable environment in order to do my experiments during my studies in Ankara University Faculty of Medicine, Neuropsychopharmacology Laboratory.

I would like to express my special gratitude and thanks to Assist. Prof. Dr. Zeynep Işıl Kalaylıoğlu for carrying out the intricate statistical analysis of the data and her contribution to my thesis.Without her help, I would not be able to complete my thesis.

Furthermore, I would like to thank to the rest of my thesis committee; Assoc. Prof. Dr Çağdaş D. Son and Assist. Prof. Dr. Mehmet Somel for their valuable comments and contribution.

I wish to send my sincerest gratitude and thanks to Prof. Dr. E. Cem Atbaşoğlu for his valuable guidance and help.

I wish to extend my thanks to Soner Mamuk for teaching and helping me in surgical procedures, animal care and data analysis and to the rest of technical staff for assisting me with my experiments. I would also like to thank to medical student Yiğit Baykara for his assistance with surgical procedures, M.D. Matilda Merve Tuğlu, Erol Rauf Ağış and whole staff for their kind helps and friendship during my studies in Ankara University Faculty of Medicine, Medical Pharmacology Department.

Moreover, I would like to express my special gratitude and thanks to Prof. Dr. Cihan Öner for showing us entirely different perspectives and an integrative standpoint of science with the arguments he guided and for teaching us to push our limits and work hard. Working in his laboratory was a milestone in my academic life and his open mind has been and will be a source of inspiration for me. I wish to extend my sincerest gratitude and thanks to Prof. Dr. Nuran Diril and Prof. Dr. Reyhan Öner who have always been supportive, encouraging and understanding and to Prof. Dr. Ali Demirsoy, Prof. Dr. Şayeste Demirezen, Prof. Dr. Mehmet Ali Onur and all the academics and people in Hacettepe University, Biology Department who have helped to free our minds and shed light on the true meaning of science.

Last but not least, I wish to send my endless appreciation to my family members; to my parents, Avatıf and Hikmet Galioğlu, for their dedication, for loving and supporting me unconditionally throughout my life and teaching me to stand up for what I believe in and move on no matter what the conditions; to my sisters Sezin Galioğlu Özaltuğ and Yeliz Galioğlu, my brother Mehmet Galioğlu and brother-in-law Emrah Özaltuğ for their endless support, love, patience, and for bringing joy to my life. You are the most precious gifts to my life!

TABLE OF CONTENTS

LIST OF TABLES

TABLES

LIST OF FIGURES

FIGURES

LIST OF ABBREVIATIONS

5-HT: 5-hydroxytryptamine or Serotonin
2-AG: 2–arachidonoyl-sn- glycerol

AA: Arachidonic acid

ABHD-12: α/β hydrolase domain-containing protein 12

ABHD-4: α/β hydrolase domain-containing protein 4

ABHD-6: α/β hydrolase domain-containing protein 6

ABPP: Activity-based protein profiling

AEA: N-arachidonoyl ethanolamine or Anandamide

AMPA: alpha-amino-3-hydroxy-5-methyl-4-isoxazolepropionic acid

AMPAR: alpha-amino-3-hydroxy-5-methyl-4-isoxazolepropionic acid receptor

AVPV: Anteroventral periventricular nucleus

BBB: Blood-brain barrier

CaER: Ca2+ - driven endocannabinoid release

cAMP: Cyclic adenosine monophosphate

CB1R or CB1: Cannabinoid type 1 receptor

CB2R or CB2: Cannabinoid type 2 receptor

CD14: Cluster of differentiation 14

CNS: Central nervous system

COX: Cyclooxygenase

COX-2: Cyclooxygenase-2

cPLA$_{2\text{-}\alpha}$: Cytosolic phospholipase $A_{2\text{-}\alpha}$

D_2: Dopamine receptor D_2

Δ^9–THC: Δ^9-tetrahydrocannabinol

DAG or DG: 1,2-

Diacylglycerol

DGL-α: Diacylglycerol lipase-α

DMH: Dorsomedial nucleus of the hypothalamus

DSE: Depolarization-induced suppression of excitation

DSI: Depolarization-induced suppression of inhibition

eCBs: Endocannabinoids

EP: E type Prostaglandin receptors

FAAH: Fatty acid amide hydrolase

GABA: Gamma- aminobutyric acid

GLA: Gamma-linolenic acid

Glu: Glutamate

GPCRs: G-protein-coupled receptors

HFIP: O-hexafluoroisopropyl

i.c.v.: Intracerebroventricular

IKK: IκB (inhibitor of kappa light chain gene enhancer in B cells) kinase

IL-1: Interleukin-1

IL-1R: Interleukin-1 receptor

IL-6: Interleukin-6

IML: Intermediolateral column of the spinal cord

ip:Intraperitoneal

IP3: Inositol trisphosphate

IRAK1: Serine-threonine kinase IL-1 receptor-associated kinase 1

IRAK4: IL-1 receptor-associated kinase-4

IRF3: Interferon Regulatory Factor 3

IRF5: Interferon regulatory factor 5

iv: Intravenous

LBP: Lipopolysaccharide binding protein

LOX: Lipoxygenase

LPO: Lateral preoptic area

LPS: Lipopolysaccharide

MAGL or MGL:Monoacylglycerol lipase

MAGs: Monoacylglycerols

MD2: Myeloid Differentiation Protein-2

mGluR1: Type-1 metabotropic glutamate receptor 1

mGluR5: Type-1 metabotropic glutamate receptor 5

MnPO: Median preoptic nucleus

mPGES-1: Microsomal Prostaglandin E synthase 1

MPO: Medial preoptic area and the lateral preoptic area

MyD88: Myeloid differentiation primary response gene 88

NAPE-PLD: N-acyl-substituted phosphatidylethanolamine specific phospholipase D

NAPEs: N-acyl-substituted phosphatidylethanolamine species

NF-κB: Nuclear factor kappa-light-chain-enhancer of activated B cells

NMDA: N-methyl-D-aspartate

NMDR: N-methyl-D-aspartate receptor

OEA: N-oleoylethanolamine

OVLT: organum vasculosum of the lamina terminalis

PAMPs: Pathogen-associated molecular patterns

P-ase: Phosphatase

PC: Phosphatidylcholine

PE: Phosphatidylethanolamine

PEA: N-palmitoylethanolamine

PG: Prostaglandin

PGE_2: Prostaglandin E_2

PG-EAs: Prostaglandin ethanolamides

PGES: Prostaglandin E synthase

PG-Gs: Prostaglandin glycerol esters

PGI_2: Prostacyclin

PI: phosphatidylinositol

PI3K: Phosphatidylinositol 3-kinase

PIP2: Phosphatidylinositol-4,5- bisphosphate

PKA: Protein kinase A

PLA_2 : Phospholipase A_2

PLC : Phospholipase C

PLC-β: Receptor-operated phospholipase C- β

po: per os

POA: Preoptic area of the hypothalamus

POAH: Preoptic anterior hypothalamic nucleus

RER: Receptor-driven endocannabinoid release

RMR: Rostral medullary raphe

sc: Subcutaneous

SEM: Standart error of the mean

$sPLA_2$: Secretory phospholipase A_2

T_{ab} : The abdominal temperature

TAK1: T ransforming growth factor-β-activated kinase 1

TIR: Toll/IL-1R/plant R gene homology

TIRAP: TIR domain-containing adaptor protein

TLR3: Toll-like receptor 3

TLR4: Toll-like receptor 4

TLRs: Toll-like receptors

TNF-α: Tumor necrosis factor

TRAF6: TNF receptor associated factor 6

TRAM: TIR-domain-containing adaptor-inducing interferon-β-related adaptor molecule

TRIF: TIR-domain-containing adaptor-inducing interferon-β

TRPV: Transient receptor potential vanilloid receptor type 1

VMPO:Ventromedial preoptic nucleus

CHAPTER 1

INTRODUCTION

1.1 The Lipid Composition of Plasma Membranes

Lipids are one of the most important building blocks in the plasma membranes. Even though lipid -to-protein ratios in membranes vary notably according to membrane function, almost all membranes contain at least one-half lipid. Plasma membrane lipids are basically composed of four types: fatty acids, glycerophospholipids, sphingolipids, and cholesterol [1]. The chemical diversity of membrane lipids controls protein trafficking, facilitates recognition between cells and leads to the production of hundreds of molecules that carry information both within and across cells [2].

1.1.1 Fatty Acids

Fatty acids contain a hydrocarbon chain with a carboxylic acid at one end. The predominant fatty acid residues are those of the C_{16} and C_{18} species; palmitic, oleic, linoleic, and stearic acids [1].

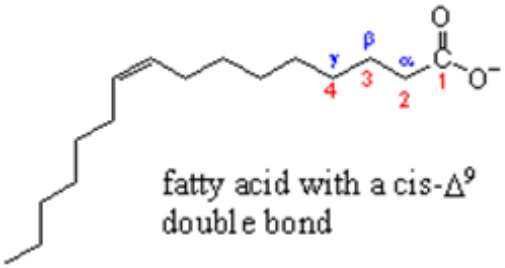

Figure 1.1. A diagram of 16-carbon fatty acid, with one *cis* double bond between carbon atoms 9 and 10 (represented as 16:1 cisΔ^9**)** [3].

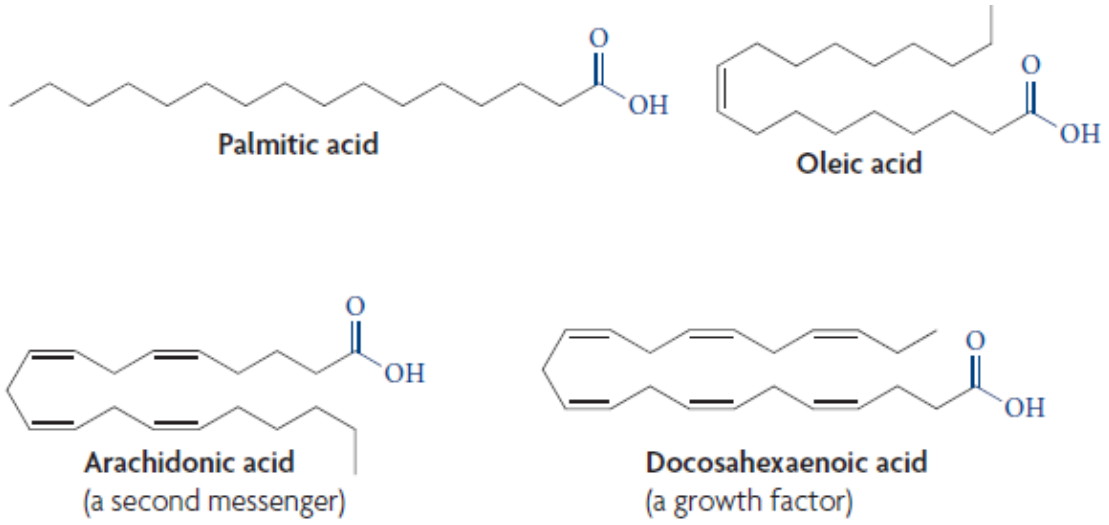

Figure 1.2. Saturated and unsaturated fatty acids [2].

Saturated fatty acids do not contain double bonds, whereas monounsaturated and polyunsaturated fatty acids contain one or more *cis* double bonds, respectively. There are two types of polyunsaturated fatty acids: ω- 6 (for example, arachidonic acid) and ω- 3 (for example, docosahexaenoic acid), which are named according to the position of the first double

bond in the carbon chain, starting from the methyl end of the molecule [2].

1.1.2 Glycerophospholipids (Phosphoglycerides)

The most commonly lipids found in the lipid bilayer are the glycerophospholipids. They comprise of *sn*-glycerol-3-phosphate esterified at its C1 and C2 positions to fatty acids (shown as R_1 and R_2 in Figure 1.3.) and at its C3 to a polar head group (shown as X in Figure 1.3.) [1]. *sn*-glycerol-3-phosphate is the parent structure common to all naturally present glycerophospholipids [4].

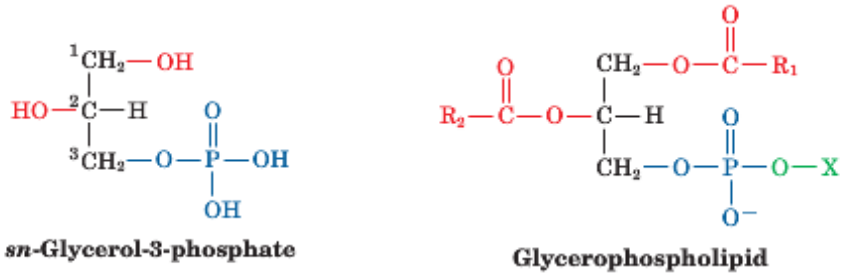

Figure 1.3. Molecular formula of *sn*-glycerol-3-phosphate and glycerophospholipid [1].

Glycerophospholipids have nonpolar aliphatic tails (hydrophobic) and polar phosphoryl-X heads (hydrophilic), and to this respect are amphiphilic molecules. In the glycerophospholipids that commonly present in biological membranes, the head groups are stemmed from polar alcohols (Figure 1.4.) [1].

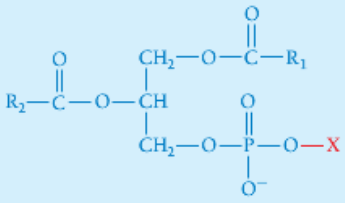

Name of X—OH	Formula of —X	Name of Phospholipid
Water	—H	Phosphatidic acid
Ethanolamine	$-CH_2CH_2NH_3^+$	Phosphatidylethanolamine
Choline	$-CH_2CH_2N(CH_3)_3^+$	Phosphatidylcholine (lecithin)
Serine	$-CH_2CH(NH_3^+)COO^-$	Phosphatidylserine
myo-Inositol	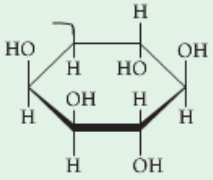	Phosphatidylinositol
Glycerol	$-CH_2CH(OH)CH_2OH$	Phosphatidylglycerol
Phosphatidylglycerol	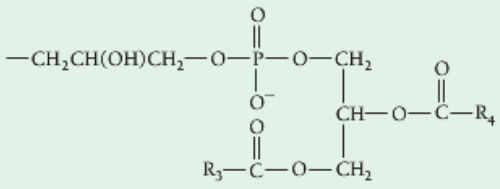	Diphosphatidylglycerol (cardiolipin)

Figure 1.4. The Common Classes of Glycerophospholipids [1].

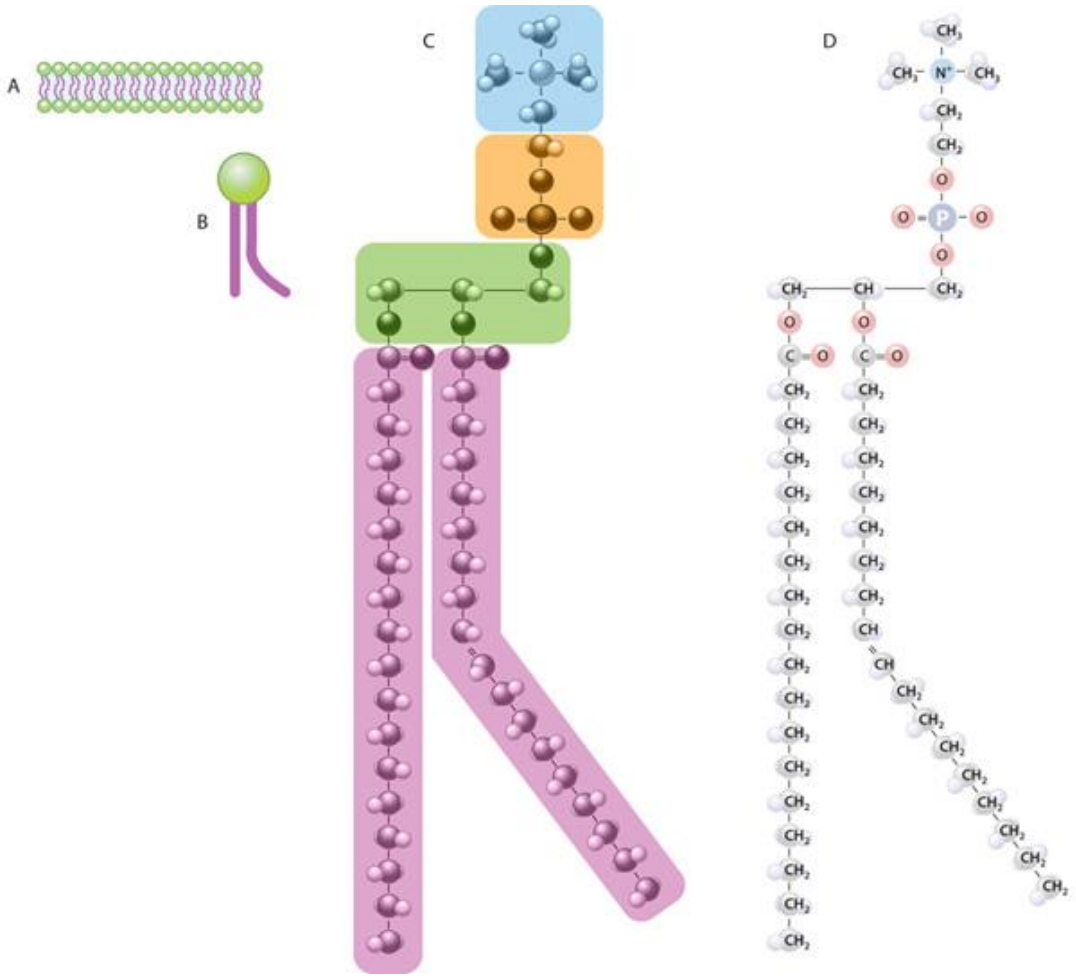

Figure 1.5. The lipid bilayer and the structure and composition of a glycerophospholipid molecule [5].**A)** The plasma membrane of a cell is a bilayer of glycerophospholipid molecules. **B)** A single glycerophospholipid molecule is composed of two major regions: a hydrophilic head (green) and hydrophobic tails (purple). **C)** The subregions of a glycerophospholipid molecule (phosphatidylcholine is shown as an example). The hydrophilic head is composed of a choline structure (blue) and a phosphate (orange). This head is connected to a glycerol (green) with two hydrophobic tails (purple) called fatty acids. **D)** This view shows the specific atoms within the various subregions of the phosphatidylcholine molecule. A double bond between two of the carbon atoms in one of the hydrocarbon (fatty acid) tails causes a slight kink on this molecule, so it appears bent [5].

1.1.3 Sphingolipids

Sphingolipids, are basically derivatives of the C_{18} lipid sphingosine. They are also major membrane components.

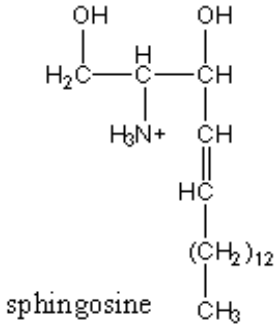

Figure 1.6. Molecular formula of sphingosine [3].

Sphingosine has a long hydrocarbon tail, and a polar domain that bears an amino group [3].

The amino group of sphingosine may form an amide bond with a carboxyl group of a fatty acid to yield ceramide.

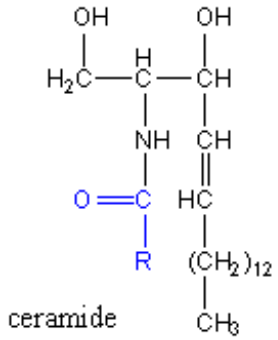

Figure 1.7. Molecular formula of ceramide [3].

Even though free ceramides are not common in biological membranes, they form the basic structure of complex lipids such as sphingomyelins, cerebrosides, and gangliosides [4].
In sphingomyelins, the terminal hydroxyl group of ceramide is esterified, usually to phosphocholine or alternatively to phosphoethanolamine, and therefore also called sphingophospholipids. They are abundant in the plasma membranes, specifically in of myelinated nerve axons which provide with electrical insulation.

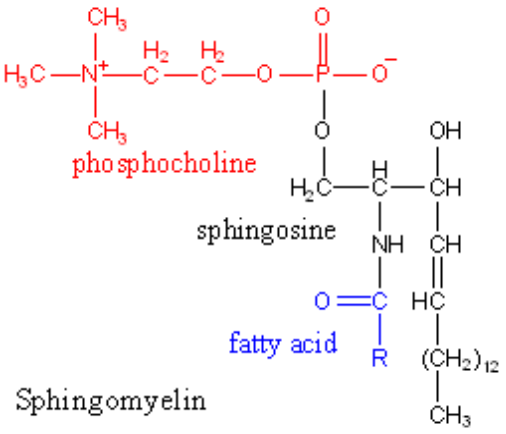

Figure 1.8. Molecular formula of sphingomyelin [3].

Cerebrosides are the simplest sphingoglycolipids. They are basically ceramides that consist of a monosaccharide group (glucose or galactose) as a polar head.

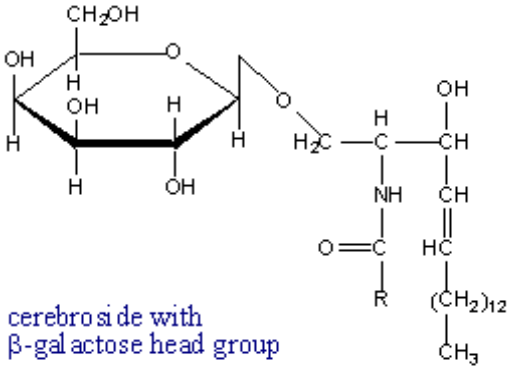

Figure 1.9. Molecular formula of cerebroside with β-galactose head group [3].

Ganglioside are ceramides that consist of a complex oligosaccharide group as a polar head. They are predominant constituents of cell surface membranes and make up a significant fraction (6%) of brain lipids [1].

Cerebrosides and gangliosides, which are also called glycosphingolipids, are usually present in the outer leaflet of the plasma membrane, with their sugar groups spreading out from the cell surface [1].

1.1.4. Cholesterol

Cholesterol is one of the basic constituent of cell membranes. It has a short branched hydrocarbon chain and a joint ring system that gives its rigidity. It is mainly hydrophobic. However, it has a polar hydroxyl group that makes it amphipathic**.**

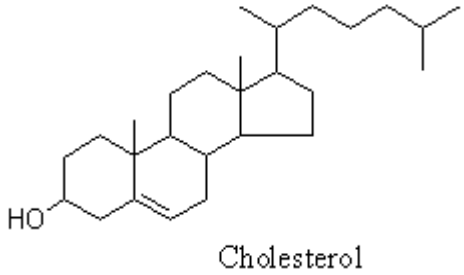

Figure 1.10. Molecular formula of cholesterol [3].

1.2 A Biologically Active Precursor Derived From Glycerophospholipids Through the Activation of Phospholipase A_2 (PLA_2) and Phospholipase C (PLC): Arachidonic Acid (AA)

Arachidonic acid (5,8,11,14-eicosatetraenoic acid) is a C_{20} polyunsaturated fatty acid which has four non-conjugated double bonds. It is an ω–6 fatty acid (the double bond at C_{14} is six carbon atoms from the methyl end (the ωcarbon atom)) and serves as the predominant precursor for lipid mediators such as prostaglandins, the major lipid mediator of inflammation, in humans [1].

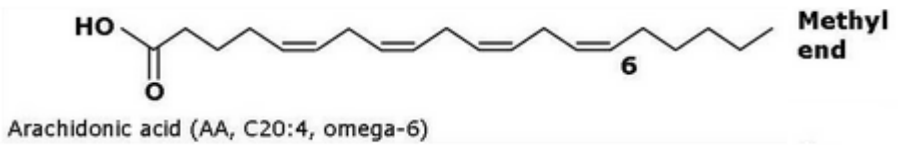

Figure 1.11. Molecular formula of Arachidonic acid (AA) (Adapted from [58]).

One of the essential fatty acids, linoleic acid (also an ω–6 fatty acid), is the precursor of arachidonic acid (AA). Linoleic acid is desaturated by a Δ^6 desaturase yielding γ-linolenic acid (GLA). Subsequent elongation and a second desaturation (this time with Δ^5 desaturase) result in the production of AA (Figure 1.12.) [1].

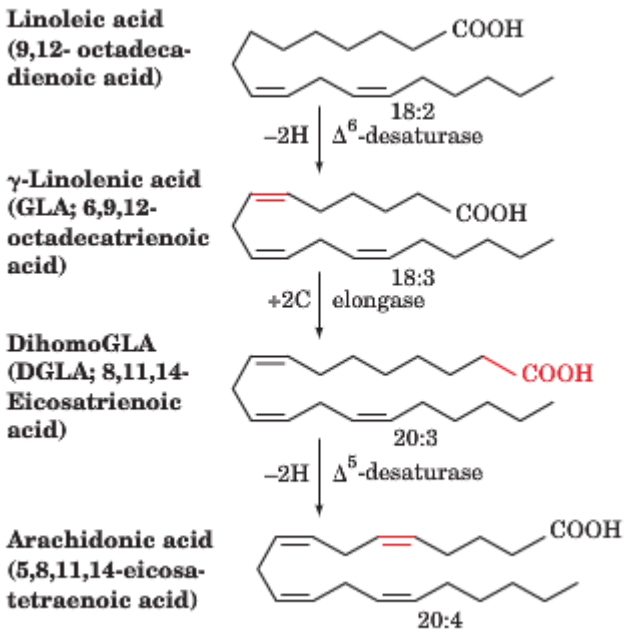

Figure 1.12. Synthesis of Arachidonic Acid (AA) (Adapted from [1]).

Under normal circumstances, arachidonate is stored in cell membranes esterified at glycerol C_2 of phosphatidylinositol and other phospholipids. When it is needed, liberation of arachidonate is accomplished by hydrolysis of phospholipids, mainly by three pathways:

1. Phospholipase A_2 (PLA_2): PLA_2 hydrolyzes acyl groups at C2 of phospholipids.

2. Phospholipase C (PLC): PLC particularly hydrolyzes the phosphatidylinositol head group yielding 1,2-diacylglycerol (DAG) and phosphoinositol. Subsequently, diacylglycerol kinase phosphorylates DAG, yielding phosphatidic acid, a substrate of

phospholipase A_2. (DAG and several forms of phosphorylated phosphoinositol are also fundamental signaling molecules, i.e. they mediate the phosphoinositide cascade).

3. The DAG and Diacylglycerol Lipase: The DAG may be hydrolyzed straightly by diacylglycerol lipase, yielding monoacylglycerol and arachidonic acid [1].

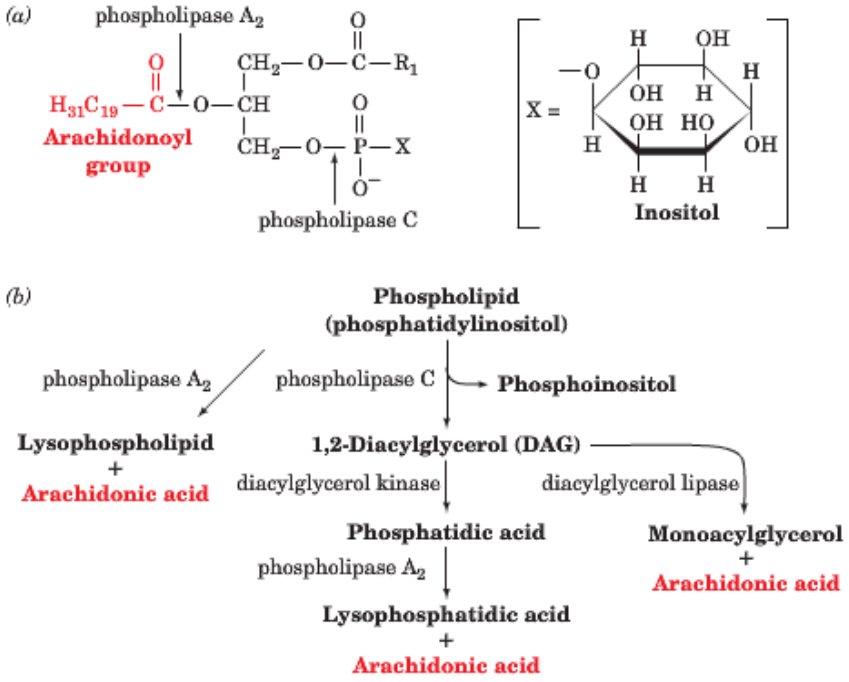

Figure 1.13. Release of arachidonic acid by phospholipase hydrolysis [1]. **(a)** The sites of hydrolytic cleavage mediated by phospholipases A_2 and C. The polar head group, X, is often inositol and its various phosphorylated forms. **(b)** Pathways of arachidonic acid liberation from phospholipids [1].

On the grounds of studies done on alternative arachidonic acid sources in recent years, however, endocannabinoids have also come into prominence as an important source of arachidonic acid in the brain.

1.3 Synthesis and Metabolism of Endocannabinoids (eCBs)

1.3.1 Endocannabinoid System

Endocannabinoids (endogenous cannabinoids) are eicosanoid (i.e., 20-carbon having arachidonic acid end-products) molecules defined as the primary endogenous agonists of cannabinoid receptors in animals [60][61][62].

Identification of a cell surface receptor that is targeted by marijuana's principle psychoactive substance, a terpenoid derivative Δ^9-tetrahydrocannabinol (Δ^9-THC) [68][69], raised questions about whether marijuana-like endogenous substances were synthesized in animals. After a while, the first endogenous marijuana-like substance *N*-arachidonoyl ethanolamine (Anandamide or AEA) was identified in pig brain [67]. 2-arachidonoyl-sn-glycerol (2-AG) was the second ligand identified and characterized as an endocannabinoid [71] [72] [73].

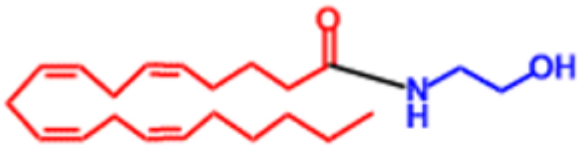

N-arachidonoyl ethanolamine (Anandamide or AEA)

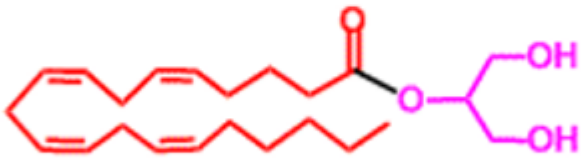

2-arachidonoyl glycerol (2-AG)

Figure 1.14. Molecular formulas of the most studied endocannabinoids, *N*-arachidonoyl ethanolamine and 2-arachidonoyl glycerol (Adapted from [59]).

Even though several endogenous molecules (e.g. noladin ether, virodhamine, and *N*-arachidonoyldopamine) have been also categorized as endocannabinoids so far, only two of them, AEA and 2-AG have been thoroughly studied and come out as the most widespread regulators of synaptic function [78].

Endocannabinoids (eCBs) are a family of lipid messengers which bind to the same cell surface receptors with marijuana. Their synthesis occur *de-novo* on demand via cleavage of membrane constituents and are produced in cells of the brain and other tissues, interacting with two subtypes of G protein-coupled cannabinoid receptors, cannabinoid type 1 receptor (CB1R) and cannabinoid type 2 receptor (CB2R). CB1R is exceedingly abundant in the brain, therefore thought to be the most responsible for THC psychoactivity. CB2R, on the other hand, is expressed in immune cells to the greatest extent [76].

eCBs function in a different manner compared to traditional neurotransmitters. Instead of being released from vesicles, they are secreted in a non-synaptic manner and bind to their cognate receptors located in the close vicinity of their sites of synthesis [66].

They have important roles in intercellular signaling processes and their ability to regulate synaptic efficacy results in a wide range of functional reorganization. They are involved in various physiological and pathophysiological processes such as fever, neuroinflammation, feeding and appetite, energy balance, pain, stress, memory, mood and sleep regulation, motor activity, cognitive functions and disfunctions [62][64][65][66][74]. Additionally, there is evidence about their involvement in regulation of cardiovascular, gastrointestinal, liver functions [75].

The endocannabinoid signalling system comprises: 1) at least two seven transmembrane-domain G-protein-coupled receptors (GPCRs), namely CB1R and CB2R; 2) the endogenous ligands of these receptors known as endocannabinoids (eCBs) of which AEA and 2-AG are the best characterized; 3) synthetic and degradative enzymes and transporters that control levels and actions of eCBs at receptors [76][78].

Endocannabinoids are markedly prevalent in mammalian cells and seem to have a prohomeostatic role when activated subsequent to transient or chronic disturbance of homeostasis, regulating actions and levels of other chemical signals in a local manner. Chemical substances which selectively manipulate actions and levels of eCBs have been and are being developed and they appear to be candidates for therapeutic drugs [76].

1.3.2 Synthesis Pathways of Endocannabinoids

Both anandamide and 2-arachidonoyl glycerol are arachidonic acid-containing lipid molecules produced from glycerophospholipids. However, their biosynthetic pathways are completely distinct [61].

In case of anadamide, a *bone fide* brain neurotransmitter, its synthesis route(s) and neural pathways in which it is employed are ambiguous [70].

According to the canonical route of anandamide biosynthesis shown in Figure 1.15. (in the center), anandamide is synthesized by According to the canonical route of anandamide biosynthesis shown in Figure 1.15. (in the center), anandamide is synthesized by a selective phospholipase D (NAPE-PLD) through hydrolysis of the phospholipid precursor, N-arachidonoyl-phosphatidylethanolamine (N-arachidonoyl-PE) [70].

N-arachidonoyl-PE is synthesized by two enzyme-mediated steps through which arachidonic acid is transferred from the sn-2 position of various phospholipids to the sn-1 position of lyso-phosphatidylcholine (PC), producing diarachidonoyl-PC. N-arachidonoyl-PE is synthesized by two enzyme-mediated steps through which arachidonic acid is transferred to the sn-1 position of lyso-phosphatidylcholine (PC), from the sn-2 position of various phospholipids, producing diarachidonoyl-PC. The free amino group of PE then receives the sn-1 arachidonoyl chain of diarachidonoyl-PC, producing N-arachidonoyl-PE. The enzymes (or enzyme) utilized in generation of diarachidonoyl-PC and N-arachidonoyl-PE have not been identified yet. However, it is

known that formation of both compounds is strictly dependent on intracellular Ca^{2+} levels of neurons. Concentration of N-arachidonoyl-PE is quite low under normal

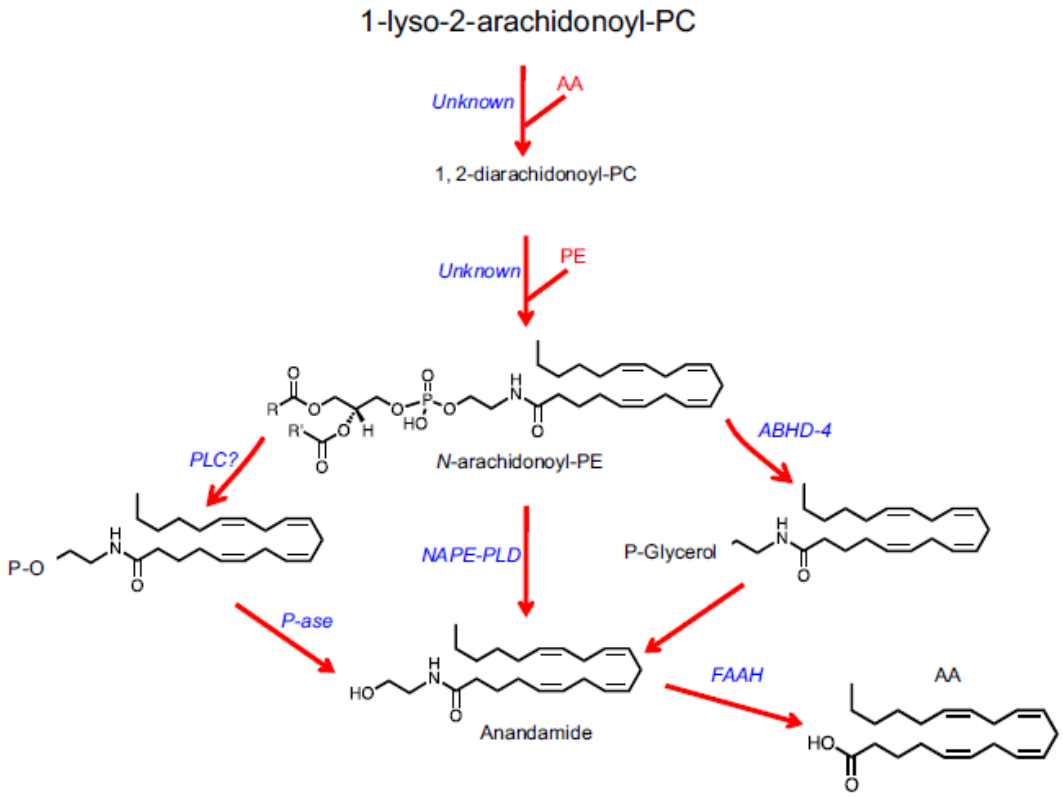

Figure 1.15. Formation and deactivation of anandamide in brain neurons [70].

circumstances (resting conditions). However, its concentration immediately and transiently elevates when neurons are subjected to stimuli that escalate intracellular Ca^{2+} levels [70].

Additionally, Figure 1.15. demonstrates two alternative routes that might be utilized. The left one shows conversion of N-arachidonoyl-PE into phospho-anandamide by an as-yet-uncharacterized PLC. Subsequently, it is dephosphorylated by a phosphatase (P-ase), forming anandamide. The right one shows hydrolization of arachidonoyl-PE by α/β hydrolase domain-containing protein 4 (ABHD-4), producing glycerophospho-

anandamide.Then anandamide is formed by glycerophospho-anandamide which looses its glycerophosphate group. Fatty acid amide hydrolase (FAAH), which is a serine amidase, is the primary intracellular degradation enzyme of anandamide. Despite FAAH seems to terminate the biological actions of anandamide, there is convincing evidence of other unraveled enzymes are also employed in this process [61] [70].

2-arachidonoyl-sn-glycerol synthesis, on the other hand, starts with the cleavage of phosphatidylinositol-4,5- bisphosphate (PIP2) in neurons (Figure 1.16.). The second messenger DAG is then produced from PIP2 through receptor-operated phospholipase C- β (PLC-β) which can be stimulated by several G protein-coupled receptors (e.g. the type-1 metabotropic glutamate receptor, mGluR5). Every checkpoint along this route can produce independent sets of signaling molecules such as DAG. DAG is utilized as a substrate by two functionally different enzymes: 1) diacylglycerol lipase-α (DGL-α), which hydrolyses DAG, forming 2-AG; 2) diacylglycerol kinase, which produces the intracellular metabolic intermediate and signalling lipid, phosphatidic acid. In addition, DAG can regulate the activity of protein kinase C and other cellular effectors [63][70].

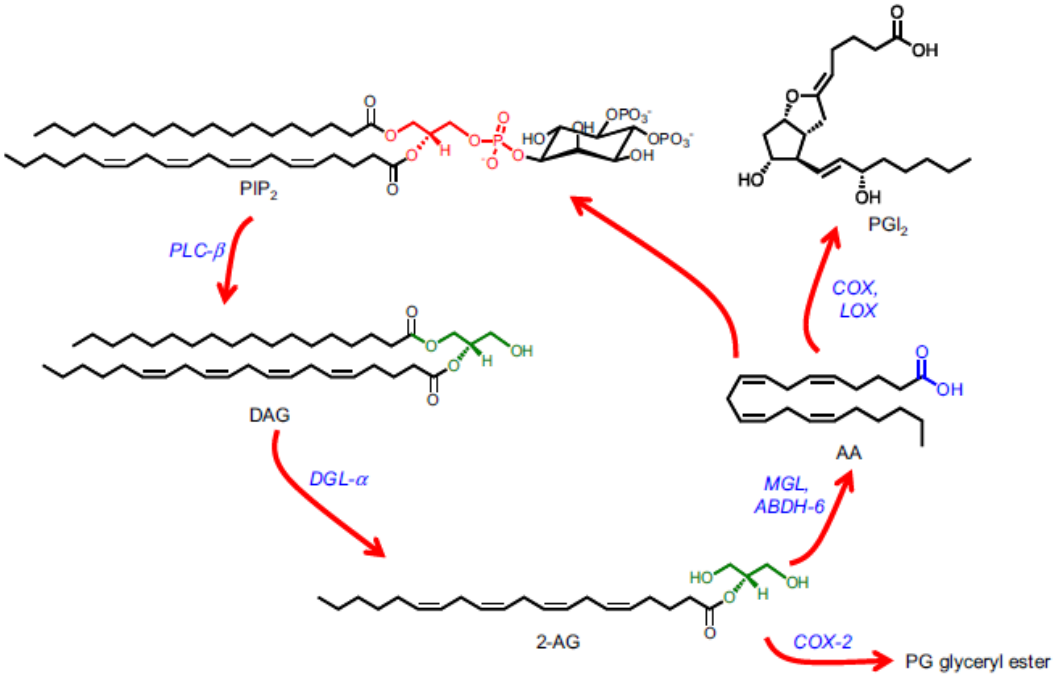

Figure 1.16. Formation and deactivation of 2-arachidonoyl-sn-glycerol (2-AG) in brain neurons [70].

The action of 2-AG is mainly terminated through hydrolysis by monoacylglycerol lipase (MGL) or α/β hydrolase domain-containing protein 6 (ABHD-6). Free non-esterified arachidonic acid is either used in the production of the eicosanoid family of compounds by COX or LOX enzymes or reinserted into cell membrane as a part of phospholipid remodelling. In addition, direct oxygenation of 2-AG by cyclooxygenase-2 (COX-2) produces a family of prostaglandin (PG) glyceryl esters. Even though these molecules do not interact with cannabinoid receptors, they exhibit important biological effects [70].

Recent studies have revealed that some specific synaptic components which comprise molecular entities that are engaged in 2-AG synthesis and degradation have also important contributions These molecular entities are assembled into a supramolecular protein complex named the '2-AG signalosome'. They specifically are found at excitatory synapses of the brain and facilitate 2-AG to function as a retrograde messenger.. However, there still are some fundamental unanswered questions about the 2- AG signalosome (e.g., its mechanism of regulation, exact molecular composition and effect on the potency of drugs such as Δ^9 –THC and cocaine) [70] [77].

2-AG is at the main center of many routes of lipid metabolism. It can interchangeably be an end-product of one pathway and a precursor of another. The diversity of its metabolic roles and its high concentration in brain tissue (about 200-fold greater than AEA's) suggest that the 2-AG in the brain may also be involved in housekeeping functions [66].

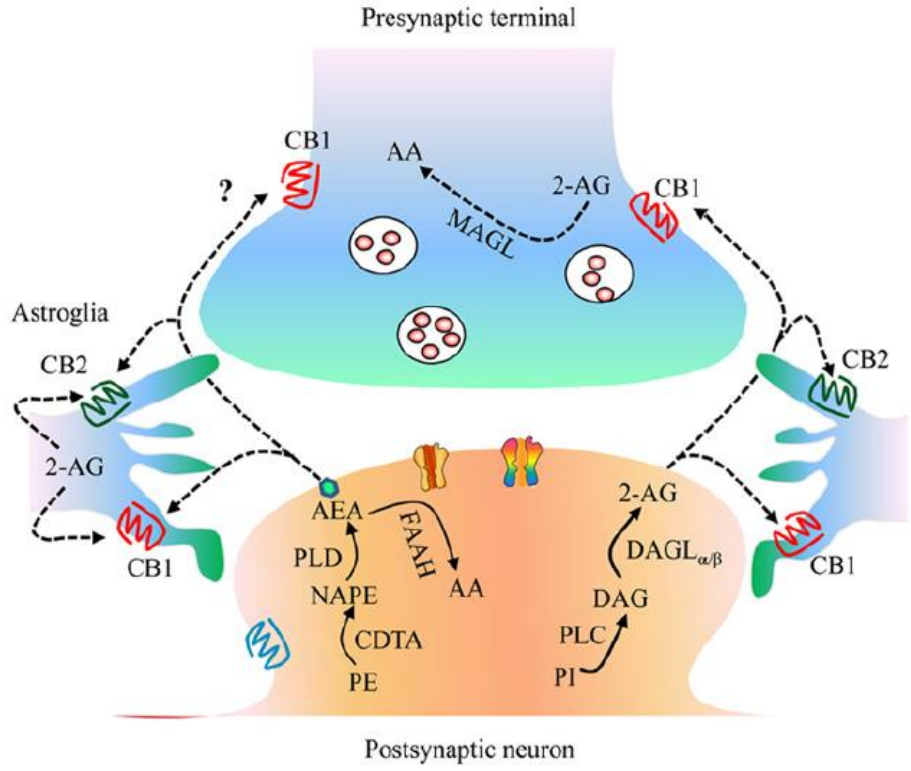

Figure 1.17. A schematic diagram illustrates the endocannabinoid system [81]. PI, phosphatidylinositol; PLC, phospholipase C; DAG, Diacylglycerol; DAGL α/β, Diacylglycerol lipase α/β; 2-AG, 2-arachidonoyl glycerol; MAGL, monoacylglycerol lipase; AEA, Anandamide ;PE, phosphatidylethanolamine ; NAPE, *N*-acyl phosphatidylethanolamine; CDTA, calcium-dependent transacylase ;PLD phospholipase D ;FAAH, fatty acid amide hydrolase; CB1,Cannabinoid Receptor Type 1;CB2,Cannabinoid Receptor Type 2.

2-AG is produced in postsynaptic neurons and its reuptake and inactivation occur in presynaptic neurons. However, it can be present in both postsynaptic and presynaptic sites (Figure 1.17). Anandamide, on the other hand, is synthesized, reuptaken and inactivated in postsynaptic neurons. CB1 receptors are expressed in presynaptic terminals and in astroglial cells. CB2 receptors are mainly expressed in astroglial cells [81].

1.3.3 Cannabinoid Receptors and Their Mechanism of Action

CB1 and CB2 are the two principal cannabinoid receptors. They are Gi/o protein-coupled receptors that regulate almost all effects of exogenous and endogenous cannabinoids. However, their distribution is remarkably distinct. CB1 is primarily found in central nervous system (CNS), while CB2 is quite scarce in CNS. CB2 is mainly expressesd in immune system cells [78][80].

CB1 receptors are one of the most extensively expressed GPCRs in the brain. Their localization to neuronal terminals strongly suggests that they have important roles in regulating synaptic function [78]. It is thought that the physiological activations of endocannabinoids and the psychoactivity of exogenous cannabinoids in the CNS occur via their action [80].

1.3.3.1 Cannabinoid Type 1 Receptor (CB1 or CB1R)

In 1990, a 473-amino acid G protein-coupled receptor encoded by a rat brain cDNA clone was identified as a cannabinoid receptor and named CB1. There are 97–99% amino acid sequence identity among human, rat and mouse CB1 receptors. In the human and rodent cortices, CB1Rs are predominantly found on axon terminals of cholecystokinin-8-positive GABA interneurons [66] [80].

Transmembrane helices of CB1R form binding sites of cannabinoids and the results of further studies (e.g. Nuclear magnetic resonance investigations) support the hypothesis that a cannabinoid interacts with a hydrophobic groove formed by helices 3 and 6 of CB1through lateral diffusion within a membrane leaflet [80].

CB1R gene takes place on 6^{th} chromosome in humans [80].CB1R has two types of NH2-terminal splice variants, short-length and full-length receptors have been identified. Short-length variants display altered ligand binding properties compared to full-length receptors and expressed at very low levels. Several polymorphisms have been identified in the CB1 receptor and even though there are some controversies about the results, some of them are correlated controversies about the results, some of them are correlated

with attention deficit/hyperactivity disorder, hebephrenic schizophrenia and obesity-related phenotypes [80].

CB1 is a Gi/o-coupled receptor and can start signalling cascades typical of this class of transducing proteins, which comprises closure of Ca^{2+} channels, opening of K^{+} channels, inhibition of adenylyl cyclase activity (with subsequent decrement of cytosolic cAMP) and deactivation of kinases which phosphorylate tyrosine, serine and threonine residues [66].

There are two main mechanisms through which CB1 receptors inhibits neurotransmitter release at synapses: 1) Short term plasticity, in which CB1 receptors are stimulated for a few seconds, involves direct G protein-dependent (likely via the βγ subunits) inhibition of presynaptic Ca^{2+}flow through voltage-gated Ca^{2+} channels 2) Long term plasticity, whose main mechanism involves inhibition of adenylyl cyclase and downregulation of the cAMP/PKA pathway by the αi/o limb [78].

CB1R is expressed broadly and abundantly in the brain. "High levels of CB1R are found in innermost layers of the olfactory bulb, hippocampus (particularly high in the dentate molecular layer and the CA3 region), lateral part of the striatum, target nuclei of the striatum (i.e., globus pallidus, entopeduncular nucleus, substantia nigra pars reticulata) and cerebellar molecular layer. Average levels are shown in other forebrain areas and in a few nuclei in the brain stem and spinal cord, which comprises the cerebral cortex, septum, amygdala, hypothalamus (ventromedial hypothalamus), lateral subnucleus of interpeduncular nucleus, parabrachial nucleus, nucleus of solitary tract (caudal and commissural portions), and spinal dorsal horn. In the thalamus, spinal ventral horn and other nuclei in the brain stem, however, CB1R is expressed at low levels. Within all these regions, inhibitory synapses generally have higher CB1 expression levels compared to excitatory synapses and these binding features are conserved across mammals [80]."

In addition, CB1 receptors can interact with some GPCRs, forming heteromeric complexes. Some of them are CB1-D2, CB1-opioid, CB1-A2A, and CB1-orexin-1 receptor complexes. These kinds of interactions can considerably alter the downstream G proteins recruited during receptor stimulation. However, the effects of

heteromerization of CB1Rs with other neuromodulatory receptors remain to be understood [78].

1.3.3.2 Cannabinoid Type 2 receptor (CB2 or CB2R)

In 1993, another type of cannabinoid receptor, cannabinoid type 2 receptor, was shown in a human cDNA clone. It comprises 360 amino acids and likewise CB1, it is a G protein coupled receptor. CB2 and CB1 receptors of human just shares 44% amino acid sequence identity. Afterwards, the mouse and rat CB2 receptors were identified. CB2 of the mouse and human share 82% amino acid sequence identity. The rat CB2, on the other hand, might be polymorphic and encodes receptors having either 369 or 410 amino acids [80].

After CB2, the peripheral cannabinoid receptor, was identified on macrophages its expression in brain cells have also been shown [80]. However, its expression in CNS is quite low compared to its expression in immune system organs. Even so, recent studies suggest a role for these receptors in the CNS (specifically in microglia and astrocytes) and shows neuronal CB2 expression in various areas of the brain specifically in somata and dendrites of them. Effects of CB2Rs on brain functions and their cellular mechanism(s), however, remain to be elucidated [78] [80].

1.4. The Stimuli in the Brain Which Leads to Increase in Endocannabinoid Levels.

Physiological stimuli and pathological conditions induce distinctive elevation of endocannabinoids in the brain. Physiological stimuli cause rapid and transient (seconds to minutes) elevations in endocannabinoids, which activate CB1Rs, regulate ion channels and inhibits neurotransmission. Pathological conditions, however, cause much slower and sustained (hours to days) elevations in the endocannabinoid tone, altering gene expression and fulfilling the activation of molecular mechanisms that prevent the synthesis and diffusion of damaging mediators. Particularly, elevations in the

endocannabinoid tone activate immune CB2Rs which reduce the synthesis of proinflammatory cytokines and enzymes involved in the production of free radicals and also activate neuronal CB1Rs which cause increase in synthesis of growth factors. However, the molecular mechanisms regulating the brain's endocannabinoid tone is still not clear [79].

Dissimilar to conventional neurotransmitters (e.g., amino acids, amines, neuropeptides) eCBs are not kept in in vesicles but synthesized *de-novo* on demand and released at once. Depolarization, activation of Gq/11-coupled receptors and synaptic stimulation are thought to be among the most important factors which induce the synthesis of eCBs in CNS. Most of the studies support the hypothesis that eCBs are synthesized via two distinct pathways: 1) PLCβ-independent and mediated by a significant elevation in intracellular Ca^{2+} levels alone (CaER) 2) PLCβ-dependent and mediated by activation of Gq/11-coupled receptors at basal (basal RER) or elevated Ca^{2+} levels (Ca^{2+}-assisted RER) (Figure 1.18.)[80].

Generally, stimulation of main Gq/11 protein-coupled receptors expressed in the CNS, including group I metabotropic glutamate receptors $mGluR_1$ and $mGluR_5$; muscarinic acetylcholine receptors M_1, M_3, and M_5; serotonin receptors 5-HT_{2A}, 5-HT_{2B}, and 5-HT_{2C}; adrenoceptors α1A, α1B, and α1D ; and histamine receptor H_1 leads to increase in endocannabinoid levels of CNS in a receptor-dependent manner [80].

It is known that macrophages subjected to lipopolysaccharide (LPS), the outer membrane of gram negative bacteria, release a burst of lipid mediators including AEA and arachidonic acid derivatives. In addition, the existence of several routes of AEA production may indicate the diversity of physiological stimuli that are able to prompt this endocannabinoid. In neural cell membranes for example, physiological stimuli such as membrane depolarization, intracellular Ca^{2+} transients and dopamine D_2 receptor activation have the ability to stimulate AEA synthesis [70].

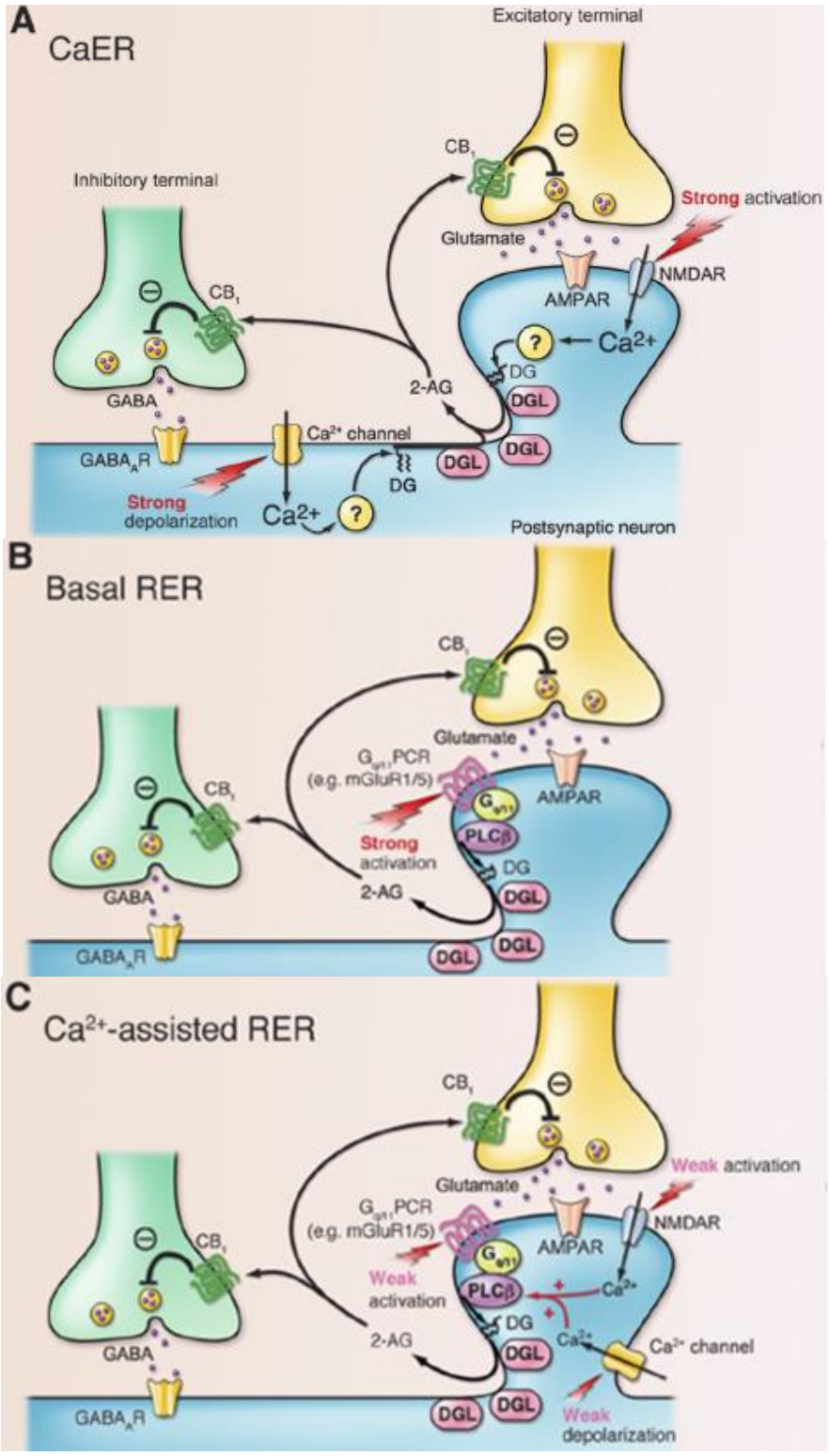

Figure 1.18. Schematic illustration of the three modes of retrograde eCB signaling [80].

A) Ca^{2+} - driven eCB release (CaER). Strong postsynaptic depolarization causes influx of Ca^{2+} through voltage-gated Ca^{2+} channels. The resultant large increase in intracellular Ca^{2+} concentration to the micromolar range induces production of diacylglycerol (DG) through unknown pathways (?) DG is converted to 2-AG (2-arachidonoyl glycerol) by DGL (diacylglycerol lipase). The produced 2-AG is then released from the postsynaptic neuron. When a large Ca^{2+} elevation is caused by activation of NMDA (*N*-methyl-D aspartate) receptors (NMDR), 2-AG is produced and released through the same pathways.

B) Basal receptor-driven endocannabinoid release (Basal-RER). At basal Ca^{2+} levels, strong activation of Gq/11-coupled receptors (e.g., mGluR1/5) stimulates PLCβ, which hydrolyzes phosphatidylinositol 4,5- bisphosphate into DG and IP3. 2-AG is then produced from DG by DGL and released

C) Ca^{2+} -assisted RER. When weak activation of Gq/11- coupled receptors coincides with small Ca^{2+} elevation (submicromolar range) through weak activation of either voltage-gated Ca^{2+} channels or NMDA receptors, PLCβ activation is enhanced. In this condition, 2-AG production can be induced and released even by weak activation of Gq/11-coupled receptors, which is subthreshold for basal RER. (Difference in Ca^{2+} levels required for CaER and Ca^{2+} -assisted RER, which is expressed as the difference in letter sizes). In any of the three modes, the released 2-AG binds to presynaptic CB1 receptors (CB1R) and suppresses neurotransmitter release [80].

In case of 2-AG, its neuronal production can be stimulated by neuronal activity (e.g., high and low-frequency stimulation of the schaffer collaterals) and elevation in the intracellular Ca^{2+} levels. In cultures of rat cortical neurons, the Ca^{2+} ionophore ionomycin and the glutamate receptor agonist NMDA induce 2-AG synthesis in a Ca^{2+}-dependent manner [66] [78][82] [83].

Even though high frequency stimulation of the schaffer collaterals induce a Ca^{2+}-dependent elevation in 2-AG level of freshly dissected hippocampal slices, this treatment has no effect on the levels of non-cannabinoid monoacylglycerols, which implies that 2-AG generation is not because of a generalized elevation in the rate of

lipid turnover. Moreover, high frequency stimulation does not have an effect on hippocampal AEA levels, which shows that the productions of AEA and 2-AG can be separately regulated. Consistent with this idea, stimulation of D_2 receptors — a powerful stimulus for AEA production in the rat striatum —has no impact on striatal 2-AG levels [66].

1.5 The Effects of Endocannabinoids on the Brain

Endocannabinoids are strong regulators of synaptic function throughout the CNS and retrograde signalling is the main mechanism through which they regulate synaptic function. In retrograde signalling, postsynaptic changes cause the production of an eCB which travels backward across synapse and interacts with CB1Rs on presynaptic neurons, altering ion channel regulation and repressing neurotransmitter release [78]. The neurotransmitters reported to be regulated via the CB1R involve glutamate, GABA, glycine, acetylcholine, norepinephrine, dopamine, serotonin, and cholecystokinin. However, the presynaptic mechanisms regulating the repression of neurotransmitter release may be different at distinct synapses [80]

DSI (depolarization-induced suppression of inhibition) and DSE (depolarization-induced suppression of excitation) are important phenomena in synaptic regulation of GABA and glutamate by eCBs, respectively. DSI is initiated by postsynaptic voltage-dependent influx of Ca^{2+} and expressed presynaptically through inhibition of transmitter release from axon terminals of GABA interneurons. DSE is also initiated by postsynaptic depolarization and causes depression in neurotransmitter release. However, DSE occurs in glutamatergic axon terminals, hence causes a reduction of excitatory input to the corresponding cell [66]

The synthesis and release of eCBs from postsynaptic neurons occurs in two states: 1) phasically in an activity-dependent manner 2) tonically under basal conditions [78][80].

Stimulation of CB1Rs regulates several types of ion channels and enzymes in a cAMP-dependent or –independent manner. Application of a cannabinoid agonist to neurons or

CB1-transfected cells stimulates A-type and inwardly rectifying K^+ channels and inhibits N- and P/Q-type Ca^{2+}channels and D- and M-type K^+ channels. Stimulation of CB1Rs also has effects on several enzymes such as focal adhesion kinase, mitogen-activated protein kinase, phosphatidylinositol-3-kinase and some enzymes of energy metabolism [80].

Even though retrograde signalling of eCBs seems to be the principal signalling mechanism, there is also evidence suggesting that eCBs signal in a non-retrograde or autocrine manner, and through astrocytes they may indirectly regulate pre- or postsynaptic functions (Figure 1.19). In non-retrograde or autocrine signalling, eCBs can regulate synaptic transmission and neural function by binding to CB1Rs or to transient receptor potential vanilloid receptor type 1 (TRPV1) located on or within the postsynaptic cell [78].

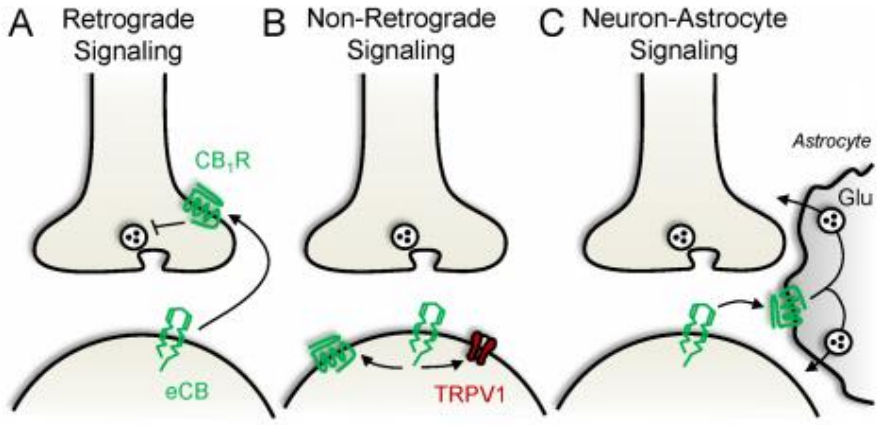

Figure 1.19. Endocannabinoid signalling at the synapse [78].

A) Retrograde endocannabinoid signaling. eCBs are mobilized from postsynaptic neurons and target presynaptic CB1Rs to suppress neurotransmitter release. **B)** Non-retrograde eCB signaling. eCBs produced in postsynaptic neurons activate postsynaptic CB1Rs or TRPV1 channels. **C)** Neuron-astrocyte eCB signaling. Modulation of eCB–independent synaptic plasticity is also one of the effects of eCBs released from postsynaptic neurons stimulate astrocytic CB1Rs, thereby triggering gliotransmission. Glu, glutamate [78].

eCBs on the CNS. In addition, eCBs have been known to regulate excitability of neurons in some brain regions. However, it is not clear whether these type of regulations occurs throughout the brain. Moreover, there are several studies indicate that the CB1R induction stimulate morphological changes of neurons [80].

There is a general consensus about the fast, point-to-point signalling process is regulated by 2-AG rather than AEA. It has been suggested that mGluR5-dependent plasticity is primarily mediated by 2-AG in the brain. This idea is due to an anatomically defined supramolecular structure called the "2-AG signalosome" in which 2-AG take place (Figure 1.20.) [70] [77].

This supramolecular complex, specifically localized to the perisynaptic zone of the dendritic spine, connecting three key proteins utilized in 2-AG production at excitatory synapses of the brain - mGluR5, PLC-β and DGLα - in a single functional unit. It has been suggested that these proteins may be held together by the scaffolding proteins Homer-cc and Homer-1a. While the excitatory axon terminals release glutamate, it binds to mGluR5 and the physical proximity of this receptor to PLC-β and DGLα eases the fast hydrolysis of PIP2 and the local accumulation of 2-AG. This accumulation lets 2-AG pass the postsynaptic membrane, cross the synaptic cleft and bind to CB1 receptors on axon terminals, weakening Ca^{2+} channel activity and repressing glutamate release. The pool of 2-AG that reaches presynaptic terminals may be immediately degraded by MGL,while the portion that fails to reach the terminals may probably be hydrolysed by α/β hydrolase domain-containing protein 6 (ABHD-6) [70][77]. It has been hypothesized that the stable association of mGluR5 and DGLα into such a complex supplies structural scaffold that enables localized formation of a signalling –competent pool of 2-AG and this pool may be different from the intracellular 2-AG pools engaged in eicosanoid synthesis and phospholipid remodeling [77].

This structural organization, however, is restricted to excitatory synapses, which have relatively lower levels of CB1 receptors. Inhibitory synapses formed by cholecystokinin-containing GABAergic interneurons have extremely high levels of CB1 and retrograde signalling have also been shown in these types of synapses. However, it is thought that

they regulate eCB-mediated retrograde signalling via a different mechanism, which is not known [70].

Figure 1.20. Schematic model of the 2-AG signalosome [70].

(mGluR5, metabotropic glutamate receptor 5; PLC-β , phospholipase C-β; DGLα, diacylglycerol lipase-α; AMPAR, AMPA receptors; NMDAR, NMDA receptors; MGL, monoacylglycerol lipase; ABHD-6, α/β hydrolase domain-containing protein 6) [70]

1.6 Biochemical Inhibition of Endocannabinoids

Endocannabinoid signalling is inactivated by enzymatic hydrolysis [88]. The intracellular hydrolysis of AEA is principally catalyzed by the enzyme fatty-acid amide

hydrolase (FAAH) which takes place in postsynaptic site. FAAH transforms AEA into free arachidonic acid and ethanolamine. AEA can also be degraded by enzymatic oxygenation [81][84][85]. Cyclooxygenase-2 can oxygenate both AEA and 2-AG, yielding prostaglandin ethanolamides (PG-EAs) and prostaglandin glycerol esters (PG-Gs), respectively [91].

The main enzyme that hydrolyzes 2-AG is monoacylglycerol lipase (MAGL or MGL), which transforms 2-AG into arachidonic acid and glycerol (Figure 1.21.) [81][90]. Almost 85% of brain 2-AG is degraded by MAGL. The remaining 15% is mostly ascribed to two uncharacterized enzymes: α/β hydrolase domain-containing protein 6 (ABHD6) and α/β hydrolase domain-containing protein 12 (ABHD12). MAGL, ABHD6, and ABHD12 have different subcellular distributions, indicating they may regulate distinct pools of 2-AG in the CNS [86].

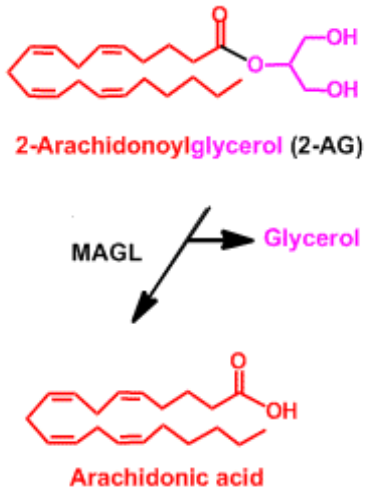

Figure 1.21. Inhibition of –AG mediated by monoacylglycerol lipase (MAGL) **(**Adapted from [59])

MAGL is a 33 kDa, peripherally associated serine hydrolase frequently located in the presynaptic site of axon terminals [81][90]. It includes the classical GXSXG consensus sequence frequently found in most of the serine hydrolases and is predicted to have an α/β-hydrolase fold by sequence homology. Its catalytic triad consists of Ser122, His269, and Asp239. Although MAGL can hydrolyze diacylglycerols and triacylglycerols, it

exquisitely prefers monoacylglycerols (MAGs) as a substrate. MAGs are transformed into free fatty acid and glycerol via the activity of MAGL [87].

It was shown that MAGL hydrolyzes 2-AG but not AEA and overexpression of MAGL decreases stimulus dependent 2-AG accumulation in primary cultures of rat brain neurons [92]. In addition, it was determined that RNA interference mediated-silencing of MAGL expression augmented 2-AG accumulation markedly in HeLa cells [93].

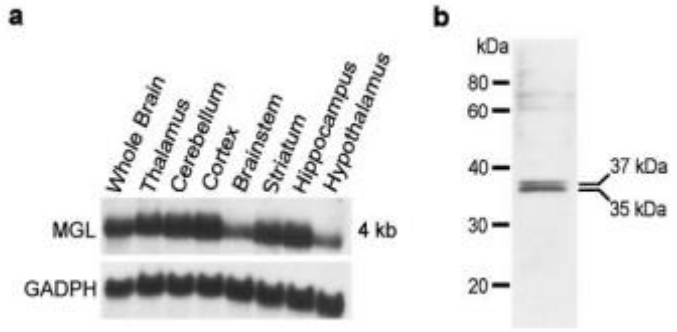

Figure 1.22. MGL expression in the rat brain [92] **a)** Northern blot analysis of MGL mRNA from various regions of the rat brain (glyceraldehyde-3-phosphate dehydrogenase (GADPH) mRNA was used as a control for loading conditions). **b)** Western Blot analysis of soluble protein from rat brain, with an immune-purified polyclonal antibody to the N-terminal region of MGL. Cortex, hippocampus and cerebellum was shown to have higher levels of MGL compared to thalamus, striatum, brainstem and hypothalamus [92].

As well as genetic studies, pharmacological studies also revealed the key role of MAGL in degradation of 2-AG. For example, JZL184, a potent, selective and irreversible inhibitor of MAGL from the *O-aryl* carbamate class, increased brain 2-AG without making significant changes in AEA levels in mice. JZL-184-treated mice displayed a comprehensive CB1-dependent behavioral effects consisting of hypothermia, analgesia and hypomotility, which suggests that 2-AG regulates various behavioral processes linked to cannabinoid pharmacology and has a widespread role in mammalian nervous system [87] [88].

In order to determine the ability of JZL184 to inhibit MAGL in vivo, male C57Bl/6 mice were pretreated with JZL184 (4-40 mg kg^{-1}, ip) and sacrificed after 4 hours from treatment. Competitive activity-based protein profiling (ABPP) of brain membrane proteomes showed that even at the lowest dose of JZL184 administered (4 mg kg^{-1}), 75% of MAGL is inhibited with minimal effects (< 20% inhibition) on other brain serine hydrolases. In addition, substrate assay analysis determined that by increasing the dose of JZL184 from 4 to 16 mg kg^{-1}, residual brain 2-AG hydrolysis activity could be further decreased from 25% to 15% of control levels. This results were consistent with a near-complete inhibition of MAGL activity as revealed by competitive ABPP. In addition, at the lowest dose of JZL184 administered (4 mg kg^{-1}), 2-AG levels were escalated by 5-fold at 4 h post-treatment and could be further escalated to 8-10-fold above baseline at higher doses of JZL 184. The escalation in brain 2-AG were coincided with substantial reductions in the levels of AA. However, FAAH was also blocked to an extent in dose dependent manner, e.g. at 16 mg kg^{-1} of JZL184 ~35% of FAAH activity remained intact [88].

In addition, it was shown that presynaptic MAGL not only degrades 2-AG secreted from activated postsynaptic neurons but also plays a role in hydrolysation of constitutively synthesized 2-AG and restrain it from accumulating around presynaptic terminals in hippocampus. This results indicate that the MAGL activity determines basal endocannabinoid tone and ceases retrograde endocannabinoid signaling [90].

1.7 Chemical Structure of KML-29 (1,1,1,3,3,3-hexafluoropropan-2-yl 4-(bis(benzo[d][1,3]dioxol-5-yl)(hydroxy)methyl)piperidine-1-carboxylate) and its Mechanism of Inhibition.

One of the most utilized MAGL inhibitors recently developed is JZL184, which is from *O-aryl* carbamate class, and has been used in many studies related to endocannabnoids. However, its most important drawback is that it displays low-level cross reactivity with

FAAH subsequent to high dosing and chronic treatments and with peripheral carboxylesterases, which can perplex certain biological studies [94].

Moreover, JZL184 is not as efficient for rats as it is for mice and humans [94]. It shows 10-fold lower activity against rat MAGL compared to those of human and mouse (Figure 1.23A) [87]. Lower potency of JZL184 against rat MAGL was also confirmed by in vitro competitive ABPP analysis of mouse and rat brain membranes (Figure 1.23B and C) [87]. JZL184 also seems to display a similar decline in activity against rat FAAH. (Figure 1.23C). Additionally, it displays equal potency against rat and mouse ABHD6 (Figure 1.23C), another 2-AG hydrolase present in the brain [87].

Rodent studies have demonstrated that dual inhibition of FAAH and MAGL causes psychotropic effects that are similar to the activity of direct cannabinoid agonists, hence, obstructs specifying biological actions of 2-AG from AEA and other N-acylethanolamines. Therefore, a robust selectivity for MAGL over FAAH and reduced cross-reactivity with other endocannabinoid-degrading enzymes is of great importance for a MAGL inhibitor [94] [95].

Short while ago, a different class of O-hexafluoroisopropyl (HFIP) carbamates, which are enhanced MAGL inhibitors, was developed. HFIP carbamates seems to accomplish their potency and selectivity for MAGL, at least partly, because of the bioisosteric nature of their leaving group which is similar to the glycerol of 2-AG (Figure 1.24.). Of those, KML29, which inhibits MAGL both in vitro and in vivo with outstanding potency and remarkably enhanced selectivity with no detectable cross-reactivity with FAAH and lower cross-reactivity with peripheral carboxyesterases, seems to be a promising inhibitor (Figure 1.25., 1.26.) [94]. In addition, KML29 displays better potency and selectivity for rat MAGL compared to JZL184 (Figure 1.27A and Table 1.1). IC_{50} value of KML29 for inhibiting rat MAGL was found 43 nM, which is nearly three-fold of its potency for mouse MAGL (IC_{50} = 15 nM). It also retained a good selectivity compared to rat FAAH (no detectable cross-reactivity) and ABHD6 (> 20-fold selectivity) (Table 1.1) and did not show any detectable off-target inhibition of other brain serine hydrolases (Figure 1.27B) [94].

It was shown that KML29 could also inhibit rat MAGL in vivo. Wistar rats administered KML29 (1–40 mg kg^{-1}, ip) or vehicle were sacrified after 4 hours and their brain tissue examined with competitive ABPP. The brain tissues of rats elucidated dose-dependent inhibition of MAGL without any detectable cross-reactivity with FAAH or ABHD6 (Figure 1.27C). KML29 inhibited > 90% of rat brain MAGL at 40 mg kg^{-1} ip and escalated brain 2-AG levels 10-fold without altering anandamide levels [94].

Rat brain lipid analysis, consistent with competitive ABPP results , demonstrated nearly 10-fold escalation in 2-AG level and decrease in endogenous free AA level proportional with the escalation in 2-AG (Figure 1.28A) . On the contrary, there were no alterations in AEA, PEA (N-palmitoylethanolamine), or OEA (N-oleoylethanolamine) levels (Figure 1.28B). In addition, 2-AG hydrolytic activity was declined by 50% at 20 mg kg^{-1} and 80% at 40 mg kg^{-1} doses of KML29 (Figure 1.28C). The remaining 20% 2-AG hydrolytic activity at 40 mg kg^{-1} is probably due to ABHD6 and ABHD12 activity since these enzymes were not inhibited by KML29 in vivo. On the other hand, brain AEA hydrolytic activity was not altered at any dose of KML29 Figure 1.28C) [94].

Moreover, even when KML29 administered chronically (6 days, 40 mg kg^{-1}, po), it displayed a comprehensive selectivity against FAAH [94].

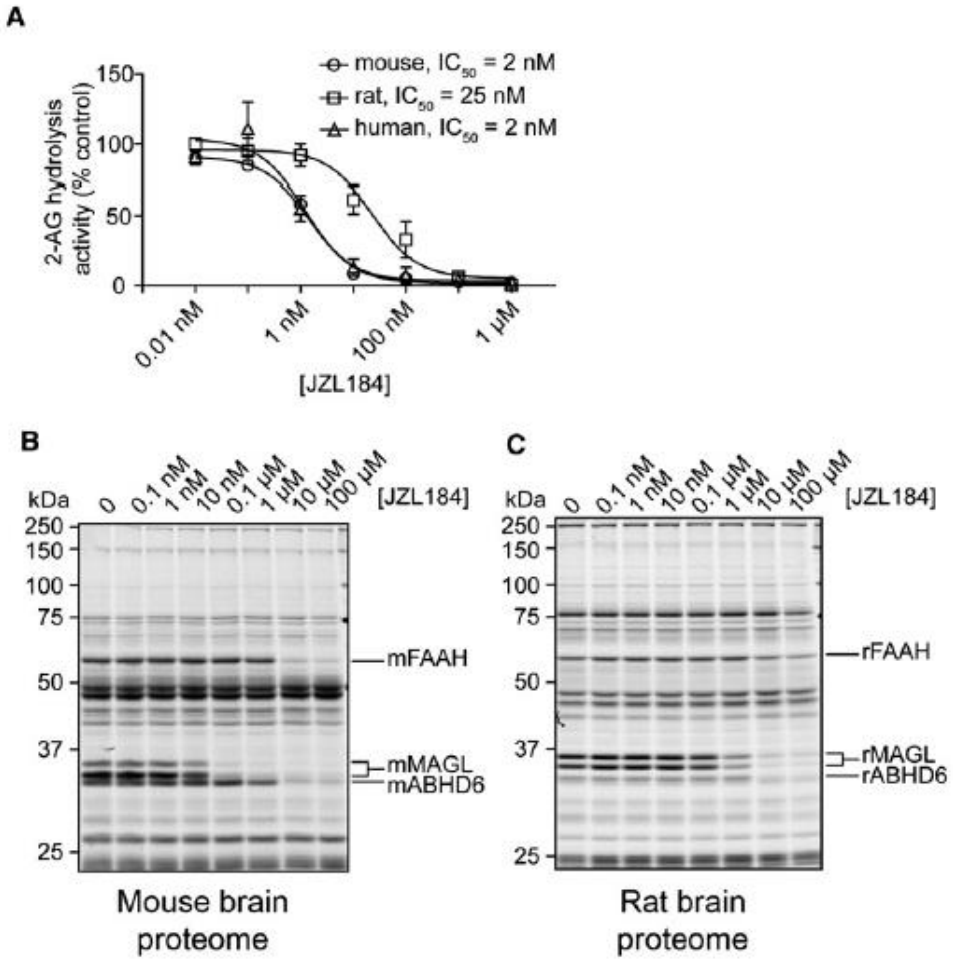

Figure 1.23. Characterization of JZL184 Inhibition of Mouse, Rat, and Human MAGL (Adapted from [87]) **A)** Blockade of recombinant MAGL orthologs by JZL184 (Data are presented as mean ± SEM of three independent experiments); **B)** and **C)** Competitive ABPP showing the effect of JZL184 on serine hydrolase activities in the mouse (B) and rat (C) brain membrane proteomes. For A–C, JZL184 was incubated with cell/tissue lysates (30 min, 37 ^{0}C) at the indicated concentrations, followed by addition of 2-AG (100 mM, 5 min, room temperature) (A) or FP-rhodamine (1 mM, 30 min, room temperature) (B and C). For B and C, control proteomes were treated with DMSO alone (mouse and rat brain MAGL migrates as a 33 and 35 kDa doublet by SDSPAGE) (Adapted from [87]).

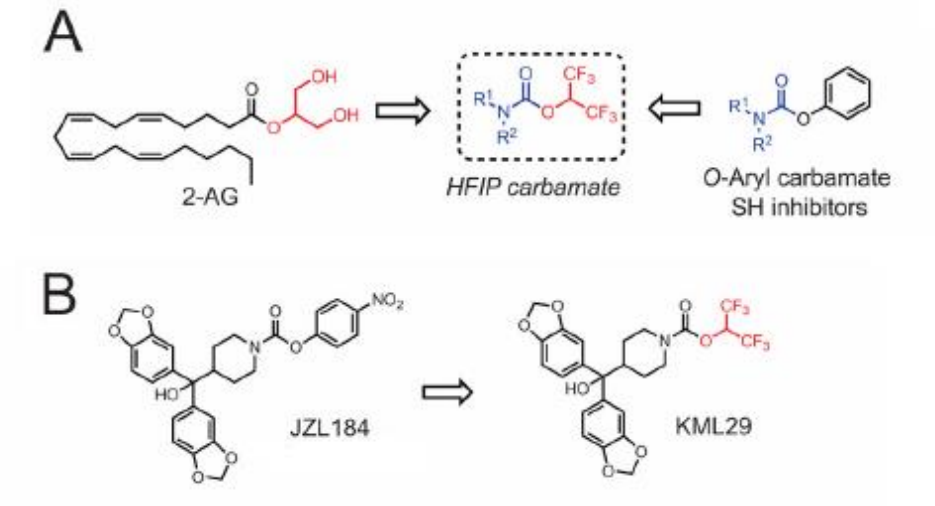

Figure 1.24. HFIP carbamates as MAGL inhibitors (Adapted from [94]).
A) The bioisosteric nature of the HFIP group compared to the glycerol head group of MAGL substrate 2-AG; **B)** KML29, HFIP carbamate analogue of JZL184 (Adapted from [94]).

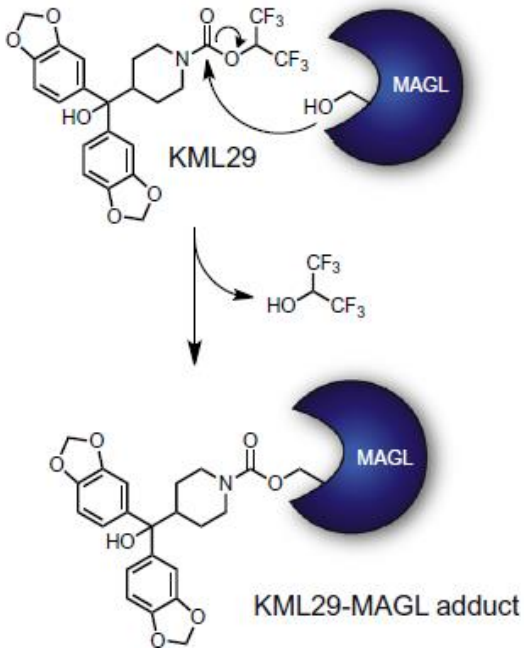

Figure 1.25. Proposed mechanism of MAGL inactivation by KML29 [94].The catalytic serine (Ser122) of MAGL attacks the activated carbamate of KML29, releasing hexafluoroisopropanol and forming a stable, carbamylated KML29-MAGL covalent adduct.

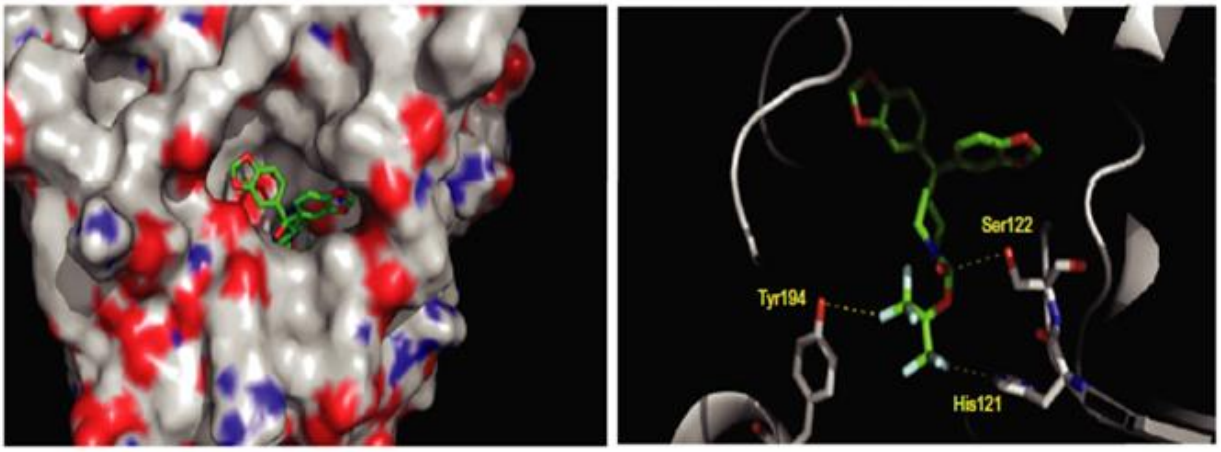

Figure 1.26. KML29-mediated inactivation of MAGL (Adapted from [94]).

Proposed docking mode of KML29 to MAGL illustrated in views of the whole protein (left image) and the active site (right image). When the catalytic Ser122 is positioned for nucleophilic attack at the carbonyl of KML29, His121 and Tyr194, which are predicted to interact with 2-AG's head group, show potentially favorable interactions with the KML29's HFIP leaving group. (RosettaLigand 3.3 (http://www.ncbi.nlm.nih.gov/pubmed/19041878) was used to perform the docking, and the MAGL structure used for docking was 3JWE from the Protein Data Bank) (Adapted from [94]).

Table 1.1. IC_{50} values for JZL184 and KML29 against mouse, rat, and human orthologs of MAGL, FAAH, and ABHD6 (Adapted from [94]).

Inhibitor IC_{50} (nM)		
	JZL184	**KML29**
MOUSE		
MAGL	10[a]	15(11-21)
FAAH	4,690[a]	>50,000
ABHD6	3,270[a]	4,870 (4,120-5,760)
RAT		
MAGL	262 (188-363)	43(36-52)
FAAH	3,570(2,540-5,020)	>50,000
ABHD6	2,940(1,441-6,010)	1,600(1,260-2,040)
HUMAN		
MAGL	3.9(1.8-8.1)	5.9(4.0-9.9)
FAAH	>50,000	>50,000

Serine hydrolase inhibition was measured by competitive ABPP where reductions in FP-Rh labeling of MAGL, ABHD6, and FAAH were quantified following preincubation of proteomic samples with the indicated inhibitor. Brain membrane proteomes were used to measure inhibition of mouse and rat enzymes, whereas human enzymes were evaluated from proteomes of transiently transfected HEK293T cells. IC50 values are reported as the mean from three independent experiments. The 95% confidence intervals are listed in the parentheses ([a] Previously determined [96] IC_{50} values) (Adapted from [94]).

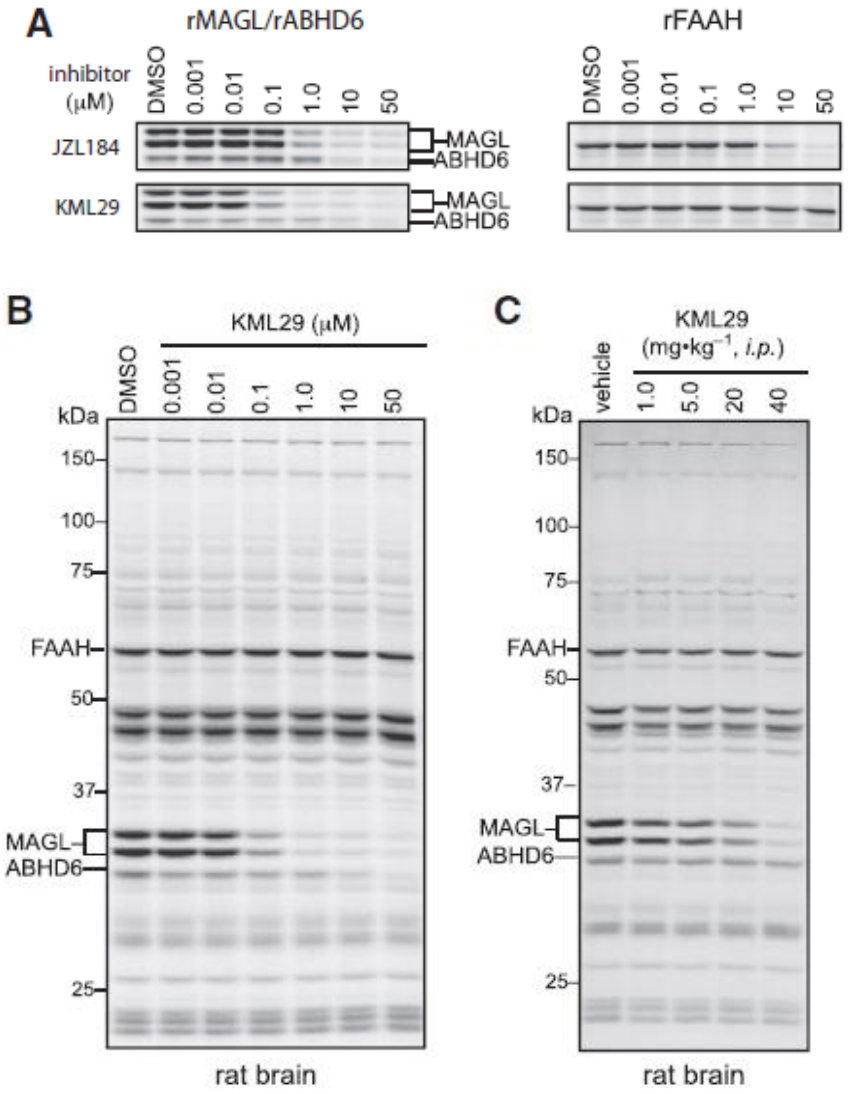

Figure 1.27. Inhibition of rat MAGL enzyme by KML29 (Adapted from [94]). **A)** Competitive ABPP gels comparing the potency and selectivity of JZL184 and KML29, against MAGL, ABHD6, and FAAH in rat brain proteomes. **B)** Full competitive ABPP gel showing KML29 activity against rat brain serine hydrolase activities, which revealed selective inhibition of MAGL at inhibitor concentrations of 1 mM or less and inhibition of ABHD6 at concentrations >1 mM. No inhibition of FAAH was detected at any tested concentration of KML29. **C)** Competitive ABPP gel of brain serine hydrolase activities from rats treated with KML29 (1–40 mg kg^{-1}, ip) for 4 hr. (Data are presented as mean ± SEM (n = 3 rats per group). *p < 0.05; **p < 0.01; ***p < 0.001 for vehicle-treated versus inhibitor-treated rats).

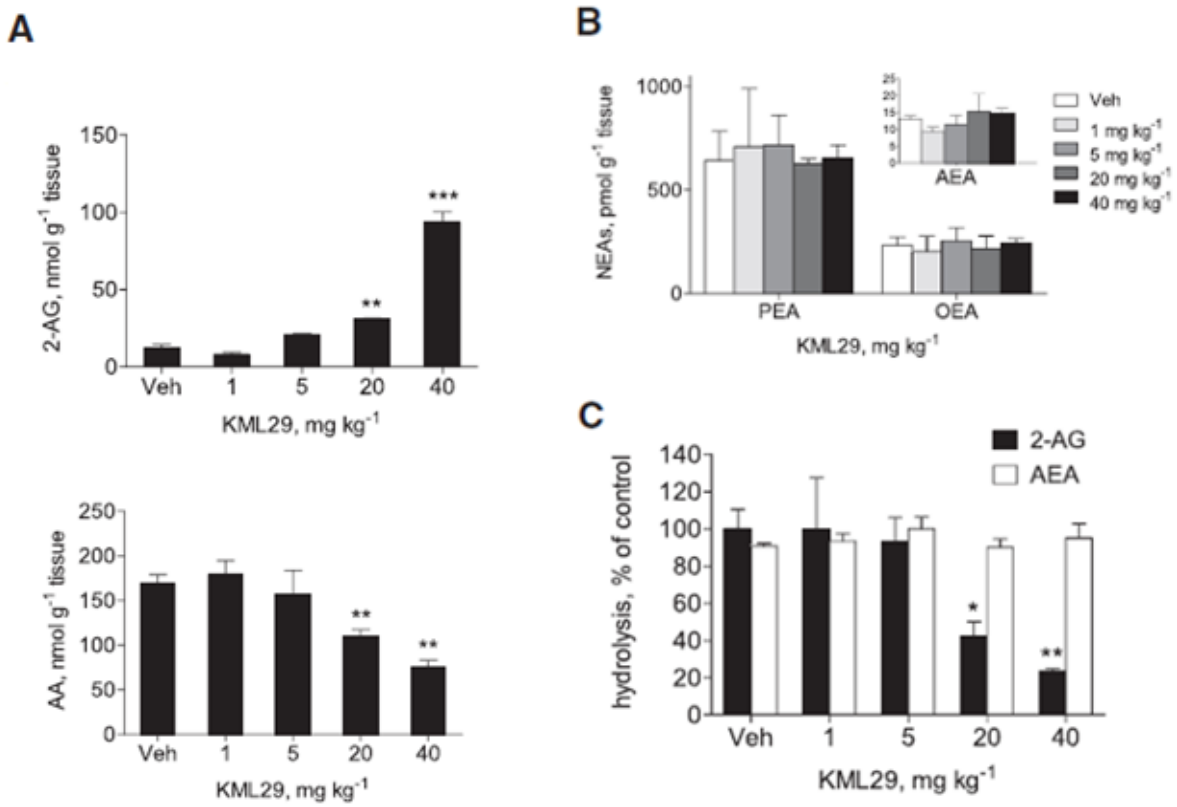

Figure 1.28. Rat brain lipid profiles of 2-AG, AA, AEA, PEA (N-palmitoylethanolamine) and OEA (N-oleoylethanolamine) treated with KML29 (Adapted from [94]).

A) Brain lipid profile of 2-AG and AA from rats treated with KML29 (1–40 mg kg^{-1}, ip). **B)** Brain lipid profile of AEA, PEA and OEA from rats treated with KML29 (1–40 mg kg^{-1}, ip) **C)** Brain MAGL and FAAH activity from rats treated with KML29 (1–40 mg kg^{-1}, ip) as measured by 2-AG and AEA hydrolysis, respectively. (Data are presented as mean ± SEM (n = 3 rats per group). *$p < 0.05$; **$p < 0.01$; ***$p < 0.001$ for vehicle-treated versus inhibitor-treated rats) (Adapted from [94]).

Additionally, in vivo characterization of KML29 in mice revealed that acute administration of the compound caused significant increase in 2-AG and decrease in AA levels of brain, respectively. Besides, KML 29 generated anti-allodynic and anti-oedematous effects in carrageenan model of inflammatory pain and partially blocked mechanical and cold allodynia in chronic constriction (sciatic nerve) injury model of neuropathic pain [112].

These data altogether suggest that KML 29 is a selective and in-vivo active probe in order to examine MAGL and 2-AG functions in rat brain, which has not been thoroughly accomplished by previously developed MAGL inhibitors [94].

1.8 Chemical Structure of Lipopolysaccharide (LPS) and Its Mechanism of Action

1.8.1 Chemical Structure of Lipopolysaccharide (LPS)

Lipopolysaccharide (LPS) is a structural entity of the outer wall of cell membrane of Gram-negative bacteria. LPS is one of the best known Pathogen-associated molecular patterns (PAMPs), which has the potency to stimulate immune system [6]. PAMPs are structural motifs present in whole group of pathogens; bacteria, viruses and fungi.

Bacterial LPS comprises three parts: a hydrophobic domain called Lipid A (or endotoxin), a core oligosaccharide and an O-antigen (a distal polysaccharide) [7]. Of those, Lipid A (or endotoxin) is the predominant PAMP of LPS.

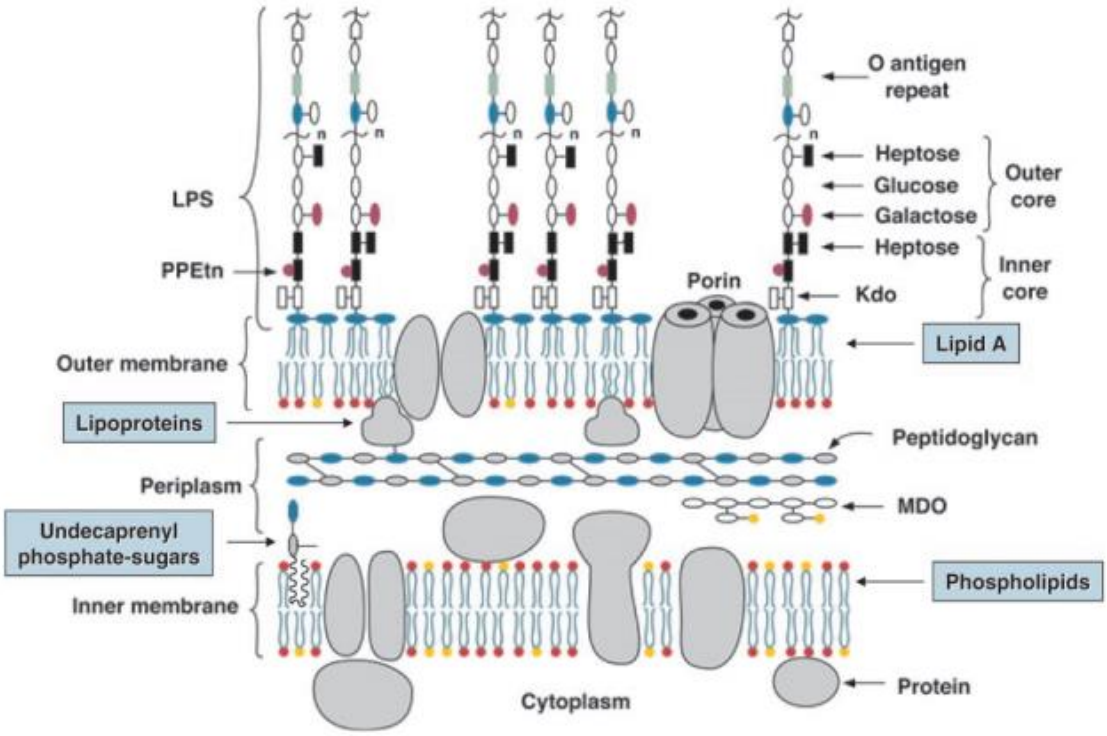

Figure 1.29. Model of the inner and outer membranes of *E. coli* K-12 [7].

1.8.2 Lipopolysaccharide (LPS) and Toll-Like Receptors (TLRs)

Host cells utilize a process known as "pattern recognition" in order to detect pathogens. PAMPs are the molecular patterns (motifs) unique to pathogens recognized by host receptors [8].

Pathogens are mainly recognized by host cells with the stimulation of Toll-like receptors (TLRs), members of the pro-inflammatory interleukin-1 receptor (IL-1R) family [20], through their PAMPs. The mammalian Toll-like receptors are germ-line encoded receptors [6] that are present in both immune cells such as macrophages, neutrophils, dendritic cells and non-immune cells such as neurons, astrocytes, fibroblasts and epithelial cells [10]. They are typical single-pass type I transmembrane-spanning proteins [10]. They comprise many extracellular leucine-rich repeats that recognize pathogens and TIR domains (Toll/IL-1R/plant R gene homology domains) in the

transmembrane and intracellular parts that trigger intracellular signaling [11]. In humans and mice there are 13 paralogous TLRs in total; humans have 10 and mice have 12 types of TLRs stimulated by different kinds of PAMPs [10].

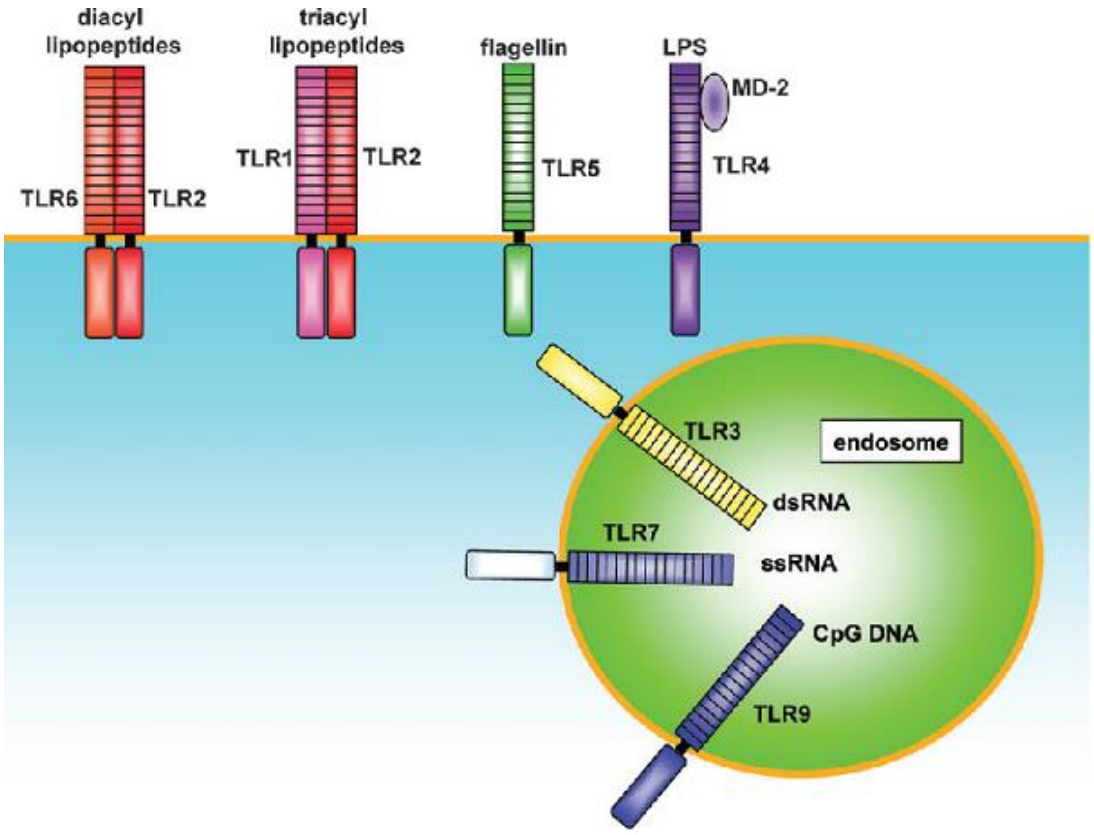

Figure 1.30. TLRs and their ligands [9].

Lipopolysaccaride stimulates TLR4 (Toll-like receptor 4) by the help of various auxillary proteins such as LBP (lipopolysaccharide binding protein), CD14 (cluster of differentiation 14) and a co-receptor known as MD2 (Myeloid Differentiation Protein-2) [11] [12].

1.8.3. Toll-Like Receptor 4 (TLR4) Signaling

TLRs are critical in order to initiate an innate immune response, one of which is inflammation, and they are considered as a bridge between innate and adaptive immunity [13].

TLR4 signalling proceeds in two distinct pathways, MyD88 (Myeloid differentiation primary response gene 88)-dependent and MyD88-independent (TRIF (TIR-domain-containing adaptor-inducing interferon-β) dependent) pathways. Expression of proinflammatory cytokines is acquired by the MyD88-dependent pathway, on the other hand Type I interferons and expression of interferon-inducible genes are acquired by the MyD88-independent pathway [6].

TLR4 signaling cascade is initiated by LPS stimulation of the receptor. Soluble protein MD-2 interacts non-covalently with TLR4 but can directly interact with LPS. Soluble shuttle protein LBP directly binds to LPS and eases its interaction with CD14 which is a soluble glycosyl phosphatidylinositol-anchored protein. Since CD14 assists LPS being transferred toTLR4/MD-2 receptor complex, it is essential in LPS recognition, hence TLR4 stimulation. Consequent to LPS detection, TLR4 go through oligomerization and utilize its downstream adaptors via interplay between TIR domains present in both TLR4 and adaptor proteins. These domains give rise to protein-protein interactions enabling signal transduction [6].

TLR4 signal transduction comprise five TIR-domain containing adaptor proteins [14]. Of those, TRAM (TRIF-related adaptor molecule) and TRIF are elements of MyD88-independent pathway [6]. TRAM integrates to the plasma membrane via myristoylation [16] and associates with TRIF, a vital adaptor protein, which leads to the stimulation of transcription factor IRF3 (Interferon Regulatory Factor 3) [17][18],and the late-phase stimulation of NF-κB (Nuclear factor kappa-light-chain-enhancer of activated B cells) and Mitogen-activated protein kinase [19]. As a result, various gene expressions, such as the Interferon β and Interferon -inducible genes are stimulated [18] leading production of Type I interferons [6]. TRIF is negatively regulated by another adaptor protein, namely sterile α and HEAT-Armadillo motifs-containing protein [14].

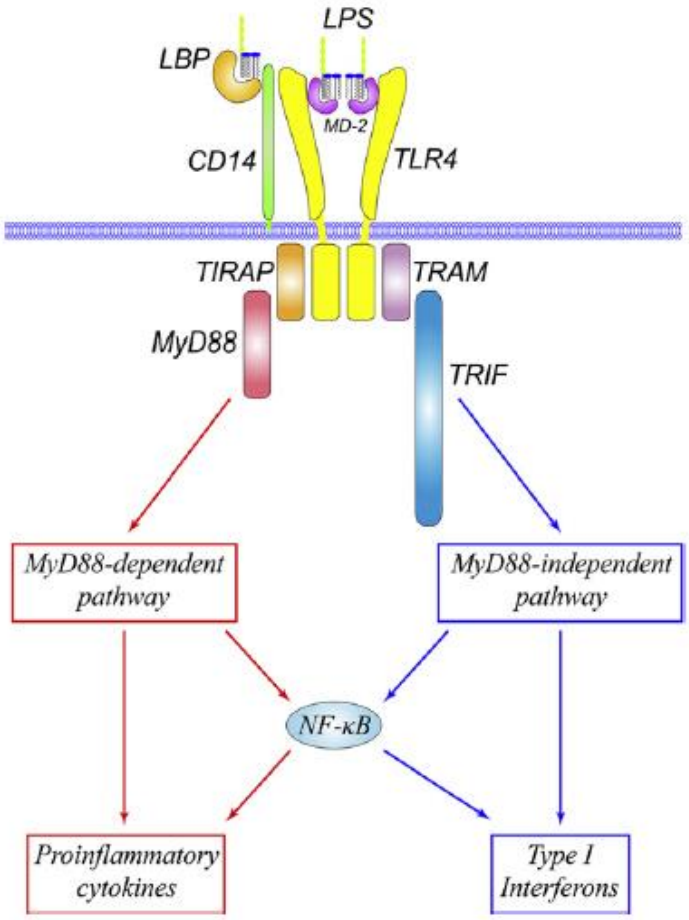

Figure 1.31. TLR4 signalling [6].

MyD88-dependent pathway, on the other hand, utilize TIRAP (MAL) (TIR domain-containing adaptor protein, MyD88-adapter-like) and MyD88 for signaling. TIRAP have a phosphatidylinositol 4,5-bisphosphate (PIP2) moiety which enables integration to the plasma membrane. Upon integration, TIRAP interacts with MyD88 and the cytoplasmic part of TLR4 leading MyD88-dependent downstream signaling [15]. Successively, MyD88 stimulates IRAK4 (IL-1 receptor-associated kinase-4), an essential protein kinase for emitting TLR signals [20]. IRAK4 utilize IRAK1 (serine-threonine kinase IL-1 receptor-associated kinase 1) and another homologous proteins in order to transmit

signals to TRAF6 (TNF receptor associated factor 6) which is also a vital adaptor protein [20].

TRAF 6, then, stimulates TAK1 (transforming growth factor-β-activated kinase 1) and TAK1 stimulates downstream IKKs (IκB (inhibitor of kappa light chain gene enhancer in B cells) kinase) and MAPK pathways whose stimulation induce another transcription factor known as AP-1 (Activator Protein 1) [6][21].

When IκB is phosphorylated by IKK complex, degradation of IκB and translocation of transcription factor NF-κB to gene promoter sites occurs respectively. NF-κB, then alters the expression of proinflammatory cytokines and further immune related genes [22].

Besides these transcription factors, IκBζ and IRF5 (interferon regulatory factor 5) are also essential factors present in MyD88-dependent pathway. IRF5 interacts with MyD88 and stimulates expression of proinflammatory cytokine genes [6].

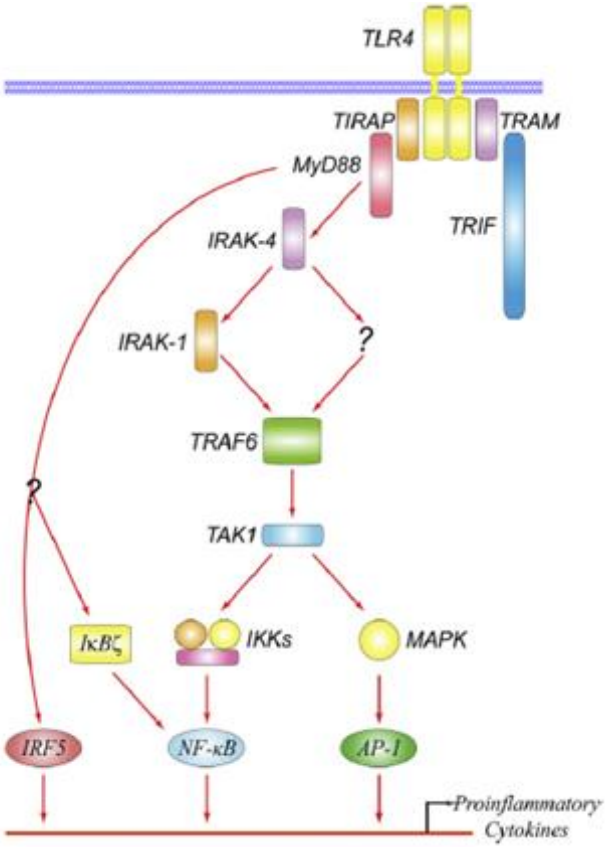

Figure 1.32. The MyD88-dependent pathway [6].

1.8.4 Induction of Inflammation by TLR Signalling

Systemic inflammation is initiated by the stimulation of cells utilized in innate immune system such as macrophages and neutrophils. When ligands such as LPS bind to TLRs of macrophages, they cause production of proinflammatory cytokines such as TNF-α (tumor necrosis factor-α), IL-1 (interleukin-1) and IL-6 (interleukin-6), production of reactive oxygen species and antimicrobial peptides and phagocytosis of microbes [10].

Upon releasing, cytokines bind to their particular cell-surface receptors on neutrophils, endothelial cells, perivascular cells of the brain and other cells of the host, which evoke complex cellular reactions. When activated macrophages release proinflammatory cytokines adjacent to infection site, released proinflammatory cytokines boost the permeability of the vascular endothelium, hence tendency of neutrophils to bind to the microvascular endothelial surface and to penetrate into plasma. Upon activation by cytokines, endothelial cells of brain vasculature [24], perivascular microglia [25], and penetrated neutrophils produce antimicrobial peptides, reactive oxygen species such as H_2O_2 and superoxide anion and lipid mediators of inflammation [10].

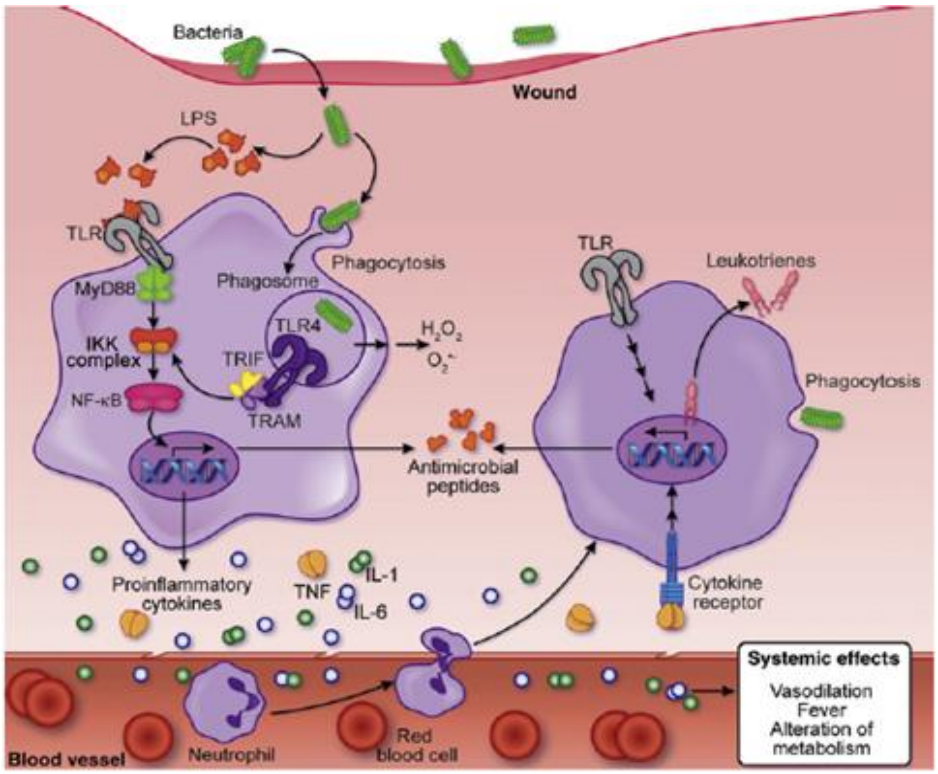

Figure 1.33. Induction of inflammation by TLR signalling [10].

As well as their impacts on infection site, cytokines have impacts throughout the body. By traveling in blood stream, they induce systemic effects such as fever, vasodilation, disrupting the effect of insulin and boosting catabolic states [10].

1.9 Production of Prostaglandins and Fever in Systemic inflammation

1.9.1 Prostaglandins as the Connection Between Systemic Inflammation and Central Nervous System (CNS)

The most important requirement in order to convert immune stimuli into central nervous system responses is the synthesis of prostaglandins [25].

When peripheral proinflammatory cytokines reach the brain, these upstream signaling molecules are transformed into downstream mediators, namely prostaglandins [26].

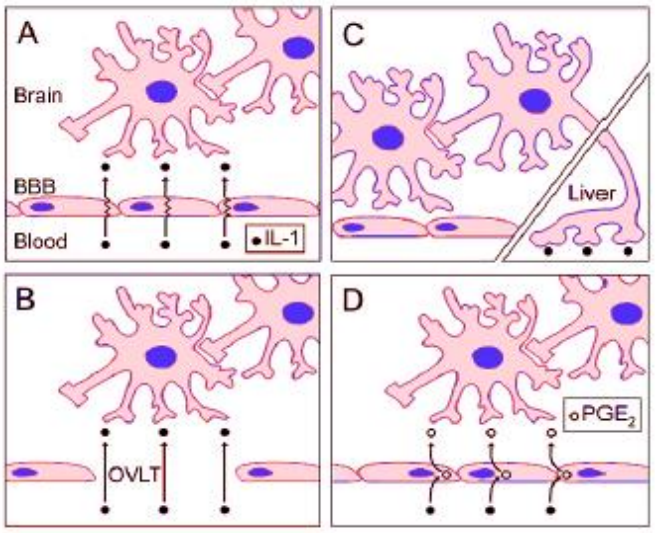

Figure 1.34. Schematic representation of four major mechanisms through which peripheral proinflammatory molecules reach the brain [26]. (A) saturable transport across the blood-brain barrier (BBB); (B) entry through the *organum vasculosum* of the *lamina terminalis* (OVLT); (C) signal transduction by sensory nerves, primarily the hepatic vagus; (D) synthesis of prostaglandin E_2 (PGE_2) in cells forming the BBB [26].

Four prevailing mechanisms through which peripheral proinflammatory molecules reach the brain has been suggested:

1) Saturable transendothelial transport; 2) Passage through the OVLT (*organum vasculosum* of the *lamina terminalis*) and the other circumventricular organs; 3) Signal transduction through sensory nerves, mainly the nervus vagus; 4) Prostaglandin production in cells which shape the BBB (Figure 1.34.) [26].

According to the first theory, peripheral cytokines have the ability to pass the BBB by carrier transport [28]. However, there have been a deviation from this theory due to studies revealed that these molecules can pass brain tissue by diffusion through basal laminae [29].

Second theory states that cytokines pass the brain via the circumventricular organs, mainly the OVLT. Since, contrary to other parts of brain vasculature, circumventricular organs have fenestrated capillaries that form leaky BBB areas [30].

Third theory suggests that pyrogens that stimulate neural terminals in peripheral tissues transform thermogenic signals into the CNS through vagal sensory fibers [31]. According to this theory, products of liver macrophages stimulates subdiaphragmatic vagal sensory afferent fibers and these inputs could be conveyed to brain via noradrenergic pathways [32][33].

Second and third theories which have associated febrile responsiveness with neural structures generally utilized lesioning of the corresponding structures [31].

In order to study vagus nerve, surgical or chemical vagotomy and for the OVLT, electrolytic, surgical or thermal ablation were utilized. However, there are controversies about those techniques used, in that, neural lesions not only have the ability to hinder signaling along the related route, but also cause unwanted side effects that alter reaction of interest (febrinergic reactions). Bilateral truncal vagotomy can be given as an example to this situation. This procedure declines fever stimulated through low doses of LPS as well as leading to malnourishment, if the animals are not kept on a liquid diet postoperatively. Malnourishment itself attenuates fever. Thus, it should be taken into consideration that vagotomized animals have declined febrinergic reactions even in the absence of malnourishment [31].

The last and most predominant theory suggests that Blood Brain Barrier itself acts as signal transducer, that is an area responsible for conversion of a signaling molecule to a different one, rather than being a prohibiting barrier [26].

Studies has revealed that endothelial and perivascular cells of the BBB stimulate production of Prostaglandin E_2 (PGE_2) synthesizing enzymes upon peripheral administration of pyrogens such as LPS, IL-1β, or TNF-α [34][35]. The PGE_2 synthesized by endothelial and perivascular cells of the BBB can easily reach neurons of circuitries responsible for thermogenesis, leading to fever [26]. There was controversies about which of these cells are involved in production of PGE_2 until recently. However, studies revealed that both endothelial and perivascular cells of the BBB are involved in this signal transduction [35] and the extent of their involvement rely on nature of pyrogens and their dose [36] [37].

1.9.2 Prostaglandin E_2 (PGE_2): Mediator of Fever

The experiments which were conducted in order to reveal which type of prostaglandin is the predominant mediator of fever revealed that mainly E series of them involved in thermogenesis [38] and aspirin-like drugs inhibit prostaglandin synthesis [39], hence alter fever. However, because of lack of precise techniques, types of prostaglandins that predominantly stimulates fever remained unclear until gene knockout models and pharmacological studies utilized together [26]. It was found that prostaglandin E_2 (PGE_2) is the dominating isoform of PGE in the brain and fundamental for stimulating fever [40] [41].

The studies about prostaglandin E receptors (EPs) [42][43] and prostaglandin synthesizing enzymes [44][45] determined that PGE_2 has a principal role in induction of three facets of polyphasic LPS fever [26].

1.9.3 Synthesis of Prostaglandin E_2 (PGE_2)

Prostanoids are a class of 20-carbon unsaturated fatty acid by-products synthesized through a cascade of intricate enzymatic reaction [27]. Liberation of unsatured fatty acid arachidonic acid (AA) from membrane phospholipids, mainly by phospholipase A_2 activity, is the first step for the synthesis of prostanoids. By the activity of cyclooxygenases (prostaglandin G/H synthases) molecular oxygen is added to AA, producing Prostaglandin G_2. Then, subsequent peroxidase activity of cyclooxygenases transforms Prostaglandin G_2 into Prostaglandin H_2. Prostaglandin G_2 and Prostaglandin H_2 are also called cycloendoperoxides and they are chemically unstable. These unstable molecules are converted to more stable molecules within a half life of thirty seconds to a few minutes [1][23][27].

Prostaglandin H_2 is immediate precursor of all prostanoids (prostaglandins, prostacyclins and thromboxanes). When it is generated, Prostaglandin H_2 is transformed into corresponding prostanid by tissue specific synthases. Prostanoids bind to their cognate receptor and display a wide variety of actions. Their large variety of actions result from the discrete types of tissue-specific synthases and receptors. Prostanoids act locally, just

in the close vicinity to the production area, that is they are autocrine and paracrine mediators [27].

The PGE_2 production cascade, like other prostanoids, comprises three enzymes; phospholipase A_2 (PLA_2), Cyclooxygenases (COX) and corresponding synthase, namely PGE synthase (PGES) [26].

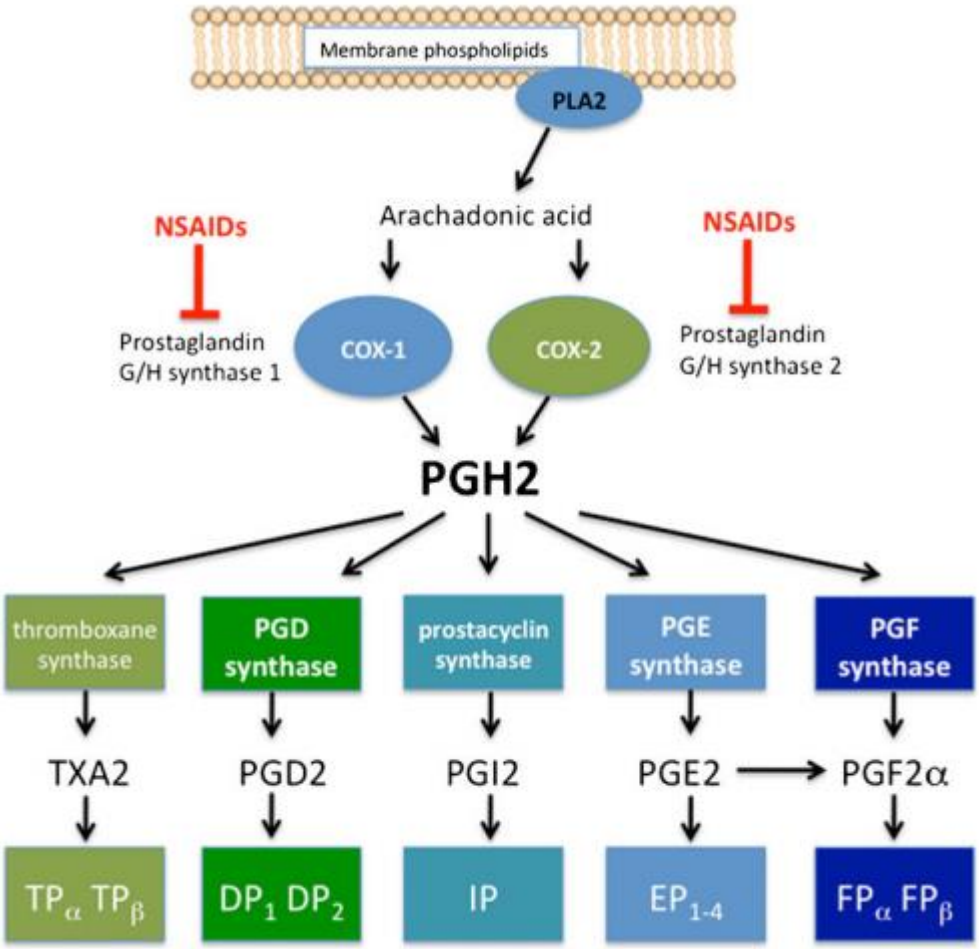

Figure 1.35. Prostanoid synthesis and action [23].

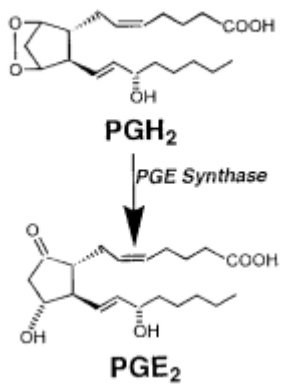

Figure 1.36. PGE synthase activity (Adapted from [46]).

It is accepted that there are two types of synthesis route of prostaglandin E_2 (PGE_2) catalyzed by distinct subsets of enzymes: moderate physiological and fast inflammatory. The inflammatory one mainly utilizes cytosolic PLA_2 ($cPLA_{2\text{-}\alpha}$) and diverse isoenzymes of secretory PLA_2 ($sPLA_2$); inducible COX, namely COX-2; and microsomal PGES 1 (mPGES-1) [26][48].

In vitro studies showed that the inducible isoforms of $sPLA_2$, COX-2 and mPGES-1 are not just co-induced by pyrogens, but also are functionally coupled to channel arachidonic acid through the PGE_2-synthesizing cascade. This kind of coupling account for the superior production of PGE_2 over other prostanoids in case of fever. Gene knockouts studies also revealed the fundamental role of COX-2 and mPGES-1 in LPS fever [26].

LPS and proinflammatory cytokines induce *de-novo* synthesis of these isoenzymes. As a consequence of LPS injection in rats, a burst of transcriptional co-expression of inflammatory enzyme isoforms occurs in three phases of polyphasic fever both in peripheral organs and in the brain [26][47].

Fever is a potent defensive measure started out by brain upon a systemic inflammatory insult by pyrogenic agents such as LPS, IL-1β, TNF-α [48]. Subsequent to the

recognition of microbial or non-microbial agents as extrinsic ones by immune cells, a multi-mediated reaction that integrates intricate physiological defence strategy of the host, that is fever, is launched [49].

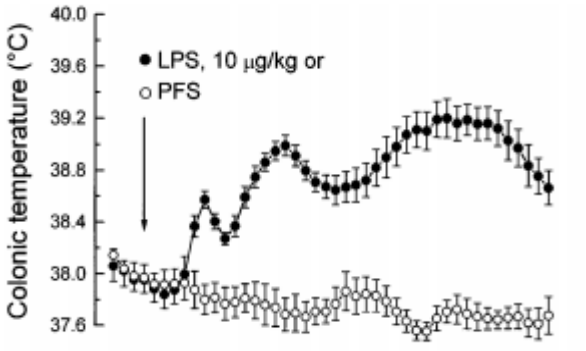

Figure 1.37. An example of fever response of Wistar rats to injection (arrow) of *Escherichia coli* 0111:B4 lipopolysaccharide (LPS; phenol extract, 10μg/kg iv) in pyrogen-free saline (PFS) and to PFS (1 ml/kg iv) [50].

A single dose of LPS injection leads to various successive increases in body temperature. Each of these increases is named "a febrile phase" and acquires different thermoregulatory mechanisms. Clinical and experimental fevers are usually polyphasic [48]. Fever inducted by LPS in rats and mice have at least three phases (*Phases 1-3*) each of which acquires *de-novo* PGE_2 synthesis, the major downstream mediator of LPS fever. The fundamental mechanism in order to initiate the activation of PGE_2-synthesizing enzymes is transcriptional upregulation [47][48].

LPS fever coincides with up-regulation of four of PGE_2-synthesizing enzymes, namely $sPLA_{2}$-IIA, $cPLA_{2-\alpha}$, COX-2, mPGES-1 and down-regulation of all PGE_2 carriers and dehydrogenases [48].

1.9.4 Prostaglandin E_2 Receptors and Their Mechanism of Action in Fever

1.9.4.1 Prostaglandin E_2 Receptors

E type Prostaglandin (EP) receptors have four subtypes: EP_1, EP_2, EP_3, and EP_4,each of which bind selectively to PGE_2[41][53].

EP receptors, members of G-protein-coupled receptors (GPCRs) (seven-transmembrane domain receptors), have mutual extracellular and membrane-spanning moieties but distinct intracellular and carboxy-terminal domains. Each receptor interacts with a specific G-protein, hence a specific second messenger system [53].

Signallings of EP subtypes have been revealed by studies utilized agonist-induced alterations in second messengers such as cAMP, Ca^{2+}, inositol phosphates and in the activity of downstream kinases. In consequence of these studies, it has been inferred that the EP_1 receptor operates through escalation in the free Ca^{2+} concentration. This escalation rely upon extracellular Ca^{2+} and takes place without detectable phosphatidylinositide response, proposing that EP_1 controls Ca^{2+} channels through an unknown G protein [52]. The EP_2 and EP_4 receptors, on the other hand, are associated with G_s and operate by elevation of cAMP. The EP_3 receptor comprise three isoforms that are produced through alternative splicing of the C-terminal tail and the fundamental signalling pathway for them is the inhibition of cAMP by G_i. However, EP receptors generally interact with more than one G protein and signal transduction pathway (Table 1.2.) [52].

Table 1.2. Signal transduction properties of EP receptor subtypes and EP_3 isoforms [52].

(Data obtained from mouse EP subtypes. PI3K, phosphatidylinositol 3-kinase; Rho, Rho family of small G proteins ;↑, increase; ↓, decrease) Adapted from [52].

Subtype	Isoform	Amino acid	G Protein	Signalling
EP_2		362	G_s	cAMP↑
EP_4		513	G_s (G_i)	cAMP↑, PI3K
EP_1		405	Unknown	Ca^{2+} ↑
EP_3	**$EP_{3\alpha}$**	366	G_i,G_{12}	cAMP↓, IP3/Ca^{2+} ↑, Rho
	$EP_{3\beta}$	362	G_i,G_{12}	cAMP↓, IP3/Ca^{2+} ↑, Rho
	$EP_{3\gamma}$	365	G_i ,G_s	cAMP↓, cAMP↑, IP3/Ca^{2+} ↑

1.9.4.2 Febrinergic Zones of the Brain and the Distribution of Prostaglandin E_2 (EP) Receptors Within Them.

The febrinergic zone of the brain, where PGE_2 generates fever, is located within the region of the brain that involves OVLT (*Organum vasculosum* of the *lamina terminals*) and the encircling POA (*Preoptic area* of the *hypothalamus*). The inference that PGE_2 has a vital role in febrinergic OVLT/POA region is based upon four observations: 1) At the time of febrile response to lipopolysaccharide (LPS), PGE_2 levels escalate in this region of the brain; 2) Administration of COX inhibitors that block PGE_2 synthesis to OVLT/POA region of the brain attenuates febrile response; 3) There is high density of PGE_2 binding in this region; 4) The firing rate of thermosensitive neurons within this febrinergic region is notably altered by PGE_2 [51].

Within this region, the thermogenesis effect of PGE_2 is more robust while it is administered to anteroventral region of the third ventricle, which involves the OVLT, the median preoptic nucleus (MnPO), and the ventromedial preoptic nucleus (VMPO), compared to other regions within the preoptic area (Figure 1.46.) [51].

Even though systemic inflammatory agents stimulates COX-2 and mPGES in quite nonspecific manner across the cerebral vasculature, the stimulation of neuronal activity

is restricted to specific hypothalamic nuclei. Therefore, it can be deduced that the expression of particular PGE_2 receptors within parenchymal cells in close vicinity of the production site establishes the action of the PGE_2 in the brain [27].

Despite the fact that all four subtypes of Prostaglandin E (EP) receptor mRNA's are expressesd on neurons of febrinergic zone of the brain [27], three of them, i.e. EP_1, EP_3, and EP_4, have divergently distinct distribution patterns in the rat OVLT/POA region [41].

It was determined that the meningeal strand, which helps the optic chiasm maintaining its activity, have only EP_1 receptor mRNA. EP_1 receptor mRNA is also determined in the medial part of the OVLT; the lateral part of it, however, comprises EP_4 receptor mRNA. In addition, low levels of EP_3 receptor mRNA is present in the OVLT. Both EP_3 and EP_4 receptor mRNAs are robustly expressesd in the POA's MnPO and in the border region of the medial preoptic area (MPO) and the lateral preoptic area (LPO), displaying an inverted Y-like shape. EP_4 receptor mRNA was also determined in the VMPO and the AVPV (anteroventral periventricular nucleus) nuclei although EP_3 receptor mRNA was not found in either of them. EP_1 receptor mRNA spreads widely throughout the POA [51].

Even though there are many studies suggest that the EP_3 receptor is the most critical receptor responsible for a robust fever response [42][43][55], there are also evidences suggest that EP_1 [43][55] and EP_4 [54] receptors are also needed in order to have a complete thermoregulatory respose to pyrogens.

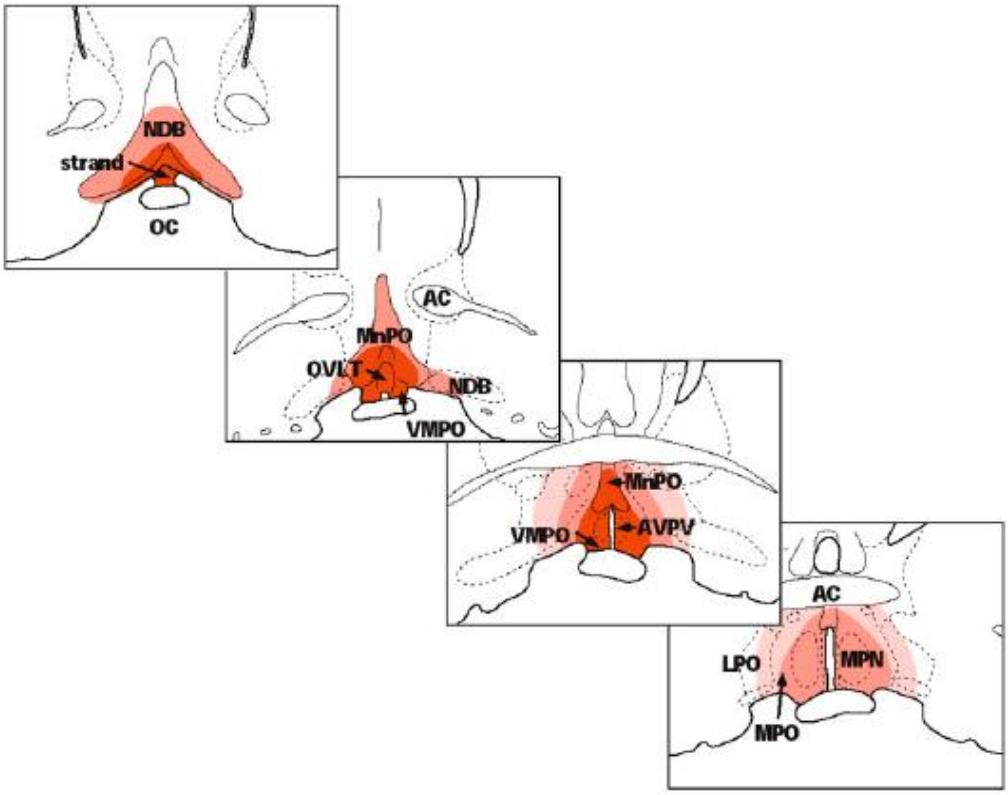

Figure 1.38. PGE_2-sensitive febrinergic zone as revealed by microinjection of PGE_1, PGE_2 and EP receptor agonists in rats [51]. Red areas represent the region where the microinjection of PGE_2 increases core temperature with darker areas representing greater increases of core temperature. (Coronal sections of the rat brain are illustrated. NDB, nucleus of the diagonal band of Broca; OC, optic chiasm; AC, anterior commissure; MnPO, median preoptic nucleus; OVLT, *organum vasculosum* of the *lamina terminalis*; VMPO, ventromedial preoptic nucleus; AVPV, anteroventral periventricular nucleus; MPN, medial preoptic nucleus; MPO, medial preoptic area; LPO lateral preoptic area) [51].

The EP_3 receptor has a number of isoforms; α and γ isoforms are strongly expressesd in the MnPO (Median preoptic nucleus) of rodents. The MnPO is the most responsive part of the brain to the pyrogenic effect of PGE_2 and the antipyretic effect of intracerebral

administration of ketorolac, a COX inhibitor, following administration of LPS. It was shown that focal elimination of EP_3 receptors in the MnPO alters fever coinciding with systemic LPS or i.c.v. (intracerebroventricular) PGE_2 administration [56].

1.9.4.3 Generation of Fever and Neural Circuitry Involved.

Body temperature, basically, shows the difference between heat production and heat loss. Body heat is produced in different tissues of the body and delivered to the skin surface by the blood in order to be emitted to the environment around the body. The thermoregulatory center, hypothalamus, regulates heat generation and loss for the purpose of maintaining the body temperature within normal range. The hypothalamus rectifies the core body temperature rather than the surface temperature. The neurons of the thermoregulatory center in the hypothalamus are thermosensitive, thus they have the ability to process input from cold and warm thermal receptors found throughout the body and produce output to make the appropriate adjustment in the body heat. The *thermostatic set point* of the thermoregulatory center is set to maintain the core temperature between the normal range (36.0 ºC - 37.5 ºC) [57].

The core temperature of the body means the temperature within the deep tissues and is kept between 36.0 ºC - 37.5 ºC under normal circumstances. Individual differences and diurnal variations is determined between this range. Core temperatures approach the lowest point in the early morning and the highest point in the late afternoon and evening [57].

The body's principal heat production source is metabolism. When an increase in body temperature is needed the sympathetic neurotransmitters epinephrine and norepinephrine are released to shift the metabolism's energy production downward and heat production upward [57].

Fever, or *pyrexia*, which is an inflammatory response, reflects an escalation in body temperature as a result of endogenous pyrogen-induced upward shift of the set point of the hypothalamic thermoregulatory center. When the set point escalates, the hypothalamus regulates physiological responses (heat production behaviours such as

shivering and vasoconstriction) so that they help the core temperature to accord with the new set point, establishing fever.

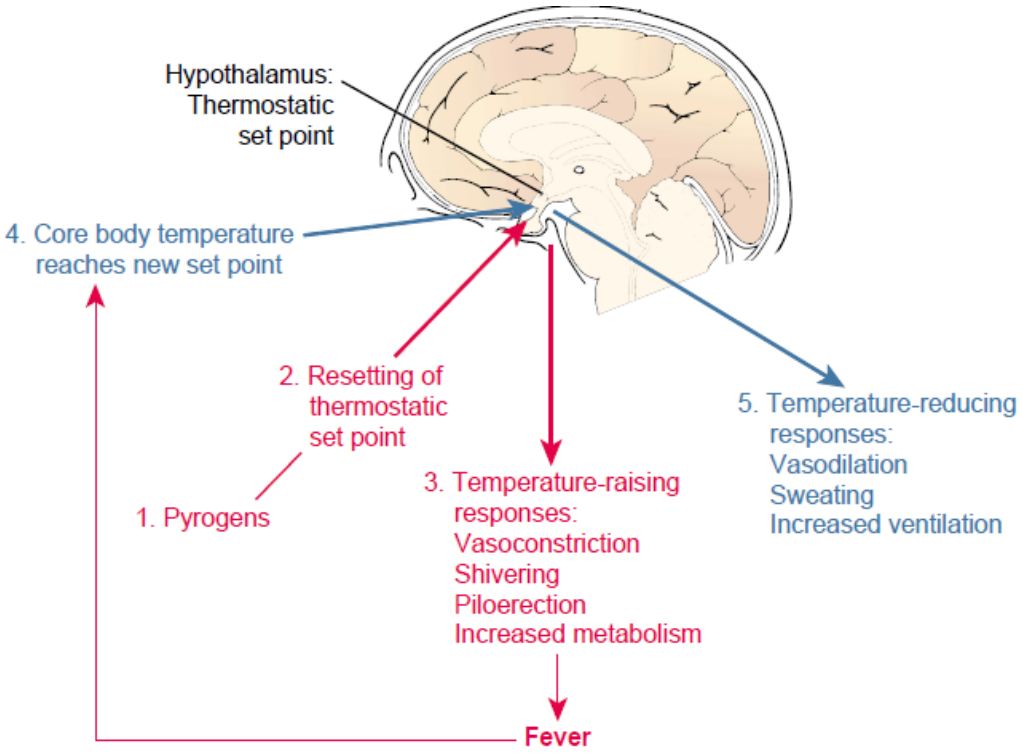

Figure 1.39. Mechanisms of fever (Adapted from [57])

1) Release of endogenous pyrogen from inflammatory cells, 2) resetting of hypothalamus thermostatic set point to a higher level (prodrome), 3) generation of hypothalamic mediated

responses that raise body temperature(chill), 4) development of fever with elevation of body to new thermostatic set point, and 5) production of temperature lowering responses (flush and defervescence) and return of body temperature to a lower level [57].

Exogenous pyrogens like lipopolysaccharide acts indirectly (through production of endogenous pyrogens such as cytokines) and therefore requires several hours to induce the rise of hypothalamic thermoregulatory set point. The endogenous pyrogens such as cytokines rise the hypothalamic thermoregulatory set point by means of prostaglandin E_2 [57].

PGE_2 is synthesized by endothelial and perivascular cells along small venules, specifically in the preoptic area. In this area it binds to EP_3R-expressing GABAergic neurons of the MnPO (median preoptic nucleus), inhibiting most of them (Figure 1.40.) [56].

Under normal circumstances, these preoptic EP_3R-expressing neurons synthesize GABA through activity of which downstream neurons of DMH (dorsomedial nucleus of the hypothalamus) and

RMR (rostral medullary raphe) that drive increase in body temperature is inhibited. Specifically,

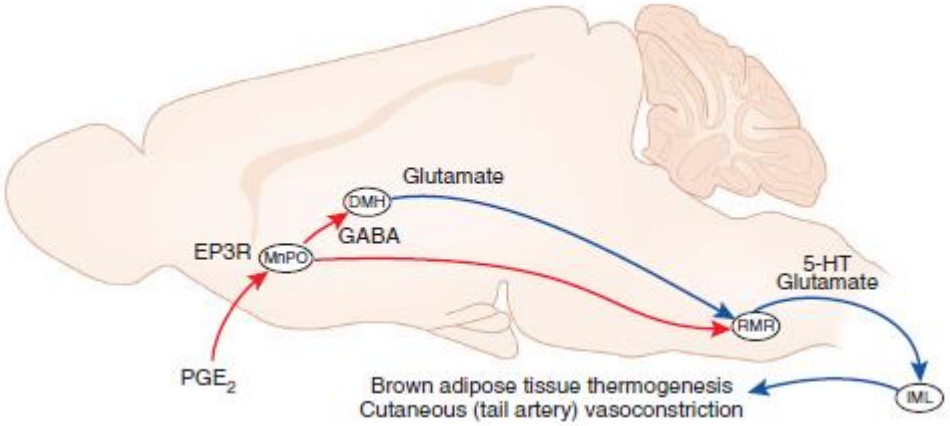

Figure 1.40. Neuronal pathways causing fever during systemic inflammation in response to PGE_2 (Adapted from [56]).

(PGE_2, Prostaglandin E_2; $EP3R$, E type Prostaglandin Receptor 3; MnPO, Median preoptic nucleus; GABA, Gamma-aminobutyric acid; DMH, Dorsomedial nucleus of the hypothalamus; RMR, Rostral medullary raphe; IML, intermediolateral column of the spinal cord. Blue arrows, excitation; Red arrows, inhibition).

the activation of α and γ EP3R isoforms inhinbit these GABAergic neuros via Gi protein–mediated inhibition of adenylate cyclase. This disinhibition leads to the activity of DMH and RMR, resulting in increase in body temperature [56].

Neurons of RMR utilize glutamate and serotonin (5-HT) to stimulate sympathetic preganglionic neurons in the IML (intermediolateral column of the spinal cord). When IML is stimulated, it activates brown adipose tissue (which rodents utilize in a cool environment) in order to produce heat and cutaneous vasoconstriction (specifically in the artery of the tail skin, which is the major means rodents utilize in a warm environment) to conserve heat. These two autonomic responses are the most fundamental ones and underlie the fever following systemic LPS or i.c.v. PGE administration [56].

Two populations of warm-sensitive (i.e., fire faster when warmed) GABAergic preoptic neurons are responsible for these responses: One of them is mainly located in the MnPO and controls tail skin vasoconstriction via projections to the RMR, stimulating sympathetic preganglionic neurons. Baseline thermoregulation is probably also regulated by these EP_3-expressing neurons of this population. The other population is located in the caudal and lateral part of dorsolateral preoptic area. Neurons of this population, on the other hand, control the thermogenesis in brown adipose tissue via their projections to the DMH, which also project to RMR. Therefore, PGE_2 within the MnPO induce autonomic heat-producing and heat-conserving pathways by binding to EP_3 receptors, which decrease activity of preoptic GABAergic neurons, thus, disinhibiting sympathetic activation of brown adipose tissue thermogenesis and tail skin vasoconstriction. As a result, body temperature increases in rodents [56].

1.10 A General Evaluation of the Endocannabinoids and Fever Generation

Endocannabinoid signalling interacts with many other signallings in the body. Of those, the interaction between endocannabinoid and eicosanoid signallings is one of the most substantial networks since it regulates inflammation and processes related to inflammation. Both systems are consist of arachidonic acid containing molecules, which results in a more complex network. Since endocannabinoids are

hydrolysed to arachidonic acid and this molecule is the active precursor for lipid mediators of inflammation such as prostaglandins, studies with the inhibitors of endocannabinoid hydrolysing enzymes have come into prominence as useful tools for revealing the functions or interactions of specific endocannabinoids. 2-AG is one of the most studied endocannabinoids. It is full agonist of both central CB1 receptor and peripheral CB2 receptor and is present a few orders of magnitude higher than AEA in animal tissues. In addition, 2-AG potentiates $GABA_A$ receptors independent from CB receptors [95]. Due to these properties, 2-AG has gained much attention in endocannabinoid studies. MAGL, the main degradation enzyme of 2-AG, have been genetically and pharmacologically altered for better understanding of the function of 2-AG and its degradation by-products.

Phospholipase A_2 enzymes have been accepted as the main source of arachidonic acid pool for cyclooxygenase-mediated production of prostaglandins until now. However, recently there have been accumulation of controversial findings. For instance, cPLA-deficient mice did not have significantly altered levels of arachidonic acid in the brain [97] and genetic or pharmacological deactivation of MAGL in mice led to a significant decline in the brain arachidonic acid [88] [89] [98] [99]. These kinds of findings have brought about the suggestion that a potential alternative non-$cPLA_2$ mechanism which controls prostaglandin synthesis in the nervous system exists. Currently, there has been a shift towards the idea that MAGL have the ability to produce a substantial arachidonic acid pool for neuroinflammatory prostaglandins. Nomura et al., showed that mice deficient in the gene that encodes MAGL *($Mgll^{-/-}$* mice) or mice treated with the MAGL-selective inhibitor JZL184 (40 mg kg^{-1}, ip) manifested loss of MAGL activity but not any other brain serine hydrolase activities and escalation of brain 2-AG with corresponding reduction in arachidonic acid levels. Deactivation of MAGL also led to decline in various prostaglandins and other eicosanoids such as PGE_2, PGD_2, PGF_2 in states of neuroinflammation [89].

In addition they investigated whether MAGL regulates eicosanoid production in states of neuroinflammation. Mice were sacrified subsequent to systemic administration to proinflammatory agent LPS (20 mg kg^{-1}, ip) for two-six hours and their brain lipids were

measured. It was demonstrated that LPS exposure caused a robust, time-dependent escalation in brain eicosanoids and these changes were notably weakened in mice treated with JZL184 or in *Mgll*$^{-/-}$ mice (Figure 1.41.). The disturbance in brain eicosanoid synthesis in MAGL-deficient animals was not reversed by CB1 or CB2 receptors antagonists rimonabant and AM630, respectively or in *Cnr1/Cnr2* $^{-/-}$ mice. These results altogether led them to suggest that the neuroprotective effects of MAGL inactivation are mainly because of decline in arachidonic acid and proinflammatory prostaglandins rather than escalation in endocannabinoid signaling [89].

In addition, it was shown that JZL184 (10 mg kg^{-1}, ip) strongly attenuated LPS (100 μg kg^{-1}, ip)-induced escalation in cytokine expression in the rat frontal cortex (FC) when administered systemically. It also decreased arachidonic acid level but this situation is not accompanied by a significant decrease in PGE_2 or increase in 2-AG levels in the rat FC. The lack of increase in 2-AG, however, might have resulted from weak affinity of JZL184 to rat MAGL [107].

There are some findings suggest that the prominent and sustained escalation in brain 2-AG leads to endocannabinoid-mediated behavioral effects in CB1 dependent manner. It is known that direct CB1 agonists boost multiple behavioral effects in rodents such as hypothermia, analgesia, hypomotility, and catalepsy (collectively named the tetrad test for cannabinoid activity). For instance, JZL184 was found to display significant analgesic effect in several pain assays, which were blocked by pretreatment with the CB1 antagonist rimonabant. JZL184 (16 mg kg^{-1}, ip) also boosted hypothermia and hypomotility substantially in mice. Rimonabant, a CB1 antagonist, blocked the hypothermic effect of JZL184 entirely, indicating hypothermic effect is mediated by CB1Rs.

In addition, JZL184 did not cause significant hypothermia, analgesia or hypomotility in CB1$^{-/-}$ mice. These data altogether suggest that JZL184 stimulates a broad array of cannabinoid behavioral effects in rodents which imitate much of the pharmacological characteristics of direct CB1 agonists [88].

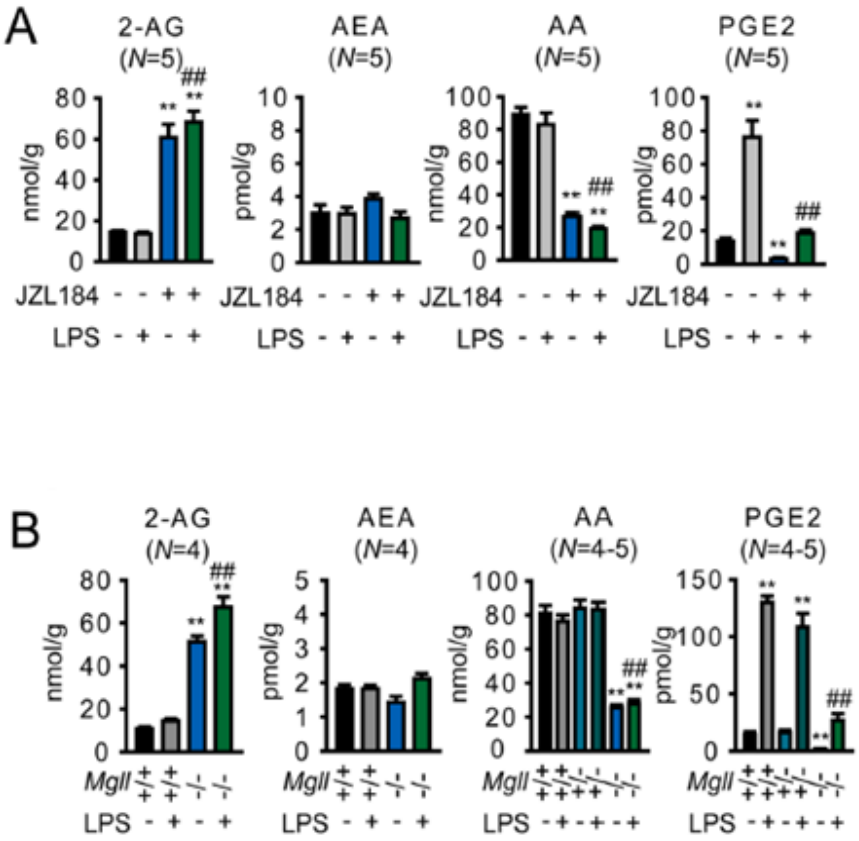

Figure 1.41. MAGL regulates arachidonic acid pathway in brain (Adapted from [89]).

A) Brain metabolite levels (determined by selected reaction monitoring using LC/MS) from mice treated with the MAGL inhibitor JZL184 (40 mg/kg, ip) or vehicle 30 min prior to administration of LPS (20 mg/kg, ip, 6 h) or vehicle. **B)** Brain metabolite levels from $Mgll^{+/+}$, $^{+/-}$, and $^{-/-}$ mice with or without LPS treatment (20 mg/kg, ip, 6 h). *$p < 0.05$ and **$p < 0.01$ for LPS-treated, JZL184-treated, or $Mgll^{-/-}$ groups compared to vehicle or $Mgll^{+/+}$ group. ##$p < 0.01$ for JZL184/LPS-treated versus LPS-treated groups, or LPS-treated $Mgll^{-/-}$ versus LPS-treated $Mgll^{+/+}$ or $Mgll^{+/-}$ groups. No statistically significant differences were observed between $Mgll^{+/-}$ and $^{+/+}$ groups. Data are presented as average ± standard error of the mean (SEM). *N*=4–5 mice/group. Experiments were performed twice and one dataset is shown (Adapted from [89]).

It has long been known that exogenous cannabinoids such as Δ^9-THC cause hypothermia [100][101][102]. Cannabinoid agonists, too, were shown to cause hypothermic response through CB1 but not CB2 receptor. A selective cannabinoid agonist WIN 55212-2 stimulated hypothermia in a dose-dependent manner in rats, which was blocked by the selective CB1 antagonist, SR141716A. However, selective CB2 antagonist did not have any effect on the WIN 55212-2-induced hypothermia. In addition, WIN 55212-2 administered directly into the POAH (preoptic anterior hypothalamic nucleus) stimulated hypothermia in an immediate and dose-dependent manner. This hypothermic response, too, was blocked by SR141716A.These results suggest that CB1 receptors, specifically within the POAH, are responsible for the hypothermia caused by cannabinoid agonist [103].

Additionally, HU-210, another synthetic cannabinoid agonist, was shown to have a deep hypothermic effect in rats. Besides, direct administration of HU-210 into the *Preoptic area* of the *hypothalamus* also led to a dose dependent decline in body temperature, indicating that it acts through affecting the thermoregulation center straightly. Coadministration of pyrogens (IL- 1 or PGE_2) and HU-210 normalized body temperature temporarily, however, it did not significantly blocked the hyperthermia caused by these pyrogens. It also did not have an effect on PGE_2 synthesis induced by LPS when investigated in ex vivo manner [109].

Effects of endogenous cannabinoids such as anandamide on body temperature was studied too. Anadamide isolated from porcine brain was shown to reduce body temperature in rats [104] and this effect was blocked by a CB1 receptor antagonist, indicating that hypothermic response caused by this receptor [105]. Another study with an endogenous cannabinoid, 2-AG, showed that inhibition of MAGL exerted dose dependent hypothermia when this endocannabinoid exogenously (iv) administered to mice [106].

Paradoxically, however, low doses of Δ^9-THC [102], anadamide and a selective CB1 agonist were shown to cause hyperthermia [111].

Results of the studies that aimed to investigate the interaction between LPS and cannabinoid agonists were consistent with the studies investigated effect of cannabinoid agonists on body temperature singly without any immunological insults. A selective CB1 receptor agonist, WIN 55,212-2, was utilized in order to determine cannabinoid effect on fever generated by LPS. It was shown that WIN 55,212-2 attenuated LPS (50 $\mu g\ kg^{-1}$ ip)-induced biphasic fever at a dose of 1 mg kg^{-1} (ip) and reduced fever at a dose of 1,5 mg kg^{-1} (ip). This decline in fever was reversed by a selective CB1 receptor antagonist, SR141716, but not by a selective CB2 receptor antagonist, SR144528. WIN 55,212-2 also blocked LPS-induced escalation in IL-6 levels in plasma which has an important role in production of fever during infection and inflammation. Additionally, the effect of Δ^9-THC on fever produced by LPS was also investigated. It was shown that Δ^9-THC significantly reduced the LPS-induced fever at a dose of 1 mg kg^{-1} (ip). This study determines the interaction of exogenous cannabinoids and synthetic cannabinoid agonists in fever generated by LPS [108].

A recent report revealed that CB1 receptor-deficient ($CB1^{-/-}$) mice did not show LPS-induced either fever or hyperalgesia, which are symptoms of sickness behaviours. Similarly, wild type mice whose CB1 receptors blocked by an antagonist (AM251) lost their ability to evoke fever when LPS administered. However, when toll-like receptor 3 (TLR3) agonist and viral mimetic Polyinosinic:Polycytidylic acid administered, $CB1^{-/-}$ mice were able to induce a strong fever response. In addition, LPS stimulated c-Fos activity in the febrinergic zone of the brain in wild-type mice but not in $CB1^{-/-}$ mice. Moreover, liver and spleen TLR4 mRNA showed a significant reduction in $CB1^{-/-}$ mice compared to wild-type mice, and their peritoneal macrophages from did not release proinflammatory cytokines as a response to LPS administration. These findings suggest that deficieny of CB1 receptors had a negative effect on TLR4's recognition of LPS which leads to sickness behaviours and that CB1 receptors have a vital role in LPS-stimulated fever [110].

These data altogether suggest that endocannabinoids and cannabinoid receptor type 1 (CB1) play important roles in sickness behaviors some of which are fever, hyperalgesia,

anorexia, activation of HPA (the hypothalamic–pituitary–adrenal) axis, and they have the ability to stimulate hypothermia and attenuate LPS-evoked fever.

1.11 The Aim of the Study

Endocannabinoids and their effects on several physiological and pathophysiological processes have been started to be unravelled and gained significant importance over the last two decades. Endocannabinoid system is now accepted as one of the primary neuromodulatory systems that plays important roles in sustaining homeostasis.

Endocannabinoid hydrolyzing enzymes have specifically been utilized in order to explore the functions of endocannabinoid signalling and its interactions with the other signalling systems. Of those, the main degradation enzyme of 2-Arachidonoyl glycerol (2-AG), monoacylglycerol lipase (MAGL), functions as a central metabolic hub, interlinking endocannabinoid system to the other lipid transmitters such as eicosanoid system. MAGL, hydrolyzing 2-AG to arachidonic acid (AA) and glycerol, generates a significant AA pool, an active precursor for lipid mediators of the brain such as prostaglandins. It remains to be understood how these by-products serve in the brain.Inhibitors selective to such degrading enzymes are unique tools to unravel both the functions of an endocannabinoids and its crosstalks with other systems since they enable to increase the level of the targeted endocannabinoid and decrease its degradation by-products. It appears that these inhibitors have a great therapeutic potential for plenty of human disorders. For this purpose, many serine hydrolyse inhibitors have been developed up to date. Of those, KML-29 with no detectable cross-reactivity with fatty acid amide hydrolyse (FAAH), the main hydrolyzing enzyme of anandamide (AEA), and with significant potency both *in vitro* and *in vivo* , is a versatile MAGL inhibitor that can be utilized both in rodent and human researches which aims to explore biological actions of 2-AG.

Systemic administration of LPS, the structural entity of the outer wall of cell membrane present in gram-negative bacteria, generates one of the most successfully utilized experimental models for investigation of stimulation of innate immune system. This type

of stimulation initiates inflammatory acute phase reactions and sickness behaviours such as fever, hyperalgesia, anorexia, activation of hypothalamic–pituitary–adrenal (HPA) axis.

Within this context, in the present study, we aimed to investigate the effect of MAGL inhibition through KML29 on an inflammatory process initiated in the brain, fever, by inducing systemic inflammation by LPS. We hypothesized that inhibition of MAGL, since it will cause an increase in 2-AG and a decrease in AA levels, may have an ameliorating effect on fever due to declined synthesis of prostaglandin E_2 in consequence of decreased AA levels and stimulation of CB1 receptors in consequence of increased 2-AG levels. For this purpose, we implemented transmitters into 24 male Wistar albino rats by surgical procedures and recorded, by means of a biotelemetric technique, to observe whether any alterations occurred in the initiated fever following administrations of KML29 and LPS simultaneously.

CHAPTER 2

MATERIALS AND METHODS

2.1 Experimental Animals

Adult Wistar albino male rats (12-16 weeks old) weighing 202-328 g. were utilized in this study. Rats provided with Ankara University Faculty of Medicine, Experimental Animals and Research Laboratory and were housed in Experimental Animals Section of Medical Pharmacology Department, Ankara University Faculty of Medicine. The surgical procedures, *in vivo* experiments and sacrification procedures were carried out in the neuropsychopharmacology laboratory of the same department. They were fed standard rat chow and water *ad libitum* and housed in an air-conditioned room at an ambient temperature of 21±1 ºC under a 12:12 h light-dark cycle (lights on at 7:00 AM) and humidity of 40%. Rats were housed in groups of three or four and seperated into one animal per macrolon cage after surgical procedures. The Local Ethical Committee of Ankara University, Faculty of Medicine for Animal Care and Use approved the experimental protocols (Approval# 2014-4-16).

In total, 24 rats were utilized and for each protocol animals were used once. Some of the rats, with at least one weak interval, were used for different protocol (e.g., saline+saline and LPS+vehicle) (Table 2.1.).

2.2 Biotelemetry Recordings and Surgical Procedure

The abdominal temperature (T_{ab}) was recorded by radiotelemetry (Mini-Mitter, Bend, OR, USA). A temperature transmitter (model VM-FM 3000) was implanted into the peritoneal cavity of each rat under aseptic conditions and general anesthesia (ketamine

80 mg/kg ip and xylasine 10 mg/kg ip) minimum a week before the day of the experiment. Following the operations, rats were placed singly in separate macrolon cages and provided with post operative care (with paying attention to their getting adequate water and granulated chow if necessary) for at least seven days. The rats reached pre-operation weight subsequent to the post operative care for at least one week were chosen randomly and utilized in experiments.

Table 2.1. Experiment Groups, Animal Codes and Basal Temperatures

Experiment Groups	Animal code	Body Weigh t (g)	mean ± SEM (g)	Basal temperature (°C)	mean ± SEM (°C)
(1) Saline (sc) + Saline (sc) ; n=9	T#1275A	238	274 ± 14.2	37.0	37.2 ± 0.11
	T#1277A	202		37.3	
	T#1278A	281		37.4	
	T#1279A	300		37.6	
	T#1280A	309		37.5	
	T#1281A	328		37.9	
	T#1282A	303		37.2	
	T#1283A	282		36.9	
	T#1284A	225		36.8	
(2) Saline (sc) + Vehicle (sc); n=9	T#1272B	251	280 ± 11.3	36.6	37.0 ± 0.09
	T#1273B	278		36.8	
	T#1274B	309		37.0	
	T#1275C	253		36.8	
	T#1277C	223		36.9	
	T#1278C	318		37.5	
	T#1282C	312		37.4	
	T#1283C	312		37.0	
	T#1284C	266		37.0	
(3) KML29 (20 mg/kg, sc); n=3	T#1269A	238	245 ± 4.6	36.7	36.7 ± 0.03
	T#1270B	254		36.7	
	T#1271B	245		36.8	

Table 2.1. Continued

(4) Saline (sc) +LPS *E. coli* O111:B4 (250 µg/kg, sc); n=7	T#1258A	250	253 ± 8.7	37.8	37.3 ± 0.16
	T#1259A	293		37.7	
	T#1260A	220		37.4	
	T#1262A	235		37.5	
	T#1263A	266		36.6	
	T#1264A	260		36.9	
	T#1265A	253		37.2	
(5) Vehicle (sc) +LPS *E. coli* O111 :B4 (250 µg/kg, sc); n=6	T#1269C	247	252 ± 10.6	36.6	37.0 ± 0.10
	T#1270C	267		37.3	
	T#1271C	247		37.1	
	T#1275B	245		37.2	
	T#1277B	215		37.0	
	T#1278B	293		36.9	
(6) KML-29 (20 mg/kg, sc)+ LPS *E. coli* O111:B4 (250µg/kg, sc) (simultaneously) ; n=7	T#1272A	249	275 ± 12.2	36.8	36.8 ± 0.06
	T#1273A	274		36.9	
	T#1274A	309		36.7	
	T#1282B	307		37.2	
	T#1283B	307		36.9	
	T#1286B	242		36.7	
	T#1287B	238		36.9	

Multiple comparisons of average basal temperatures and body weights between groups of 1, 2, 4, 5, 6 were made by one-way ANOVA. Average basal temperature analysis were followed with the Fisher's Least Significant Difference (LSD) post-hoc test with Bonferonni correction (One-way ANOVA results for average basal temperature without bonferonni correction: [F (4, 37): 2.769; p: 0.043]). Without bonferonni correction p=0.013 for group1 vs group 6; p=0.016 for group 4 vs group 6; with bonferonni correction p=0.128 for group1 vs group 6; p=0.157 for group 4 vs group 6. Results show no statistically significant difference in average basal temperatures between groups after multiple testing adjustment. One-way ANOVA results for body weights: [F (4, 37):1.096; p: 0.375]. There is no statistically significant difference in body weights between groups.

The experiments were started at 9 AM each time. On the day of experiment the rats were taken from Experimental Animals Section and placed onto the receivers (series TR-3000) in the neuropsychopharmacology laboratory of the same section in their cages and were allowed to adapt to the environment and reach a steady T_{ab} at an ambient temperature of 24 ±1 ºC.

The receivers utilized to detect the signals come from the transmitters implanted into the peritoneal cavity of the rats and direct them to a personel computer via an interface. The frequencies of these signals are converted to temperature per-minute by a specific software, namely Vital View, present in the computer.

After the rats reaching a steady T_{ab}, the treatments were started and adminstration of drugs were done between 11.30 AM-12.30 PM. Subsequent to the tratments, recordings were taken until the following morning. Ten hours following the injections were taken into consideration in order to make calculations. The baseline T_{ab} was calculated as the average of 30 minutes preceding the injection. T_{ab} changes were calculated as ΔT for every minute and all the analyses were performed based on ΔT.

$$\Delta T = T_{ab} \text{ per-minute following the injection} - \text{Baseline } T_{ab} \quad (2.1)$$

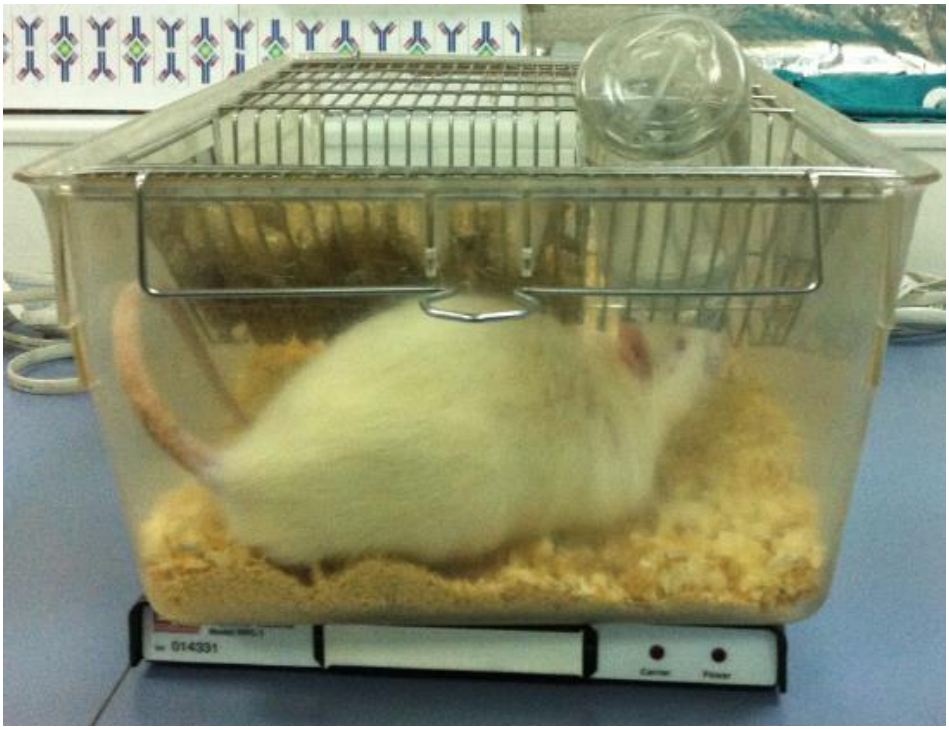

Figure 2.1. An example of rat, which was implanted a transmitter into its peritoneal cavity, whose cage placed onto the receiver.

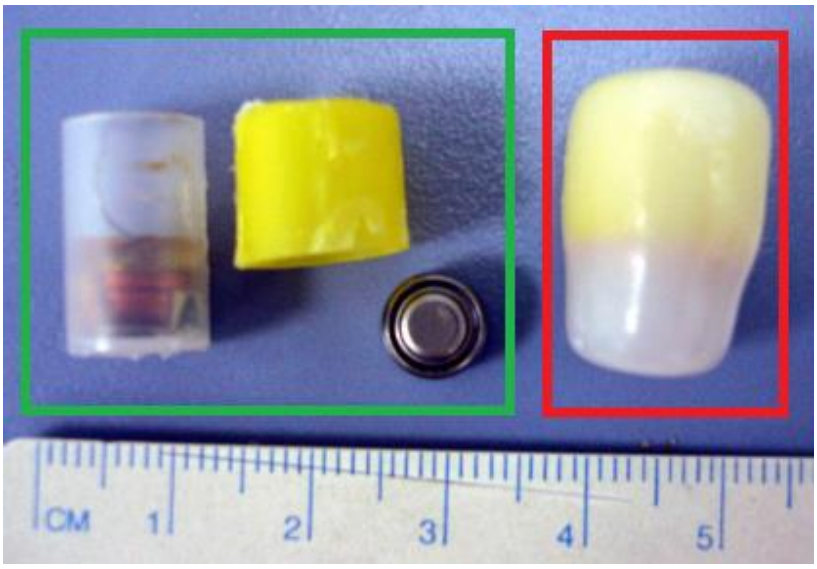

Figure 2.2. An example of a Mini Mitter VM-FM 3000 transmitter (in red rectangle) and parts of it (in green rectangle).

2.3 Experimental Protocols

2.3.1 Saline (5 ml/kg, sc) + Saline (5 ml/kg, sc) Protocol; n=9

5 ml/kg sterile apyrogenic saline solution (0.9% NaCl) was used and both injections were done subcutaneously (sc) in simultaneous manner.

2.3.2 Saline (5 ml/kg, sc) + Vehicle (5 ml/kg, sc) Protocol; n=9

For saline injection 5 ml/kg sterile apyrogenic saline solution (0.9 % NaCl) and for the vehicle injection 5 ml/kg freshly prepared vehicle was used. In order to prepare vehicle, 0.17 N solution of NaOH, which was prepared by diluting 1ml of 1N solution of NaOH by a factor of 5.85, was mixed to 1.5 N solution of HCl, which was prepared by diluting

1ml of 2N solution of HCl by a factor of 1.3, at the rate of 1.8/2 (1.8 ml of 0.17N solution of NaOH in final volume of 2 ml). These calculations were made in order to keep the final percentage of the NaCl in the solution close to the 0.9 % NaCl. After mixing in vortex mixer for about 1 minute the solution was kept in the sonicator adjusted to 50 ºC for 5 minutes. It was aimed to keep the final pH close to physiological pH (between 7.0-7.8). Therefore, after the sonication process pH meter was used to confirm the final pH and if necessary it was added minute amounts of HCl and /or NaOH to get a pH close to physiological one. Finally it was added 15 µl of Tween-80 to get the solution ready for injection. Both injections were done subcutaneously in simultaneous manner.

Figure 2.3. An example of subcutaneous neck injection in rats [113].

2.3.3 KML29 (20 mg/kg, sc) Protocol; n=3

For preparation of 20 mg/ kg KML29 (Cayman Chemicals Company, USA, Batch#0453632-13), KML29 bottle which was kept in -20 ºC transferred to + 4 ºC and kept there for 30 minutes.

After that, the bottle was held in room temperature for about 10-15 minutes. In order to get 20 mg/kg of final concentration, it was aimed to get 4 mg/ml of KML29 solution since injections were done by the volume of 5ml/kg. In order to keep the final percentage of the NaCl in the solution close to the 0.9 %, it was added 0.17 N solution of NaOH at the rate of 1.8/2 (1.8 ml of 0.17N solution of NaOH in final volume of 2 ml) to weighed KML29. After mixing in vortex mixer for about 1 minute the solution was kept in the sonicator adjusted to 50 ºC for 5 minutes. It was aimed to keep the final pH close to physiological pH between 7.0-7.8. Therefore, after the sonication process pH meter was used to confirm the final pH and 1.5N solution of HCl added step by step at the rate of 0.2/2 (0.2 ml of 1.5 N solution of HCl in final volume of 2 ml) to get a pH close to physiological one. Finally it was added 10 µl of Tween-80 to get the solution ready for injection. The final concentration allowed to inject approximately 20 mg/kg dose of KML29. Injections were done subcutaneously.

2.3.4 Saline (5 ml/kg, sc) +LPS *E. coli* O111:B4 (250 µg/kg, sc) Protocol; n=7

For saline injection 5 ml/kg sterile apyrogenic saline solution (0.9 % NaCl) and for the LPS *E. coli* O111:B4 (Sigma-Aldrich Co. LLC, USA, Lot#012M4098V) injection 250 µg/kg of prepared solution was used. LPS *E. coli* O111:B4 was aliquoted as a stock solution of 2 mg/ml under aseptic conditions and kept at -20 ºC till it was used. On the day of experiment LPS bottle was held in the room temperature for about 10-15 minutes then it was further diluted to get 50 µg/ml of concentration with sterile apyrogenic saline solution since injections were done by the volume of 5 ml/kg. Both injections were done subcutaneously in simultaneous manner.

2.3.5 Vehicle (5 ml/kg, sc) +LPS *E. coli* O111:B4 (250 µg/kg, sc) Protocol; n=6

For the vehicle injection 5 ml/kg freshly prepared vehicle and for the LPS *E. coli* O111:B4 injection 250 µg/kg of prepared solution was used. Preparation of vehicle was made as described in protocol 2.3.2 and LPS *E. coli* O111:B4 solution as described in protocol 2.3.4. Both injections were done subcutaneously in simultaneous manner.

2.3.6 KML29 (20 mg/kg, sc) +LPS *E. coli* O111:B4 (250 µg/kg, sc) (simultaneously) Protocol; n=7

Preparations of 20 mg/kg KML29 was made as described in protocol 2.3.3 and LPS *E. coli* O111:B4 solution as described in protocol 2.3.4. Both injections were done subcutaneously in simultaneous manner (KML29 injection to the left side and LPS *E. coli* O111:B4 to the right side of the neck).

2.4. Statistical Analysis

ΔT values and body weights were expressesd as means ± SEM (Standard error of the mean). Comparisons of average baseline temperatures and body weights of the groups were made by one-way ANOVA through SPSS for windows (version 15.0) statistical package (SPSS Inc., Chicago, IL, USA). The analysis of average baseline temperatures were followed with the Fisher's Least Significant Difference (LSD) post-hoc test with Bonferroni correction (Overall type I error was taken to be 0.25 and 0.25/5=0.05 was taken as nominal significance level per pairwise comparison).

Bayesian random effects spline regression was used to investigate the differences between the groups in terms of Tab profiles over time. Analyses were carried out using Markov chain Monte Carlo (MCMC) method. MCMCglmm and ggplot2 of R statistical

package (version 3.1.2) were used for statistical modeling and analysis of the data and producing the plots respectively. Bonferroni correction was made as multiple testing adjustment (Overall type I error was taken to be 0.20 and 0.20/4=0.05 was taken as nominal significance level per pairwise comparison).

CHAPTER 3

RESULTS AND DISCUSSION

In this study, the effect of MAGL inhibition on the fever initiated by LPS was investigated. For this purpose, 6 different protocols have been prepared and used.

3.1. Control Experiments

Saline(sc)+saline(sc) and saline(sc)+vehicle(sc) experiments were performed as controls. For each group, randomly chosen 9 rats (totally 18 rats) were utilized.

Saline+saline (5 ml/kg each) protocol was performed in order to observe whether injection stress caused any significant changes in the body temperature. Since we were planning to do two injections, i.e. KML29 and LPS injections simultaneously, we aimed to see the effect of two simultaneous saline injections. In addition, saline+saline protocol was also performed as the control of Saline+LPS experiments because saline was used as dissolver for LPS. As shown in Figure 3.1, the injection time was accepted as 0 in the time line (shown with arrow in the graph) and there was no apparent change in the T_{ab} of this group following saline+saline injections until the 420^{th} minute. The T_{ab} increase started at the 420^{th} minute continued until the end of the observation period (600 min) (Since rats are nocturnal animals, when the lights are turned off (at 7 PM) their body temperature increase naturally as a result of circadian rhythm).

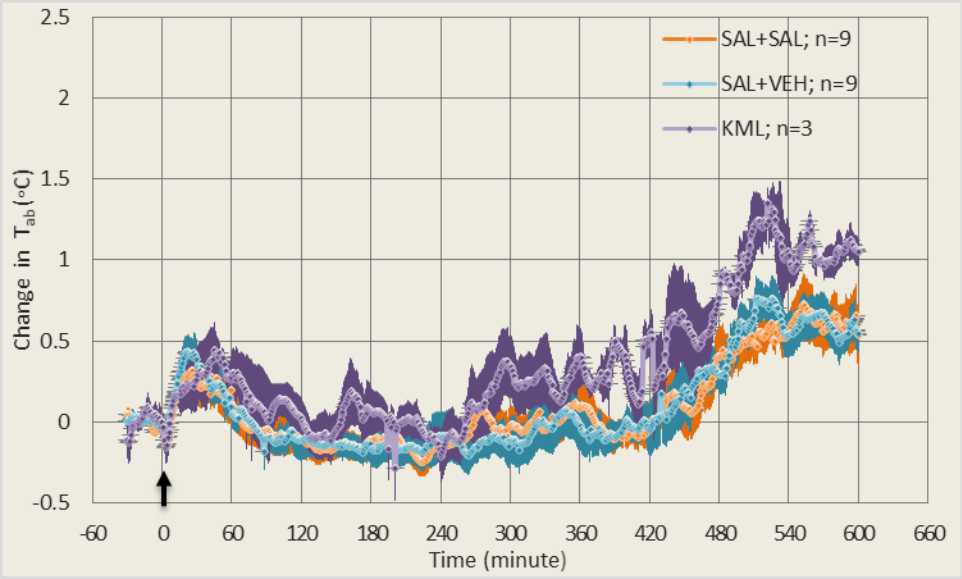

Figure 3.1. Overlapped lines of changes in T_{ab}s (ΔT) following Saline (5 ml/kg, sc) +Saline (5 ml/kg, sc) (n=9); Saline (5 ml/kg, sc) +Vehicle (5 ml/kg, sc) (n=9) and approximately 20 mg/kg of KML29 (sc, n=3) injections. Injections were done at time 0 (Indicated by arrow). Each point represent the mean ±SE of the T_{ab} observations of animals. (Precise concentrations of KML29 injections: 19.98 mg/kg, 19.95 mg/kg, 17.15 mg/kg, average concentration:18 mg/kg)

The transient escalation in ΔT_{ab} just after the injection was due to handling and injection procedure and known as "stress response".

In addition, saline+vehicle (5 ml/kg each) protocol was performed in order to observe whether vehicle injection caused any significant changes in the body temperature. In this set of experiment we aimed to see the effect of simultaneous saline and vehicle injections as the control of KML29 and LPS injections. Overlapped lines of changes in the T_{ab}s (ΔT) following Saline (sc)+Saline (sc) and Saline (sc)+Vehicle (sc) injections are shown in Figure 3.1. As can be seen, the two lines display quite similar trends and there is no statistically significant difference between them (data is shown in appendix). The transient escalation in ΔT_{ab} just after the injection was also due to the stress response. There was no change in the T_{ab} of this group following saline+vehicle

injections until the 420th minute. As a result of circadian rhythm, the T_{ab} increase which started at the 420th minute continued until the end of observation period (600 min).

In order to determine which dose of KML29 would be appropriate to use, we performed another set of control experiment. Due to the findings explained in the section 1.7 (Figure 1.27. and 1.28) limited blockade of MAGL appeared to be a safer and more appropriate way for our study. Therefore, we considered to utilize approximately 20 mg/kg of KML29 in our experiments.

Before utilizing a dose of 20 mg/kg in our experiments, we wanted to confirm that this dose is ineffective on body temperature when administered singly (without simultaneous injection of saline). Since empirical data was enough for determining the dose, we used three rats. As shown in Figure 3.1., administration of approximate 20 mg/kg of KML29 does not alter (decrease) body temperature in rats.

3.2 Saline (5ml/kg, sc)+LPS *E. coli* O111:B4 (250 µg/kg, sc) Experiments

In order to confirm the fever LPS *E. coli* O111:B4 causes, we injected dose of 250 µg/kg subcutaneously.

As can be seen in figure 3.2 the fever caused by LPS *E. coli* O111:B4 250 µg/kg (sc) has three characteristic phases:

1) Initiation (Latency) of fever: The point where the body temperature increases steadily and reaches 0.5˚C of ΔT.

2) Fever Peak: The point where the body temperature reaches the maxima.

3) Fever Plateau: The point where the body temperature proceeds near the maxima reached previously.

According to the figure 3.2., Saline 5 ml/kg (sc)+LPS *E. coli* O111:B4 250 µg/kg (sc) caused body temperature to increase about 3.5 hours after the injection (initiation of fever) and it reached to the maxima ($\Delta T = 1.8 \pm 0.16$) in approximately 2.5 hours and continued until the end of observation period (fever plateau).

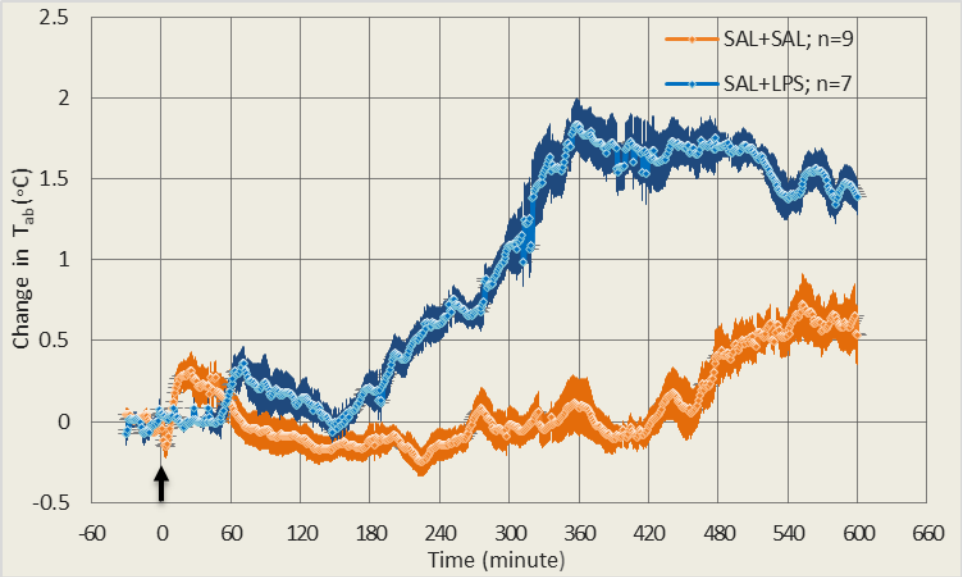

Figure 3.2. Overlapped lines of changes in T_{ab}s (ΔT) following Saline (5 ml/kg, sc)+Saline (5 ml/kg, sc) (n=9) and Saline (5 ml/kg, sc)+LPS *E. coli* O111:B4 (250 µg/kg, sc) (n=7) injections. Injections were done at time 0 (Indicated by arrow).

In order to analyse whether the difference between saline+saline and saline+LPS O111:B4 lines of changes in the T_{ab}s are statistically significantly different, Bayesian estimation -Markov chain Monte Carlo (MCMC) method was used. Since LPS O111:B4+Saline line displays two different trends; i.e., quadratic between 0-250th minute and concave between 250-600th minute, mixed effects quadratic regression was used for the first part (0-250th minute) and mixed effects spline regression (low rank thin spline) for the second part (250-600th minute) of analysis.

Beta1 is the parameter that shows the association between treatments and temperature changes and its being in the interval that includes zero indicates that ΔT between these two groups is not statistically significantly different than zero. Analysis of the

first part revealed that with 95% posterior interval Beta1 equals to -0.05829 (-0.5178, 0.40187); that is the temperature change (ΔT) for ≤ 250th minute between these two groups are statistically insignificant.

Analysis of second part (≥ 250 minute), on the other hand, revealed that with 95% posterior interval Beta1 equals to 2.415 (2.269, 2.563); that is the temperature change (ΔT) for ≥ 250th minute between these two groups is statistically significant with 5% Type I error. This value indicates that the with 95% posterior interval temperature change in salin+LPS O111:B4 group is approximately 2.4 fold larger compared to saline+saline group (this result is adjusted for time; that is at any fixed time point ΔT of saline+LPS O111:B4 group is 2.4 fold higher compared to ΔT of saline+saline group at the same time point) (Figure 3.3).

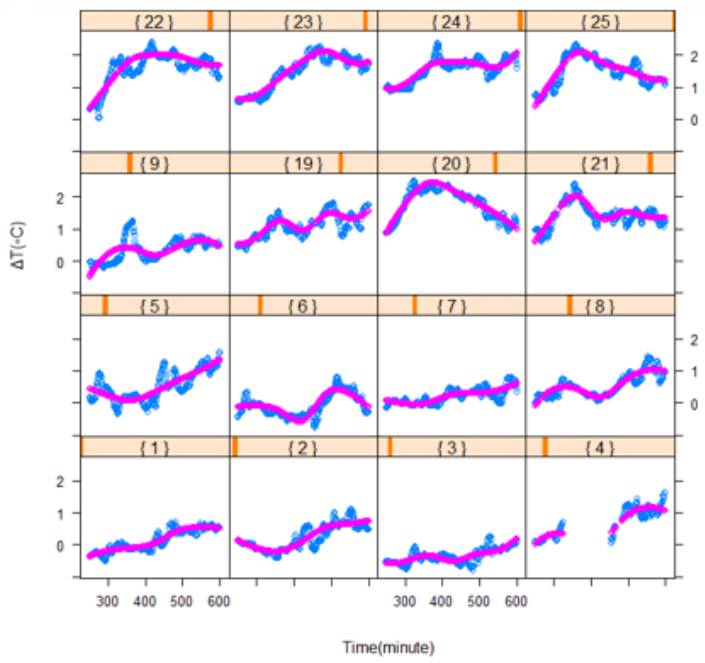

Figure 3.3. Statistical model (mixed effects spline regression (low rank thin spline)) fitted to ≥ 250 minute of saline+saline (n=9) and saline+LPS O111:B4 (n=7) groups. Blue lines indicate the observed points in the experiments and pink lines indicate to what extent the fitted model captured those observed points (α= 0.05 was taken as nominal significance level per pairwise comparison).

3.3 Simultaneous KML29 (20 mg/kg, sc)+LPS *E. coli* O111:B4 (250 µg/kg, sc) Experiments

In this set of experiment we administered approximate 20 mg/kg of KML29 and 250 µg/kg of LPS *E. coli* O111:B4 subcutaneously in simultaneous manner to 7 outbred Wistar albino rats. KML29 injection was done to the left side and LPS *E. coli* O111:B4 injection to the right side of the neck.

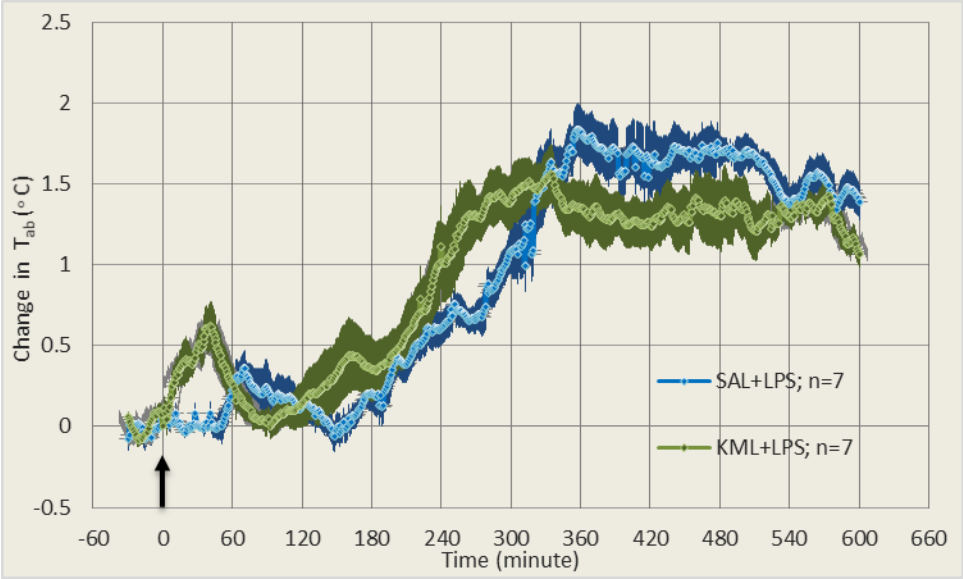

Figure 3.4. Overlapped lines of changes in T_{ab}s (ΔT) following simultaneous Saline (5 ml/kg, sc) + LPS *E. coli* O111:B4 (250 µg/kg, sc) (n=7) and approximate 20 mg/kg KML29 (sc)+LPS *E. coli* O111:B4 (250 µg/kg, sc) (n=7) injections.Injections were done at time 0 (Indicated by arrow). (Precise concentrations of KML29 injections: 20 mg/kg, 20 mg/kg, 17.7 mg/kg, 17.7 mg/kg, 20.08 mg/kg, 20.08 mg/kg, 16 mg/kg; average concentration:18.79 mg/kg)

According to the figure 3.4., administration of KML29 20 mg/kg (sc) simultaneously with LPS *E. coli* O111:B4 250 µg/kg (sc) caused body temperature to increase about 3.5 hours after the injection (initiation of fever) and it reached to the maxima (ΔT= 1.5±0.18) in approximately 2.2 hours and continued until the end of the observation period (fever plateau).

Statistical analysis was made by using Bayesian estimation -Markov chain Monte Carlo (MCMC) method. Due to the reasons explained in section 3.1.2. mixed effects quadratic regression was used for the first part (0-250th minute) and mixed effects spline regression for the second part (250-600th minute) of analysis.

Analysis of the first part revealed that with 95% posterior interval Beta1 equals to 0.1479 (-0.3516, 0.6394); that is the temperature change (ΔT) for ≤ 250th minute between these two groups are statistically insignificant.

Analysis of second part (≥ 250 minute) revealed that with 95% posterior interval Beta1 equals to -1.717 (-1.863, -1.571); that is the temperature change (ΔT) for ≥ 250th minute between these two groups is statistically significant with 5% Type I error. This value indicates that with 95% posterior interval the temperature change in KML29+LPS O111:B4 group is approximately 1.7 fold lesser compared to saline+LPS O111:B4 group (this result is adjusted for time).

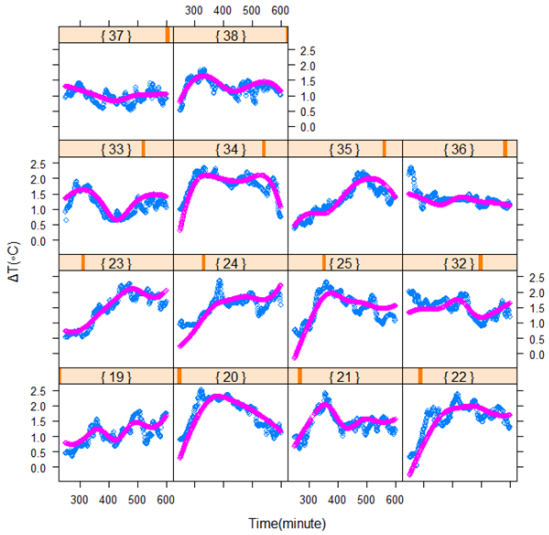

Figure 3.5. Statistical model (mixed effects spline regression) fitted to ≥ 250 minute of saline+LPS O111:B4 (n=7) and KML29+LPS O111:B4 (n=7) groups. Blue lines indicate the observed points in the experiments and pink lines indicate to what extent the fitted model captured those observed points (α= 0.05 was taken as nominal significance level per pairwise comparison).

3.4 Vehicle+LPS *E. coli* O111:B4 (250 µg/kg, sc) Experiments

This set of experiment is designed to examine whether the ameliorating effect of the KML29 on fever arised from the vehicle. For this purpose, 6 outbred Wistar albino rats were utilized. 5 ml/kg of vehicle and 250 µg/kg were injected subcutaneously in simultaneous manner (Figure3.6.).

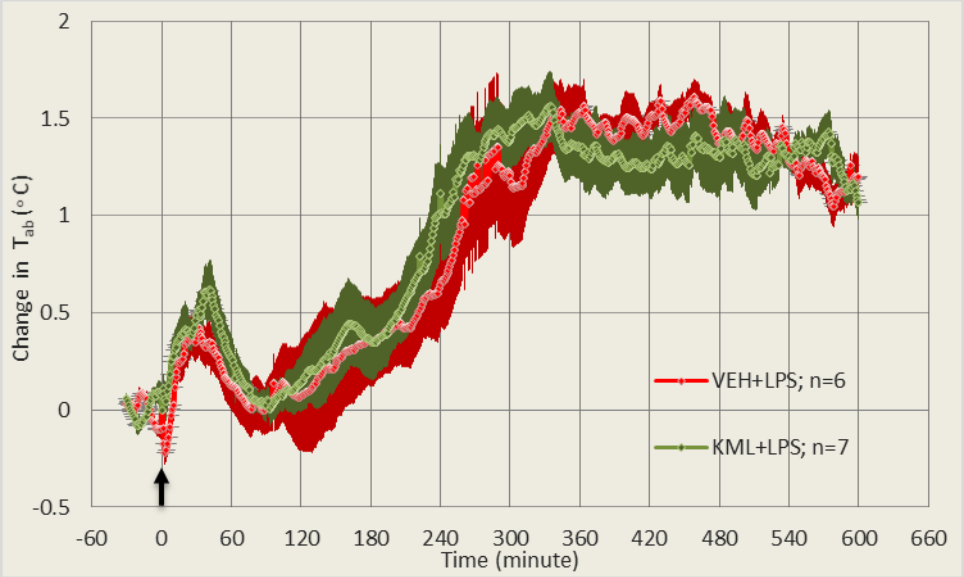

Figure 3.6. Overlapped lines of changes in T_{ab}s (ΔT) following simultaneous Vehicle (5 ml/kg, sc)+LPS *E. coli* O111:B4 (250 µg/kg, sc) (n=6) and approximate 20 mg/kg KML29 (sc)+LPS *E. coli* O111:B4 (250 µg/kg, sc) (n=7) injections. Injections were done at time 0 (Indicated by arrow).

According to the figure 3.6., administration of Vehicle 5 ml/kg (sc) simultaneously with LPS *E. coli* O111:B4 250 µg/kg (sc) caused body temperature to increase about 3.5 hours after the injection (initiation of fever) and it reached to the maxima (ΔT= 1.5±0.12) in approximately 2.5 hours and continued until the end of the observation period (fever plateau).

Statistical analysis of comparison between saline+LPS O111:B4 and Vehicle+LPS O111:B4 was carried out by using Bayesian estimation -Markov chain Monte Carlo (MCMC) method. Mixed effects cubic regression was used for the first part (0-250th

minute) and mixed effects spline regression for the second part (250-600th minute) of analysis.

Analysis of the first part revealed that with 95% posterior interval Beta1 equals to 0.04548 (-0.4281, 0.5147); that is the temperature change (ΔT) for ≤ 250th minute between these two groups are statistically insignificant.

Analysis of second part (≥ 250 minute) revealed that with 95% posterior interval Beta1 equals to -0.855 (-1.006, -0.8037); that is the temperature change (ΔT) for ≥ 250th minute between these two groups is statistically significant with 5% Type I error. This value indicates that with 95% posterior interval the temperature change in Vehicle+LPS O111:B4 group is approximately 0.8 fold less compared to saline+LPS O111:B4 group (this result is adjusted for time).

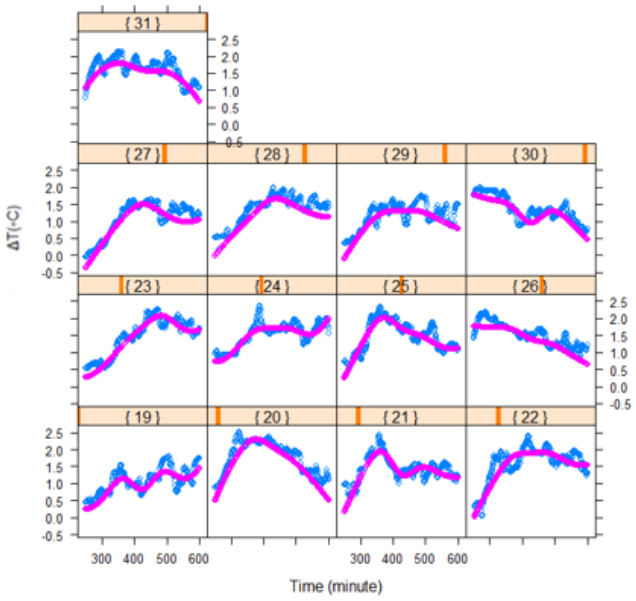

Figure 3.7. Statistical model (mixed effects spline regression) fitted to ≥ 250 minute of saline+LPS O111:B4 (n=7) and Vehicle+LPS O111:B4 (n=6) groups. Blue lines indicate the observed points in the experiments and pink lines indicate to what extent the fitted model captured those observed points (α= 0.05 was taken as nominal significance level per pairwise comparison).

In order to discriminate among the effect of vehicle and the effect of KML29, another statistical test was carried out. Statistical analysis of the comparison between Vehicle+LPS O111:B4 and KML29+LPS O111:B4 groups was also carried out by using Bayesian estimation -Markov chain Monte Carlo (MCMC) method. Mixed effects quadratic regression was used for the first part (0-250th minute) and mixed effects spline regression for the second part (250-600th minute) of analysis.

Analysis of the first part revealed that with 95% posterior interval Beta1 equals to 0.0917 (-0.4212, 0.5979); that is the temperature change (ΔT) for $\leq$ 250th minute between these two groups are statistically insignificant.

Analysis of second part ($\geq$ 250 minute) revealed that with 95% posterior interval Beta1 equals to -0.7223 (-0.8535, -0.5917); that is the temperature change (ΔT) for $\geq$ 250th minute between these two groups is statistically significant with 5% Type I error. This value indicates that with 95% posterior interval the temperature change in KML29+LPS O111:B4 group is approximately 0.7 fold lesser compared to Vehicle+LPS O111:B4 group (this result is adjusted for time). This result shows that KML29, apart from the effect of vehicle, has an ameliorating effect on the fever induced by LPS O111:B4.

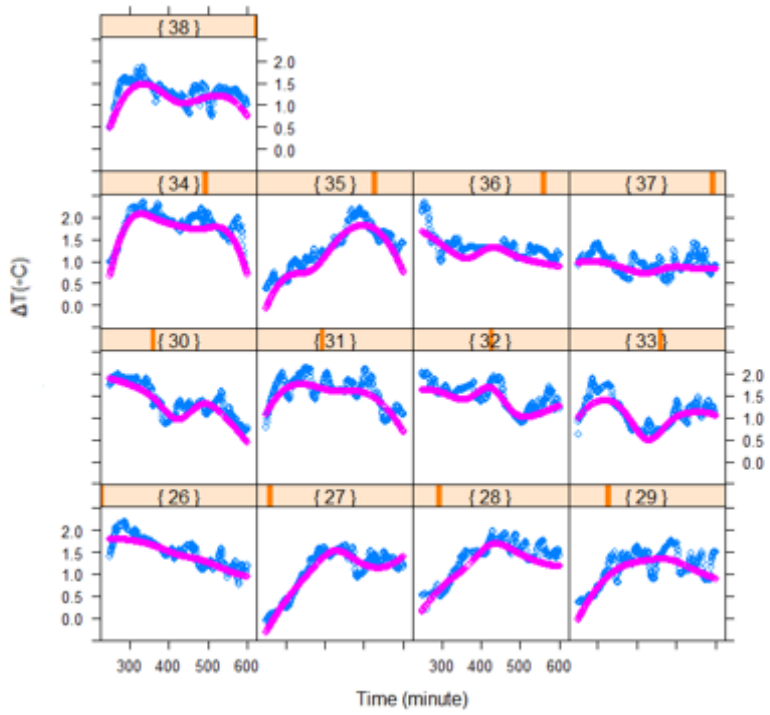

Figure 3.8. Statistical model (mixed effects spline regression) fitted to ≥ 250 minute of Vehicle+LPS O111:B4 (n=6) and KML29+LPSO111:B4 (n=7) groups. Blue lines indicate the observed points in the experiments and pink lines indicate to what extent the fitted model captured those observed points (α= 0.05 was taken as nominal significance level per pairwise comparison).

Table 3.1. Beta1 results of comparisons between groups

		Saline+Saline vs **Saline+LPS**	**Saline+LPS** vs **KML29+LPS**	**Saline+LPS** vs **Vehicle+LPS**	**Vehicle+LPS** vs **KML29+LPS**
Beta1	**< 250th minute**	**-0.05829**	**0.1479**	**0.04548**	**0.0917**
		95% post. interval (-0.5178, 0.40187)	95% post.interval (-0.3516, 0.6394)	95% post. interval (-0.4281, 0.5147)	95% post. interval (-0.4212, 0.5979)
	> 250th minute	**2.415**	**-1.717**	**-0.855**	**-0.7223**
		95% post. interval (2.269 , 2.563)	95% post. interval (-1.863, -1.571)	95% post. interval (-1.006, -0.8037)	95% post. interval (-0.8535, -0.5917)

LPS: LPS *E. coli* O111:B4; post.: posterior

Monoacylglycerol lipase inhibition is known to cause prominent effects on lipid metabolism due to the interactive nature of endocannabinoid signalling. Specifically, accumulation of evidence that indicates MAGL's ability to produce a substantial arachidonic acid pool for neuroinflammatory prostaglandins and its genetic and pharmacological inactivation's altering 2-AG and prostaglandin levels including PGE_2 led to the idea that MAGL inhibition could have a neuroprotective effects in states of inflammation [89] [107].

In the current study, we hypothesized that MAGL's inhibition may have an ameliorating effect on LPS induced fever, an inflammatory procees generated by brain, either by increasing 2-arachidonoyl glycerol or decreasing arachidonic acid levels or both.

As shown in section 3.2 administration of 250 μg/kg, sc LPS *E. coli* O111:B4+ 5ml/kg, sc saline caused ΔT to increase significantly (with 5% type 1 error, 2.4 fold) compared to saline+saline injection. Comparative analysis of saline+LPS *E. coli* O111:B4 and KML29(20 mg/kg, sc) +LPS *E. coli* O111:B4(250 μg/kg, sc) (section 3.3) revealed that administration of KML29 simultaneously with LPS *E. coli* O111:B4 significantly decreased ΔT (with 5% type 1 error, 1.7 fold) compared to saline+LPS *E. coli* O111:B4. Administration of KML29 simultaneously with LPS *E. coli* O111:B4 resulted in decreased plateau phase of fever compared to LPS *E. E. coli* O111:B4+saline administration.

Even though comparative analysis of salin+LPS *E. coli* O111:B4 and vehicle+LPS *E. coli* O111:B4 (section 3.4) revealed that administration of vehicle simultaneously with LPS *E. coli* O111:B4, too, significantly decreased ΔT (with 5% type 1 error, 0.8 fold) compared to saline+LPS *E. coli* O111:B4, further analysis performed for discriminating the effect of KML29 from the effect of vehicle on LPS-induced fever showed that simultaneous KML29+LPS *E. coli* O111:B4 administration significantly decreased ΔT (with 5% type 1 error, 0.7 fold) compared to simultaneous vehicle+ LPS *E. coli* O111:B4. Therefore, we can conclude that apart from the effect of vehicle, KML29 had a significant but modest protective effect at a dose of 20 mg/kg.

It could be argued that the modest protection of KML29 at a dose of 20 mg/kg might have been strengthened by using higher doses of KML29. However, since one of vital aspect of fever studies is to use an inffecetive dose (when injected singly) of compound of interest and high doses might have cause decline in body temperature, we did not prefer to use higher doses of KML29.

In addition, it should also be taken into consideration that the modest protection of KML29 against LPS-induced fever might have been caused by its solubility difficulties. It was reported that KML29 requires sonication in the vehicle before injection. Specifically, mild heating and prolonged sonication have been recommended in case of p.o. or i.p. administration [94]. Even though we followed the essentials of those recommended procedures in our protocols, the difficulties in the dissolvation might have affected the inhibition ability of KML29.

Depending on these results it can be speculated that MAGL activation and hence degradation of 2-AG needs to be elevated in order fever induced by LPS to reach the maxima and maintain fever near this peak. That is, the ratio of incline in fever is related with 2-AG's degradation by MAGL.

Even though it was reported that mice exposed to LPS had a robust and time-dependent escalation in brain eicosanoids (e.g., PGE_2) which was notably weakened with the treatment of JZL184 or in *Mgll*$^{-/-}$ mice [89], we might speculate that the ameliorating effect of KML29 is likely due to elevation in endogenous 2-arachidonoyl glycerol levels and its effect on CB1 receptors rather than decrease in AA and hence in PGE_2 since studies with COX inhibitors resulted in a much robust reduction in LPS-induced fever due to the complete blockade of the prostaglandin synthesis [114][115][116].

A study reports that pretreatment with nonhypothermic dose of a cannabinoid receptor agonist WIN 55,212-2, antagonized the LPS-induced biphasic fever with the first peak at 180 min and the second at 300 min postinjection (Figure 3.9.). WIN 55,212-2 dose dependently lowered the maxima and plateau phase of LPS-induced fever, which is consistent with our results (Figure 3.4.).

The inhibitory effect of this agonist was reversed by a CB1 receptor antagonist, SR141716, but not with a CB2 receptor antagonist, SR144528, implying this effect was due to CB1 receptors. Besides, Δ^9 – THC, an exogenous cannabinoid agonist also reduced LPS-induced fever in a dose dependent manner [108].

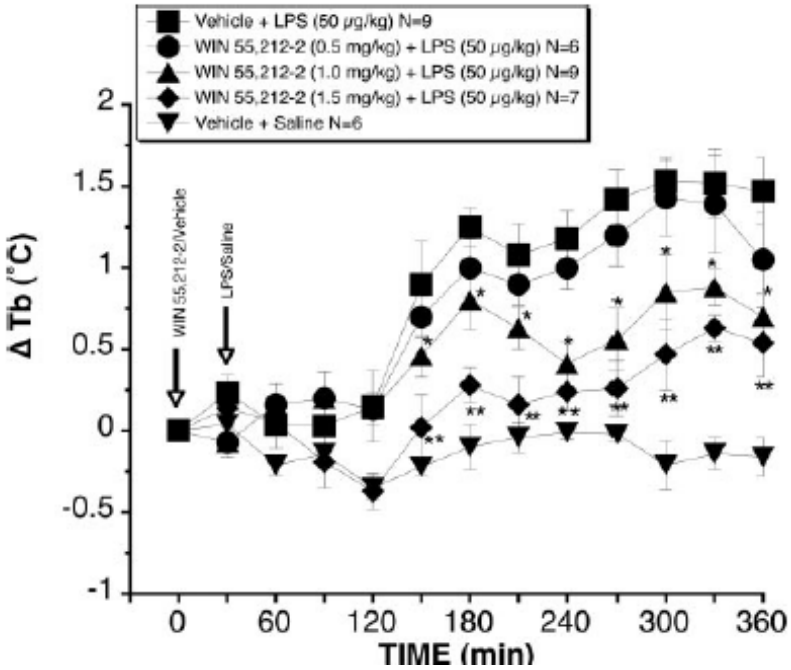

Figure 3.9. Effect of i.p. pretreatment with WIN 55,212-2 (0.5–1.5 mg/kg, -30 min) on LPS induced fever. LPS was injected at time 0. Data are expressed as the mean±S.E.M. from baseline. N, number of rats. ΔTb, variation in body temperature. *, $p < 0.05$; **, $p < 0.01$. Vehicle + LPSversus WIN 55,212-2 +LPS at various concentrations [108].

In addition, the measurement of IL-6 levels of WIN 55,212-2-exposed rats at 3 and 5 hrs after LPS injection revealed that the plasma levels of this cytokine reduced significantly ($p < 0.05$) compared to those of did not exposed to this cannabinoid agonist [108]. Since IL-6 is accepted as one of the most predominant circulating mediators of LPS-induced fever [117] [118] [119], the reduction of IL-6 ,which is parallel to the peaks of this fever, may also be one of the reasons for the reduction in these peaks.

There are several reports which provide evidence that cannabinoids have a suppressive effect on peripheral circulating cytokines in inflammatory states [122], specifically through CB1 receptors [120] [121]. These suppressive effect of synthetic cannabinoid agonists on peripheral cytokines, which is mainly mediated by CB1 receptors, may partly account for the remission of inflammatory states, however, the exact mechanism that leads to this amelioration is still unknown.

As well as synthetic cannabinoids, growing evidence suggest that in situations 2-AG's endogenous accumulation due to the lack of MAGL activation or 2-AG's de-novo biosynthesis, a significant remmision in inflammatory states occurs. For instance, JZL184 was shown to decrease plasma cytokine levels [107]. It was also reported that MAGL inhibitors JZL184 and URB602 suppressed formalin-induced pain via peripheral CB1 and CB2 receptors [123]. Attenuation in mechanical and cold allodynia through CB1 receptor mechanism in nerve-injured mice which exposed to JZL184 was also reported [124]. In addition, KML29 generated anti-allodynic and anti-oedematous effects in murine inflammatory pain and partially blocked mechanical and cold allodynia in sciatic nerve injury pain models [112]. MAGL inactivation by JZL184 in mice model of inflammatory bowel disease revealed that elevation in 2-AG levels reduced macroscopic and histological colon alteration and colonic release of proinflammatory cytokines. MAGL inhibiton contributed to the integrity of the intestinal barrier function, which followed by reduction in endotoxemia, peripheral and brain inflammation [125]. These reports, consistent with our results, suggest that MAGL plays a vital role in generation of inflammatory states and inactivation of this enzyme can provide with protection against inflammation via elevation of 2-AG levels.

However, another metabolic route that determines 2-AG's fate should also be taken into account, specifically in states of inflammation. 2-AG can also be metabolized by primary inducible inflammatory enzyme, COX-2. 2-AG's oxygenation by COX-2 results in the production of prostaglandin glycerol esters [127]. It was suggested that these COX-2 derived endogenous metabolites themselves could serve as inflammatory lipid mediators, however, their mechanism of action remains to be understood [80] [126] [128].

It seems that neural cells have the ability to steer 2-AG toward different metabolic routes (i.e., oxygenation into prostaglandin glycerol esters or hydrolysis to form arachidonic acid) depending on the signalling need of the cell. However, what causes the preference of one route over another is still unkown [70]. This alternative metabolic pathway may become more important when the primary hydrolytic enzymes of 2-AG, MAGL, is blocked and changes in COX-2 activity may alter endocannabinoid signalling [80].

It is possible that in the fever phases that have decreased COX-2 expressions relatively, 2-AG's degradation through COX-2 would be less and hence endogenous levels of 2-AG will further increase. This situation may result in two possible effects: The further escalation in 2-AG levels may augment this endocannabinoid's ameliorating effects and the possible negative effects of 2-AG's oxygenation by-products with COX-2 (i.e., prostaglandin glycerol esters) may also decrease.

We might suggest that such an influence seems to play a role in the efficacy of KML29 on endocannabinoid signalling in LPS-induced fever. Our results suggest that the protective effect of KML29 gets stronger at plateau phase of the fever which has decreased COX-2 levels, relatively. It was reported that COX-2 expression in hypothalamus of intravenous LPS (50 μg/kg)-treated rats peaked at Phase 2 (almost 1.6 hour after injection) and robustly declined in Phase 3 (5 hours from injection) [47]. Consistent with this data, KML29 administration led to a decrease in plateau phase and this decrease was maintained until the end of the observation time (10 hours)(Figure 3.4.). Therefore, we might speculate that the ameliorating effect of MAGL inhibiton by KML29 coincides with times that COX-2 is present in low levels.

It was elucidated that the augmentation of endocannabinoid signalling is closely related to decreased oxygenation of them by COX-2 and substrate-selective COX-2 inhibitors (SSCIs) was shown to decrease anxiety-like behaviours by augmenting endocannabinoid signalling in mice [129]. This strategy could also be used in the further studies related to LPS-induced fever. Since usage of SSCIs would prevent oxygenation of 2-AG by COX-2 without affecting prostaglandin synthesis and non-eCB lipids, it could be utilized for

further investigation of whether the protective effect of MAGL inhibition would be strengthened if it was used simultaneously with SSCIs.

CHAPTER 4

CONCLUSION

- In the current study we aimed to examine whether KML29, a selective and irreversible inhibitor of Monoacylglycerol lipase would have a protective effect on an inflammatory process, fever, induced by subcutaneously administered Lipopolysaccharide in rats. Our results indicate that KML29 has a modest but significant ameliorating effect on LPS-induced fever, specifically during the plateau phase.

- The protective effect of Monoacylglycerol lipase inhibition is likely to be due to the increase in 2-Arachidonoyl glycerol levels rather than the decrease in the arachidonic acid levels as a robust decline in arachidonic acid levels would have resulted in a much robust suppression of the fever.

- KML29's protective impact due to MAGL inhibition appears to take effect specifically at the times that COX-2 expression declines, which is the plateau phase of fever. This finding is consistent with the recent studies which suggests that COX-2 has the ability to limit endocannabinoids' ameliorating effects on inflammation.

- In line with the recent reports that indicates MAGL's vital role in the generation of inflammatory states, our findings imply that the activation of this enzyme is an important aspect of generation of LPS-induced fever and inhibition of MAGL has a protective effect on fever as well as other inflammatory conditions, specifically due to the increased 2-AG levels.

- In conclusion, this study shows that MAGL inhibiton has an ameliorating effect on fever initiated by LPS in rats. In addition, it is suggestive of the COX-2 levels during the MAGL inhibiton should be considered as an important aspect for the efficacy of MAGL inhibition.

- MAGL is considered as a metabolic hub and the effects of its inhibition have come into prominence as protection against inflammatory states. However, the mechanism of its protection and the effect of other metabolic pathways such as 2-AG's oxygenation by COX-2 and resulting by-products (i.e., prostaglandin glycerol esters) on fever and other inflammatory states remain to be elucidated and further studies are warranted.

REFERENCES

[1] Voet D, Voet JG, Biochemistry, 4th Edition, 2011, JOHN WILEY & SONS INC.,USA.

[2] D. Piomelli , G. Astarita , R. Rapaka, *A neuroscientist guide to lipidomics*Nat Rev Neurosci. 2007 Oct; 8(10):743-54.

[3] https://www.rpi.edu/dept/bcbp/molbiochem/MBWeb/mb1/part2/lipid.htm#Fattyacids 03\03\2014

[4] Yeagle L.P.,The Structure of Biological Membranes,2nd edition,2005,CRC PressLLC,USA,Chapter1

[5] http://www.nature.com/scitable/topicpage/cell-membranes-14052567 03\06\2014

[6] Lu YC, Yeh WC, Ohashi PS, *LPS/TLR4 signal trasduction pathway*Cytokine. 2008 May; 42(2):145-51.

[7] Raetz CR, Whitfield C. *Lipopolysaccharide endotoxins.* Annu Rev Biochem. 2002; 71:635-700.

[8] http://www.nature.com/scitable/topicpage/toll-like-receptors-sensors-that-detect-infection-14396559 08\19\2014

[9] Takeda K, Akira S. *Toll-like receptors in innate immunity*. nt Immunol. 2005 Jan; 17(1):1-14. Review.

[10] Moresco EM, LaVine D, Beutler B. *Toll-like receptors.* Curr Biol. 2011 Jul 12;21(13):R488-93. Review.

[11] Kawai T., Akira S. *TLR Signalling.* Cell Death Differ. 2006 May; 13(5):816-25.

[12] Park BS, Song DH, Kim HM, Choi BS, Lee H, Lee JO. *The structural basis of lipopolysaccharide recognition by the TLR4-MD-2 complex.* Nature. 2009 Apr 30; 458(7242):1191-5.

[13] Akira S, Takeda K. *Toll-like receptor signalling.* Nat Rev Immunol. 2004 Jul; 4(7):499-511. Review

[14] O'Neill LA, Bowie AG. *The family of five: TIR-domain-containing adaptors in*

Toll-like receptor signalling. Nat Rev Immunol. 2007 May; 7(5):353-64. Review.

[15] Kagan JC, Medzhitov R. *Phosphoinositide-mediated adaptor recruitment controls Toll-like receptor signaling.* Cell. 2006 Jun 2; 125(5):943-55.

[16] Rowe DC, McGettrick AF, Latz E, Monks BG, Gay NJ, Yamamoto M, Akira S, O'Neill LA, Fitzgerald KA, Golenbock DT. *The myristoylation of TRIF-related adaptor molecule is essential for Toll-like receptor 4 signal transduction.* Proc Natl Acad Sci U S A. 2006 Apr 18; 103(16):6299-304.

[17] Yamamoto M, Sato S, Hemmi H, Hoshino K, Kaisho T, Sanjo H, Takeuchi O, Sugiyama M, Okabe M, Takeda K, Akira S. *Role of adaptor TRIF in the MyD88-independent toll-like receptor signaling pathway.* Science. 2003 Aug 1; 301(5633):640-3.

[18] Yamamoto M, Sato S, Hemmi H, Uematsu S, Hoshino K, Kaisho T, Takeuchi O, Takeda K, Akira S. *TRAM is specifically involved in the Toll-like receptor 4-mediated MyD88-independent signaling pathway.* Nat Immunol. 2003 Nov; 4(11):1144-50.

[19] Covert MW, Leung TH, Gaston JE, Baltimore D. *Achieving stability of lipopolysaccharide-induced NF-kappa B activation.* Science. 2005 Sep 16; 309(5742):1854-7.

[20] Suzuki N, Suzuki S, Duncan GS, Millar DG, Wada T, Mirtsos C, Takada H, Wakeham A, Itie A, Li S, Penninger JM, Wesche H, Ohashi PS, Mak TW, Yeh WC. *Severe impairment of interleukin-1 and Toll-like receptor signalling in mice lacking IRAK-4.* Nature. 2002 Apr 18; 416(6882):750-6.

[21] Sato S, Sanjo H, Takeda K, Ninomiya-Tsuji J, Yamamoto M, Kawai T, Matsumoto K, Takeuchi O, Akira S. *Essential function for the kinase TAK1 in innate and adaptive immune responses.* Nat Immunol. 2005 Nov; 6(11):1087-95.

[22] Bensinger SJ, Tontonoz P. *Integration of metabolism and inflammation by lipid-activated nuclear receptors.* Nature. 2008 Jul 24; 454(7203):470-7. Review

[23] Cunningham C, Skelly DT. *Non-steroidal anti-inflammatory drugs and cognitive function: are prostaglandins at the heart of cognitive impairment in dementia and delirium?* J Neuroimmune Pharmacol. 2012 Mar; 7(1):60-73.

[24] Yamagata K, Matsumura K, Inoue W, Shiraki T, Suzuki K, Yasuda S, Sugiura H, Cao C, Watanabe Y, Kobayashi S. *Coexpression of microsomal-type*

prostaglandin E synthase with cyclooxygenase-2 in brain endothelial cells of rats during endotoxin-induced fever. J Neurosci. 2001 Apr 15; 21(8):2669-77.

[25] Elmquist JK, Breder CD, Sherin JE, Scammell TE, Hickey WF, Dewitt D, Saper CB. *Intravenous lipopolysaccharide induces cyclooxygenase 2-like immunoreactivity in rat brain perivascular microglia and meningeal macrophages*. J Comp Neurol. 1997 May 5; 381(2):119-29.

[26] Romanovsky AA, Almeida MC, Aronoff DM, Ivanov AI, Konsman JP, Steiner AA, Turek VF. *Fever and hypothermia in systemic inflammation: recent discoveries and revisions.* Front Biosci. 2005 Sep 1; 10:2 193-216. Review.

[27] Zhang J, Rivest S. *Is survival possible without arachidonate metabolites in the brain during systemic infection?* News Physiol Sci. 2003 Aug; 18:137-42.

[28] Banks WA, Kastin AJ, Durham DA. *Bidirectional transport of interleukin-1 alpha across the blood-brain barrier.* Brain Res Bull. 1989 Dec; 23 (6):433-7.

[29] Mercier F, Kitasako JT, Hatton GI. *Fractones and other basal laminae in the hypothalamus.* J Comp Neurol. 2003 Jan 13; 455(3):324-40.

[30] Blatteis CM, Bealer SL, Hunter WS, Llanos-Q J, Ahokas RA, Mashburn TA Jr. *Suppression of fever after lesions of the anteroventral third ventricle in guinea pigs.* Brain Res Bull. 1983 Nov; 11(5):519-26.

[31] Romanovsky AA, Sugimoto N, Simons CT, Hunter WS. *The organum vasculosum laminae terminalis in immune-to-brain febrigenic signaling: a reappraisal of lesion experiments.* Am J Physiol Regul Integr Comp Physiol. 2003 Aug; 285(2):R420-8.

[32] Blatteis CM, Sehic E. *Fever: how may circulating pyrogens signal the brain?* News Physiol Sci. 1997; 12: 1–9.

[33] Watkins LR, Maier SF, Goehler LE. *Cytokine-to-brain communication: a review & analysis of alternative mechanisms*. Life Sci. 1995; 57(11):1011-26. Review.

[34] Yamagata K, Matsumura K, Inoue W, Shiraki T, Suzuki K, Yasuda S, Sugiura H, Cao C, Watanabe Y, Kobayashi S. *Coexpression of microsomal-type prostaglandin E synthase with cyclooxygenase-2 in brain endothelial cells of rats during endotoxin-induced fever.* J Neurosci. 2001 Apr 15; 21(8):2669-77.

[35] Ek M, Engblom D, Saha S, Blomqvist A, Jakobsson PJ, Ericsson-Dahlstrand A. *Inflammatory response: pathway across the blood-brain barrier.* Nature. 2001 Mar 22; 410(6827):430-1.

[36] Schiltz JC,Sawchenko PE. *Distinct brain vascular cell types manifest inducible cyclooxygenase expression as a function of the strength and nature of immune insults.* J Neurosci. 2002 Jul 1; 22(13):5606-18.

[37] Konsman JP, Vigues S, Mackerlova L, Bristow A, Blomqvist A. *Rat brain vascular distribution of interleukin-1 type-1 receptor immunoreactivity: relationship to patterns of inducible cyclooxygenase expression by peripheral inflammatory stimuli.* J Comp Neurol. 2004 Apr 19; 472(1):113-29.

[38] Milton AS, Wendlandt S. *A possible role for prostaglandin E1 as a modulator for temperature regulation in the central nervous system of the cat.* J Physiol. 1970 Apr; 207(2):76P-77P.

[39] Vane JR. *Inhibition of prostaglandin synthesis as a mechanism of action for aspirin-like drugs.* Nat New Biol. 1971 Jun 23; 231(25):232-5.

[40] Blatteis CM, Sehic E. *Prostaglandin E_2: A putative fever mediator*. In: Mackowiak PA, editor. Fever Basic Mechanisms and Management. Philadelphia: Blackwell Science Inc; 1997. pp. 117–145

[41] Oka T. *Prostaglandin E_2 as a mediator of fever: the role of prostaglandin E (EP) receptors.* Front Biosci. 2004 Sep 1; 9:3046-57.

[42] Ushikubi F, Segi E, Sugimoto Y, Murata T, Matsuoka T, Kobayashi T, Hizaki H, Tuboi K, Katsuyama M, Ichikawa A, Tanaka T, Yoshida N, Narumiya S. *Impaired febrile response in mice lacking the prostaglandin E receptor subtype EP3*. Nature. 1998 Sep 17; 395(6699):281-4.

[43] Oka T, Oka K, Kobayashi T, Sugimoto Y, Ichikawa A, Ushikubi F, Narumiya S, Saper CB. *Characteristics of thermoregulatory and febrile responses in mice deficient in prostaglandin EP1 and EP3 receptors.* J Physiol. 2003 Sep 15; 551(Pt 3):945-54.

[44] Li S, Wang Y, Matsumura K, Ballou LR, Morham SG, Blatteis CM. *The febrile response to lipopolysaccharide is blocked in cyclooxygenase-2(-/-), but not in cyclooxygenase-1(-/-) mice*. Brain Res. 1999 Apr 17; 825(1-2):86-94.

[45] Engblom D, Saha S, Engström L, Westman M, Audoly LP, Jakobsson PJ, Blomqvist A. *Microsomal prostaglandin E synthase-1 is the central switch during immune-induced pyresis*. Nat Neurosci. 2003 Nov; 6(11):1137-8.

[46] Narumiya S, Sugimoto Y, Ushikubi F. *Prostanoid receptors: structures, properties, and functions.* Physiol Rev. 1999 Oct;79(4):1193-226

[47] Ivanov AI, Pero RS, Scheck AC, Romanovsky AA. *Prostaglandin E(2)-synthesizing enzymes in fever: differential transcriptional regulation.* Am J Physiol Regul Integr Comp Physiol. 2002 Nov; 283(5):R1104-17.

[48] Ivanov AI, Romanovsky AA. *Prostaglandin E_2 as a mediator of fever: synthesis and catabolism.* Front Biosci. 2004 May 1; 9: 1977-93.

[49] Fraga D, Zanoni CI, Rae GA, Parada CA, Souza GE. *Endogenous cannabinoids induce fever through the activation of CB1 receptors.* Br J Pharmacol. 2009 Aug;157(8):1494-501

[50] Romanovsky AA, Simons CT, Kulchitsky VA. *"Biphasic" fevers often consist of more than two phases.* Am J Physiol. 1998 Jul; 275(1 Pt 2):R323-31.

[51] Oka T. *Prostaglandin E_2 as a mediator of fever: the role of prostaglandin E (EP) receptors*. Front Biosci. 2004 Sep 1; 9:3046-57. Review.

[52] Sugimoto Y, Narumiya S. *Prostaglandin E receptors*. J Biol Chem. 2007 Apr 20; 282(16):11613-7.

[53] Turrin NP, Rivest S. *Unraveling the molecular details involved in the intimate link between the immune and neuroendocrine systems*. Exp Biol Med (Maywood). 2004 Nov; 229(10):996-1006.

[54] Oka T, Oka K, Scammell TE, Lee C, Kelly JF, Nantel F, Elmquist JK, Saper CB. *Relationship of EP(1-4) prostaglandin receptors with rat hypothalamic cell groups involved in lipopolysaccharide fever responses*. J Comp Neurol. 2000 Dec 4; 428(1):20-32.

[55] Lazarus M, Yoshida K, Coppari R, Bass CE, Mochizuki T, Lowell BB, Saper CB. *EP3 prostaglandin receptors in the median preoptic nucleus are critical for fever responses.* Nat Neurosci. 2007 Sep; 10(9):1131-3.

[56] Saper CB, Romanovsky AA, Scammell TE. *Neural circuitry engaged by prostaglandins during the sickness syndrome.* Nat Neurosci. 2012 Jul 26; 15(8):1088-95.

[57] http://m-learning.zju.edu.cn/G2S/eWebEditor/uploadfile/20111121083505_460699365083.pdf 10/04/14

[58] http://www.eufic.org/article/en/health-and-lifestyle/healthy-eating/artid/The-importance-of-omega-3-and-omega-6-fatty-acids/ 10/02/2014

[59] http://www.biologie.uni-freiburg.de/data/bio2/schroeder/Cannabis_sativa_de.html 10/03/2014

[60] Di Marzo V. *Targeting the endocannabinoid system: to enhance or reduce?* Nat Rev Drug Discov. 2008 May; 7(5):438-55.

[61] Wang J, Ueda N. *Biology of endocannabinoid synthesis system.* Prostaglandins Other *Lipid* Mediat. 2009 Sep; 89(3-4):112-9.

[62] Di Marzo V. *Endocannabinoids: synthesis and degradation*. Rev Physiol Biochem Pharmacol. 2008; 160:1-24.

[63] Di Marzo V. *Endocannabinoid signaling in the brain: biosynthetic mechanisms in the limelight.* Nat Neurosci. 2011 Jan; 14(1):9-15.

[64] Marsicano G, Lutz B. *Neuromodulatory functions of the endocannabinoid system.* J Endocrinol Invest. 2006; 29(3 Suppl):27-46. Review.

[65] Piomelli D. *The endocannabinoid system: a drug discovery perspective*. Curr Opin Investig Drugs. 2005 Jul; 6(7):672-9.

[66] Piomelli D. *The molecular logic of endocannabinoid signaling*. Nat Rev Neurosci. 2003 Nov; 4(11):873-84.

[67] Devane WA, Hanus L, Breuer A, Pertwee RG, Stevenson LA, Griffin G, Gibson D, Mandelbaum A, Etinger A, Mechoulam R. *Isolation and structure of a brain constituent that binds to the cannabinoid receptor.* Science. 1992 Dec 18; 258(5090):1946-9.

[68] Devane WA, Dysarz FA 3rd, Johnson MR, Melvin LS, Howlett AC. *Determination and characterization of a cannabinoid receptor in rat brain.* Mol Pharmacol. 1988 Nov; 34(5):605-13.

[69] Matsuda LA, Lolait SJ, Brownstein MJ, Young AC, Bonner TI. *Structure of a cannabinoid receptor and functional expression of the cloned cDNA.* Nature. 1990 Aug 9; 346(6284):561-4.

[70] Piomelli D. *More surprises lying ahead. The endocannabinoids keep us guessing.* Neuropharmacology. 2014 Jan; 76 Pt B: 228-34.

[71] Mechoulam R, Ben-Shabat S, Hanus L, Ligumsky M, Kaminski NE, Schatz AR, Gopher A, Almog S, Martin BR, Compton DR, et al. *Identification of an endogenous 2-monoglyceride, present in canine gut, that binds to cannabinoid receptors.* Biochem Pharmacol. 1995 Jun 29; 50(1):83-90.

[72] Sugiura T, Kondo S, Sukagawa A, Nakane S, Shinoda A, Itoh K, Yamashita A, Waku K. *2-Arachidonoylglycerol: a possible endogenous cannabinoid receptor ligand in brain.* Biochem Biophys Res Commun. 1995 Oct 4; 215(1):89-97.

[73] Stella N, Schweitzer P, Piomelli D. *A second endogenous cannabinoid that modulates long-term potentiation.* Nature. 1997 Aug 21; 388(6644):773-8.

[74] Fride E. *Endocannabinoids in the central nervous system--an overview*. Prostaglandins Leukot Essent Fatty Acids. 2002 Feb-Mar; 66(2-3):221-33.

[75] Navarrete M, Díez A, Araque A. *Astrocytes in endocannabinoid signalling*. Philos Trans R Soc Lond B Biol Sci. 2014 Oct 19; 369(1654). pii: 20130599.

[76] Di Marzo V. *The endocannabinoid system: its general strategy of action, tools for its pharmacological manipulation and potential therapeutic exploitation*. Pharmacol Res. 2009 Aug; 60(2):77-84.

[77] Jung KM, Sepers M, Henstridge CM, Lassalle O, Neuhofer D, Martin H, Ginger M, Frick A, Di Patrizio NV, Mackie K, Katona I, Piomelli D, Manzoni OJ. *Uncoupling of the endocannabinoid signalling complex in a mouse model of fragile X syndrome.* Nat Commun. 2012; 3:1080

[78] Castillo PE, Younts TJ, Chávez AE, Hashimotodani Y. *Endocannabinoid signaling and synaptic function.* Neuron. 2012 Oct 4;76(1):70-81

[79] Witting A, Chen L, Cudaback E, Straiker A, Walter L, Rickman B, Möller T, Brosnan C, Stella N. *Experimental autoimmune encephalomyelitis disrupts endocannabinoid-mediated neuroprotection.* Proc Natl Acad Sci U S A. 2006 Apr 18;103(16):6362-7.

[80] Kano M, Ohno-Shosaku T, Hashimotodani Y, Uchigashima M, Watanabe M. *Endocannabinoid -Mediated Control of Synaptic Transmission.* Physiol Rev. 2009 Jan; 89(1):309-80.

[81] Xu JY, Chen C. *Endocannabinoids in Synaptic Plasticity and Neuroprotection.* Neuroscientist. 2014 Feb 25.[Epub ahead of print]

[82] Stella N, Schweitzer P, Piomelli D. *A second endogenous cannabinoid that modulates long-term potentiation.* Nature. 1997 Aug 21; 388(6644):773-8.

[83] Stella N, Piomelli D. *Receptor-dependent formation of endogenous cannabinoids in cortical neurons.* Eur J Pharmacol. 2001 Aug 17; 425(3):189-96.

[84] Sugiura T, Kobayashi Y, Oka S, Waku K. *Biosynthesis and degradation of anandamide and 2-arachidonoylglycerol and their possible physiological significance*. Prostaglandins Leukot Essent Fatty Acids. 2002 Feb-Mar; 66(2-3):173-92.

[85] Piomelli D, Tarzia G, Duranti A, Tontini A, Mor M, Compton TR, Dasse O, Monaghan EP, Parrott JA, Putman D. *Pharmacological profile of the selective FAAH inhibitor KDS-4103 (URB597).* CNS Drug Rev. 2006 Spring; 12(1):21-38.

[86] Blankman JL, Simon GM, Cravatt BF. *A comprehensive profile of brain enzymes that hydrolyze the endocannabinoid 2-arachidonoylglycerol*. Chem Biol. 2007 Dec; 14(12):1347-56.

[87] Long JZ, Nomura DK, Cravatt BF. *Characterization of monoacylglycerol lipase inhibition reveals differences in central and peripheral endocannabinoid metabolism*. Chem Biol. 2009 Jul 31; 16(7):744-53.

[88] Long JZ, Li W, Booker L, Burston JJ, Kinsey SG, Schlosburg JE, Pavón FJ, Serrano AM, Selley DE, Parsons LH, Lichtman AH, Cravatt BF. *Selective blockade of 2-arachidonoylglycerol hydrolysis produces cannabinoid behavioral effects.* Nat Chem Biol. 2009 Jan; 5(1):37-44.

[89] Nomura DK, Morrison BE, Blankman JL, Long JZ, Kinsey SG, Marcondes MC, Ward AM, Hahn YK, Lichtman AH, Conti B, Cravatt BF. *Endocannabinoid hydrolysis generates brain prostaglandins that promote neuroinflammation*. Science. 2011 Nov 11; 334(6057):809-13.

[90] Hashimotodani Y, Ohno-Shosaku T, Kano M. *Presynaptic monoacylglycerol lipase activity determines basal endocannabinoid tone and terminates retrograde endocannabinoid signaling in the hippocampus.* J Neurosci. 2007 Jan 31; 27(5):1211-9.

[91] Kozak KR, Crews BC, Morrow JD, Wang LH, Ma YH, Weinander R, Jakobsson PJ, Marnett LJ. *Metabolism of the endocannabinoids, 2-arachidonylglycerol and anandamide, into prostaglandin, thromboxane, and prostacyclin glycerol esters and ethanolamides.* J Biol Chem. 2002 Nov 22;277(47):44877-85

[92] Dinh TP, Carpenter D, Leslie FM, Freund TF, Katona I, Sensi SL, Kathuria S, Piomelli D. *Brain monoglyceride lipase participating in endocannabinoid inactivation.* Proc Natl Acad Sci U S A. 2002 Aug 6; 99(16):10819-24.

[93] Dinh TP, Kathuria S, Piomelli D. *RNA interference suggests a primary role for monoacylglycerol lipase in the degradation of the endocannabinoid 2-arachidonoylglycerol.* Mol Pharmacol. 2004 Nov; 66(5):1260-4.

[94] Chang JW, Niphakis MJ, Lum KM, Cognetta AB 3rd, Wang C, Matthews ML, Niessen S, Buczynski MW, Parsons LH, Cravatt BF. *Remarkably selective inhibitors of monoacylglycerol lipase bearing a reactive group that is bioisosteric with endocannabinoid substrates.* Chem Biol. 2012 May 25; 19(5):579-88.

[95] Ueda N, Tsuboi K. *Discrimination between two endocannabinoids.* Chem Biol. 2012 May 25; 19(5):545-7.

[96] Long JZ, Jin X, Adibekian A, Li W, Cravatt BF. *Characterization of tunable piperidine and piperazine carbamates as inhibitors of endocannabinoid hydrolases.* J Med Chem. 2010 Feb 25; 53(4):1830-42.

[97] Rosenberger TA, Villacreses NE, Contreras MA, Bonventre JV, Rapoport SI. *Brain lipid metabolism in the cPLA$_2$ knockout mouse.* J Lipid Res. 2003 Jan; 44(1):109-17.

[98] Schlosburg JE, Blankman JL, Long JZ, Nomura DK, Pan B, Kinsey SG, Nguyen PT, Ramesh D, Booker L, Burston JJ, Thomas EA, Selley DE, Sim-Selley LJ,Liu QS, Lichtman AH, Cravatt BF. *Chronic monoacylglycerol lipase blockade causes functional antagonism of the endocannabinoid system*. Nat Neurosci. 2010 Sep;13(9):1113-9

[99] Nomura DK, Blankman JL, Simon GM, Fujioka K, Issa RS, Ward AM, Cravatt BF, Casida JE. *Activation of the endocannabinoid system by organophosphorus nerve agents.* Nat Chem Biol. 2008 Jun; 4(6):373-8.

[100] Holtzman D, Lovell RA, Jaffe JH, Freedman DX. *1-delta9-tetrahydrocannabinol: neurochemical and behavioral effects in the mouse.* Science. 1969 Mar 28; 163(3874):1464-7.

[101] Lomax P, Campbell C. *Phenitrone and marihuana induced hypothermia.* Experientia. 1971 Oct 15;27(10):1191-2

[102] Taylor DA, Fennessy MR. *Biphasic nature of the effects of delta9-tetrahydrocannabinol on body temperature and brain amines of the rat*. Eur J Pharmacol. 1977 Nov 15;46(2):93-9

[103] Rawls SM, Cabassa J, Geller EB, Adler MW. *CB1 receptors in the preoptic anterior hypothalamus regulate WIN 55212-2 [(4,5-dihydro-2-methyl-4(4-morpholinylmethyl)-1-(1-naphthalenyl-carbonyl)-6H-pyrrolo[3,2,1ij]quinolin-6-one]-induced hypothermia*. J Pharmacol Exp Ther. 2002 Jun;301(3):963-8

[104] Crawley JN , Corwin RL, Robinson JK, Felder CC, Devane WA, Axelrod J. *Anandamide, an endogenous ligand of the cannabinoid receptor, induces hypomotility and hypothermia in vivo in rodents* Pharmacol Biochem Behav. 1993 Dec; 46(4):967-72.

[105] Costa B, Vailati S, Colleoni M. *SR 141716A, a cannabinoid receptor antagonist, reverses the behavioural effects of anandamide-treated rats*. Behav Pharmacol. 1999 May; 10(3):327-31.

[106] Burston JJ, Sim-Selley LJ, Harloe JP, Mahadevan A, Razdan RK, Selley DE, Wiley JL. *N-arachidonyl maleimide potentiates the pharmacological and biochemical effects of the endocannabinoid 2-arachidonylglycerol through inhibition of monoacylglycerol lipase.* J Pharmacol Exp Ther. 2008 Nov; 327(2):546-53.

[107] Kerr DM, Harhen B, Okine BN, Egan LJ, Finn DP, Roche M. *The monoacylglycerol lipase inhibitor JZL184 attenuates LPS-induced increases in cytokine expression in the rat frontal cortex and plasma: differential mechanisms of action.* Br J Pharmacol. 2013 Jun; 169(4):808-19.

[108] Benamar K, Yondorf M, Meissler JJ, Geller EB, Tallarida RJ, Eisenstein TK, Adler MW. *A novel role of cannabinoids: implication in the fever induced by bacterial lipopolysaccharide.* J Pharmacol Exp Ther. 2007 Mar;320(3):1127-33

[109] Ovadia H, Wohlman A, Mechoulam R, Weidenfeld J. *Characterization of the hypothermic effect of the synthetic cannabinoid HU-210 in the rat. Relation to the adrenergic system and endogenous pyrogens.* Neuropharmacology. 1995 Feb; 34(2):175-80.

[110] Duncan M, Galic MA, Wang A, Chambers AP, McCafferty DM, McKay DM, Sharkey KA, Pittman QJ. *Cannabinoid 1 receptors are critical for the innate immune response to TLR4 stimulation.* Am J Physiol Regul Integr Comp Physiol. 2013 Aug 1; 305(3):R224-31.

[111] Fraga D, Zanoni CI, Rae GA, Parada CA, Souza GE. *Endogenous cannabinoids induce fever through the activation of CB1 receptors.* Br J Pharmacol. 2009 Aug; 157(8):1494-501.

[112] Ignatowska-Jankowska BM, Ghosh S, Crowe MS, Kinsey SG, Niphakis MJ, Abdullah RA, Tao Q, O' Neal ST, Walentiny DM, Wiley JL, Cravatt BF, Lichtman AH. *In vivo characterization of the highly selective monoacylglycerol lipase inhibitor KML29: antinociceptive activity without cannabimimetic side effects.* Br J Pharmacol. 2014 Mar;171(6):1392-407

[113] http://www.portalroedores.com.br/twister/caractersticas-informaes-biolgicas-e-procedimentos 01/23/2015

[114] Engström Ruud L, Wilhelms DB, Eskilsson A, Vasilache AM, Elander L, Engblom D, Blomqvist A. *Acetaminophen reduces lipopolysaccharide-induced fever by inhibiting cyclooxygenase-2.* Neuropharmacology. 2013 Aug; 71:124-9.

[115] Roth J, Hübschle T, Pehl U, Ross G, Gerstberger R. *Influence of systemic treatment with cyclooxygenase inhibitors on lipopolysaccharide-induced fever and circulating levels of cytokines and cortisol in guinea-pigs.* Pflugers Arch. 2002 Jan; 443(3):411-7.

[116] Steiner AA, Li S, Llanos-Q J, Blatteis CM. *Differential inhibition by nimesulide of the early and late phases of intravenous- and intracerebroventricular-LPS-induced fever in guinea pigs.* Neuroimmunomodulation. 2001; 9(5):263-75.

[117] Harré EM, Roth J, Pehl U, Kueth M, Gerstberger R, Hübschle T. *Selected contribution: role of IL-6 in LPS-induced nuclear STAT3 translocation in sensory circumventricular organs during fever in rat.* J Appl Physiol (1985). 2002 Jun; 92(6):2657-66.

[118] Cartmell T, Poole S, Turnbull AV, Rothwell NJ, Luheshi GN. *Circulating interleukin-6 mediates the febrile response to localised inflammation in rats*. J Physiol. 2000 Aug 1; 526 Pt 3:653-61.

[119] Chai Z, Gatti S, Toniatti C, Poli V, Bartfai T. *Interleukin (IL)-6 gene expression in the central nervous system is necessary for fever response to lipopolysaccharide or IL-1 beta: a study on IL-6-deficient mice.* J Exp Med. 1996 Jan 1; 183(1):311-6.

[120] Roche M, Diamond M, Kelly JP, and Finn DP. *In vivo modulation of LPS induced alterations in brain and peripheral cytokines and HPA axis activity by cannabinoids*. J Neuroimmunol. 2006; 181:57–67

[121] Smith SR, Terminelli C, Denhardt G. *Effects of cannabinoid receptor agonist and antagonist ligands on production of inflammatory cytokines and anti-inflammatory interleukin-10 in endotoxemic mice*. J Pharmacol Exp Ther. 2000 Apr; 293(1):136-50.

[122] Gallily R, Yamin A, Waksmann Y, Ovadia H, Weidenfeld J, Bar-Joseph A, Biegon A, Mechoulam R, Shohami E. *Protection against septic shock and suppression of tumor necrosis factor alpha and nitric oxide production by dexanabinol (HU-211), a nonpsychotropic cannabinoid*. J Pharmacol Exp Ther. 1997 Nov; 283(2):918-24.

[123] Guindon J, Guijarro A, Piomelli D, Hohmann AG. *Peripheral antinociceptive effects of inhibitors of monoacylglycerol lipase in a rat model of inflammatory pain.* Br J Pharmacol. 2011 Aug; 163(7):1464-78.

[124] Kinsey SG, Long JZ, O'Neal ST, Abdullah RA, Poklis JL, Boger DL, Cravatt BF, Lichtman AH. *Blockade of endocannabinoid-degrading enzymes attenuates neuropathic pain.* J Pharmacol Exp Ther. 2009 Sep; 330(3):902-10.

[125] Alhouayek M, Muccioli GG, Lambert DM, Delzenne NM, Cani PD. *Increasing endogenous 2- arachidonoylglycerol levels counteracts colitis and related systemic inflammation.* FASEB journal: official publication of the Federation of American Societies for Experimental Biology. 2011; 25:2711–2721.

[126] Alhouayek M, Muccioli GG. *COX-2-derived endocannabinoid metabolites as novel inflammatory mediators.* Trends Pharmacol Sci. 2014 Jun; 35(6):284-92.

[127] Kozak KR, Rowlinson SW, Marnett LJ. *Oxygenation of the endocannabinoid, 2-arachidonylglycerol, to glyceryl prostaglandins by cyclooxygenase-2*. J Biol Chem. 2000 Oct 27; 275(43):33744-9.

[128] Hermanson DJ, Gamble-George JC, Marnett LJ, Patel S. *Substrate-selective COX-2 inhibition as a novel strategy for therapeutic endocannabinoid augmentation*. Trends Pharmacol Sci. 2014 Jul; 35(7):358-67.

[129] Hermanson DJ, Hartley ND, Gamble-George J, Brown N, Shonesy BC, Kingsley

PJ, Colbran RJ, Reese J, Marnett LJ, Patel S. *Substrate-selective COX-2 inhibition decreases anxiety via endocannabinoid activation.* Nat Neurosci. 2013 Sep; 16(9):1291-8.

APPENDIX A

Models Used in Statistical Analyses

A.1 Saline+Saline (n=9) vs. Vehicle+Saline (n=9)

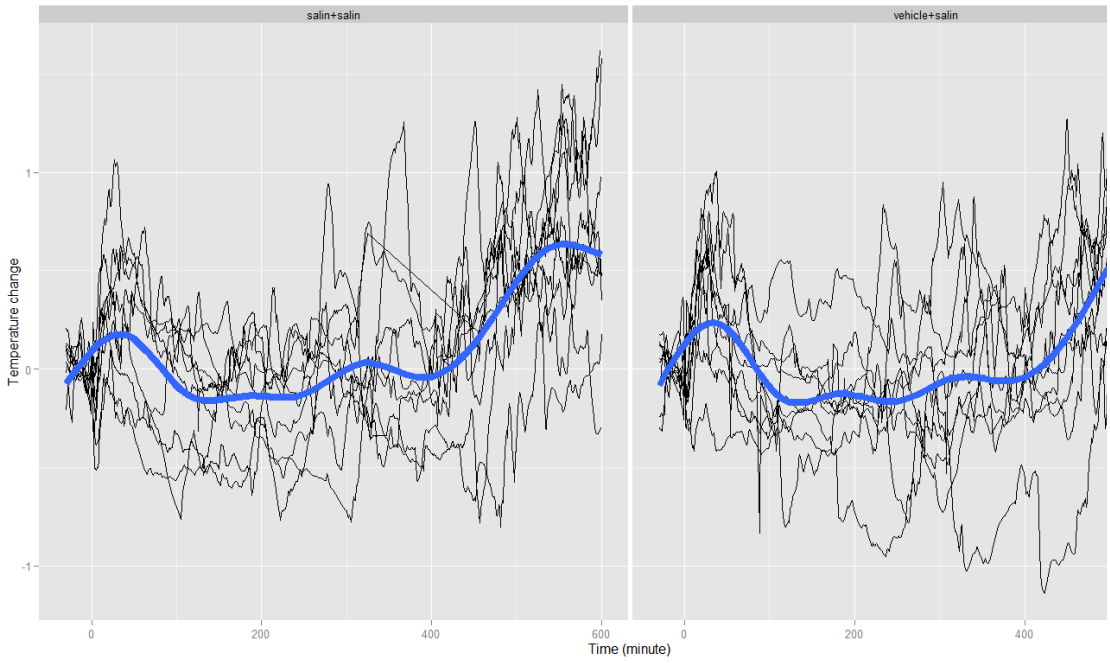

Figure A.1. Empirical graphs (Spagetthi plot and mean curve) of Saline+Saline (on the left) and Vehicle+Saline (on the right). (Mean curve is shown in blue and obtained by smoothing the mean of data at each time point. LOESS is used for smoothing).

Modeling for data analysis: Mixed effects quadratic regression model was used (Overall (mean) temperature change is 2nd degree polynomial in time. Intercept and linear term (i.e. rate of change in temperature over time) changes from rat to rat).

$$Yij = beta0 + betas1_i\ tij + betas2_i\ tij^2 + b0_i + b1_i\ tij + beta1 * trt \quad (A.1)$$

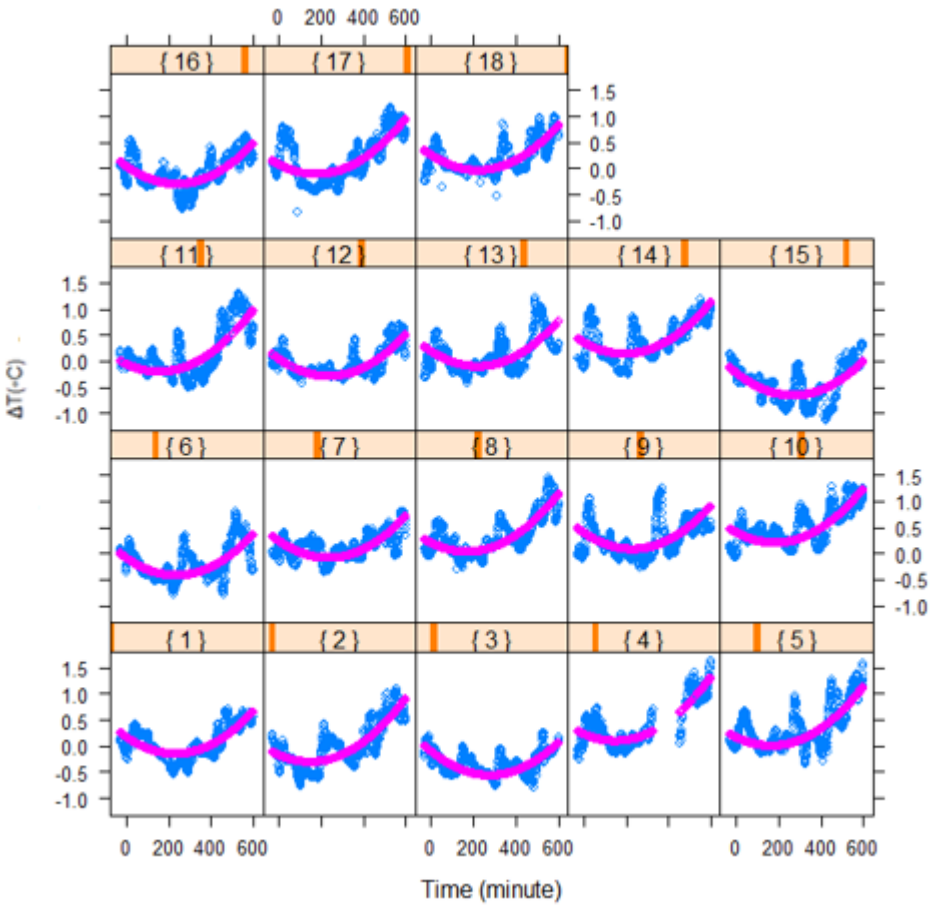

Figure A.2. Statistical model (mixed effects quadratic regression) fitted to 0-600 minutes of Saline+Saline (n=9) and Vehicle+Saline (n=9) groups. Blue lines indicate the observed points in the experiments and pink lines indicate to what extent the fitted model captured those observed points (α= 0.05 was taken as nominal significance level per pairwise comparison).

Beta1 estimate = 0.007049

Standard error of Beta1 estimate= 1.892e-03

	2.5%	25%	50%	75%	97.5%
Beta1	-3.682e-01	-1.166e-01	6.119e-03	1.312e-01	3.734e-01

95% posterior interval = (-0.3682, 0.3734)

Result: There is no statistically signficant difference between Saline+Saline and Vehicle+Saline groups with 95% posterior interval in terms of T_{ab} changes (Beta1 = 0.007049 (-0.3682,0.3734)).

A.2 Saline+Saline (n=9) vs. Saline+ LPS O111:B4 (n=7)

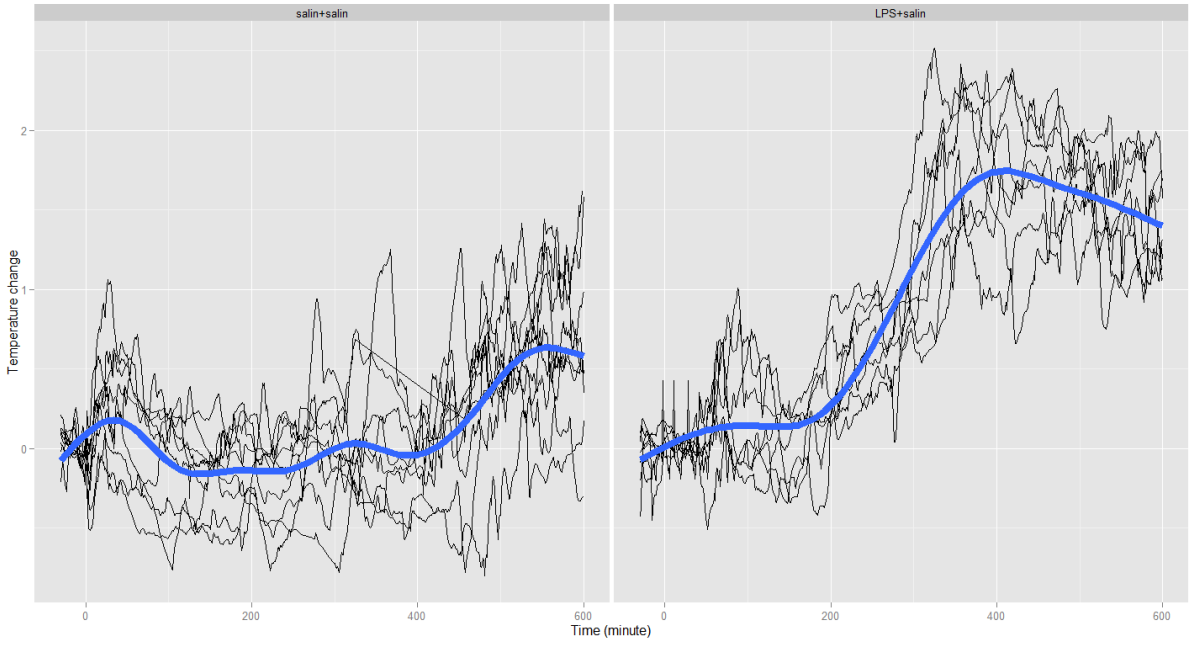

Figure A.3. Empirical graphs (Spagetthi plot and mean curve) of Saline+Saline (on the left) and Saline+LPS (on the right). (Mean curve is shown in blue and obtained by smoothing the mean of data at each time point. LOESS is used for smoothing).

In saline+saline graph there is a quadratic change over time (i.e., there is a slight increase initially, then a gradual decrease and a stabilization followed by an increase again over time).

In the Saline+LPS graph, however, there are two sharp trends (time slots), first being between 0-250 minutes and second between 250-600 minutes. The first one displays a quadratic trend and the second one a concave (i.e., an increase reaching a saturation point followed by a decrease) trend. It is likely that there is no difference in between two groups for the first time slot (≤ 250 mins), however, there is a difference for the second time slot (≥ 250 mins). Therefore, different models were used for the statistical analyses of these two distinct strata.Best model representing the data is chosen based on the deviance information criteria.

The analysis to determine whether there is a statistically significant difference between two groups for the first time slot (≤ 250 mins) in terms of changes in $T_{ab:}$

With interaction:

The analysis for whether interaction term should take place in the model:

$$Yij = beta0 + betas1\ tij + betas2\ tij^2 + b0i + b1i\ tij + b2i\ tij^2 + beta1 * trt * tij + beta2 * trt*tij^2 \quad (A.2)$$

H0: No interaction effect → H0: beta1 = beta2= 0 (M1); H1: Model above (M2).

LRT= Deviance of M2 – Deviance of M1 = (-2634.8148) - (-2634.9381) = 0.

Result: Do not reject H0: no need to put interaction effect. That is the effect of time on the changes in T_{ab}s is not a parameter that changes from a group to another.Therefore, there is no need to use interaction term in the model. Having determined that, the need for the below analysis came out.

Without interaction

Mixed effects quadratic regression

$$Yij = beta0 + betas1\ tij + betas2\ tij^2 + b0_i + b1_i\ tij + b2_i\ tij^2 + beta1 * trt \quad (A.3)$$

Beta1 estimate = -0.05829

Standard Error of Beta1 estimate = 0.002382

	2.5%	25%	50%	75%	97.5%
trt	-0.5178	-0.209310	-0.0577987	0.09314	0.40187

95% posterior interval = (-0.5178, 0.40187)

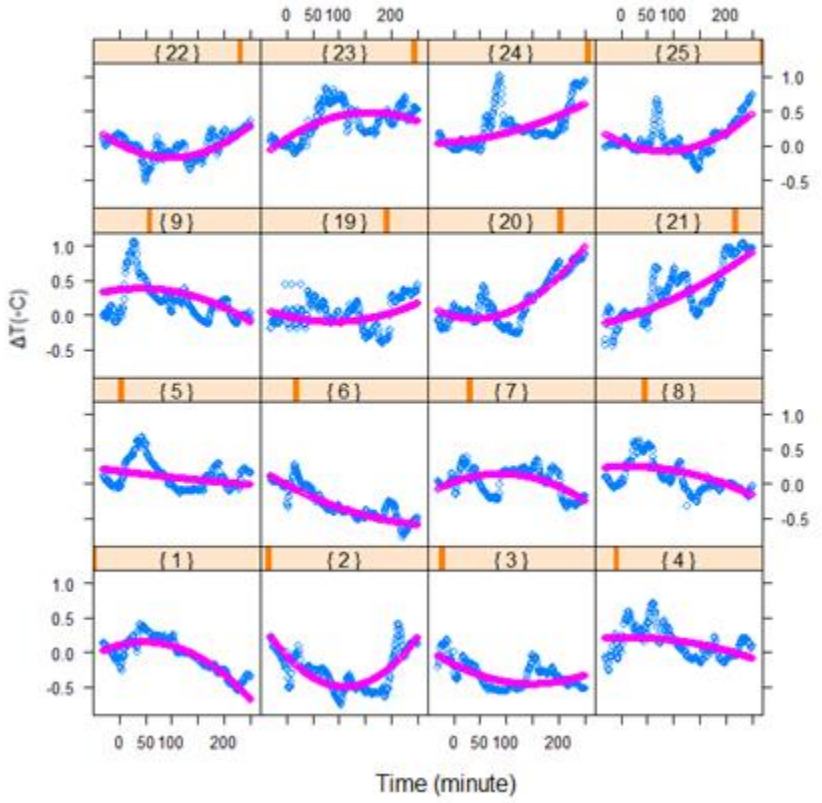

Figure A.4. Statistical model (mixed effects quadratic regression) fitted to ≤ 250 minute of Saline+Saline (n=9) and Saline+LPS O111:B4 (n=7) groups. Blue lines indicate the observed points in the experiments and pink lines indicate to what extent the fitted model captured those observed points (α= 0.05 was taken as nominal significance level per pairwise comparison).

Betas1 estimate = -0.003170

Standard error of Betas1 estimate = 0.001207

	2.5%	25%	50%	75%	97.5%
trt	-0.2318	-0.077399	-0.0047032	0.07131	0.23060

95% posterior interval = (-0.2318, 0.23060)

Betas2 estimate = 0.001377

Standard error of Betas2 estimate = 0.001315

	2.5%	25%	50%	75%	97.5%
trt	-0.2554	-0.080131	0.0015053	0.08284	0.25392

95% posterior interval = (-0.2554, 0.25392)

Result: For the first time slot (≤ 250 mins), there is no statistically signficant difference between Saline+Saline and Saline+LPS groups with 95% posterior interval in terms of T_{ab} changes (Beta1= -0.05829 (-0.5178, 0.40187)).

In addition, both groups' rate of change with respect to time are statistically insignificant (Betas1 = -0.003170 (-0.2318, 0.23060), Betas2 = 0.001377 (-0.2554, 0.25392)), that is temperature changes in both groups do not significantly differs wth respect to time.

The analysis to determine whether there is a statistically significant difference between two groups for the first time slot (≥ 250 mins) in terms of changes in T_{ab}:

Without interaction

Mixed effects spline regression (low rank thin spline):

$$Yij = beta0 + betass1\ tij + betas1\ |tij-a1|^3 + betas2\ |tij-a2|^3 + betas3\ |tij-a3|^3 + betas4\ |tij-a4|^3 + betas5\ |tij-a5|^3 + b1i\ tij + bs1i|tij-a1|^3 + bs2i\ |tij-a2|^3 + bs3i\ |tij-a3|^3 + bs4i\ |tij-a4|^3 + bs5i|tij-a5|^3 + beta1*trt \quad (A.4)$$

Beta1 estimate = 2.415

Standard error of Beta1 estimate = 7.677e-04

	2.5%	25%	50%	75%	97.5%
trt	2.269	2.364	2.415	2.465	2.563

95% posterior interval = (2.269, 2.563)

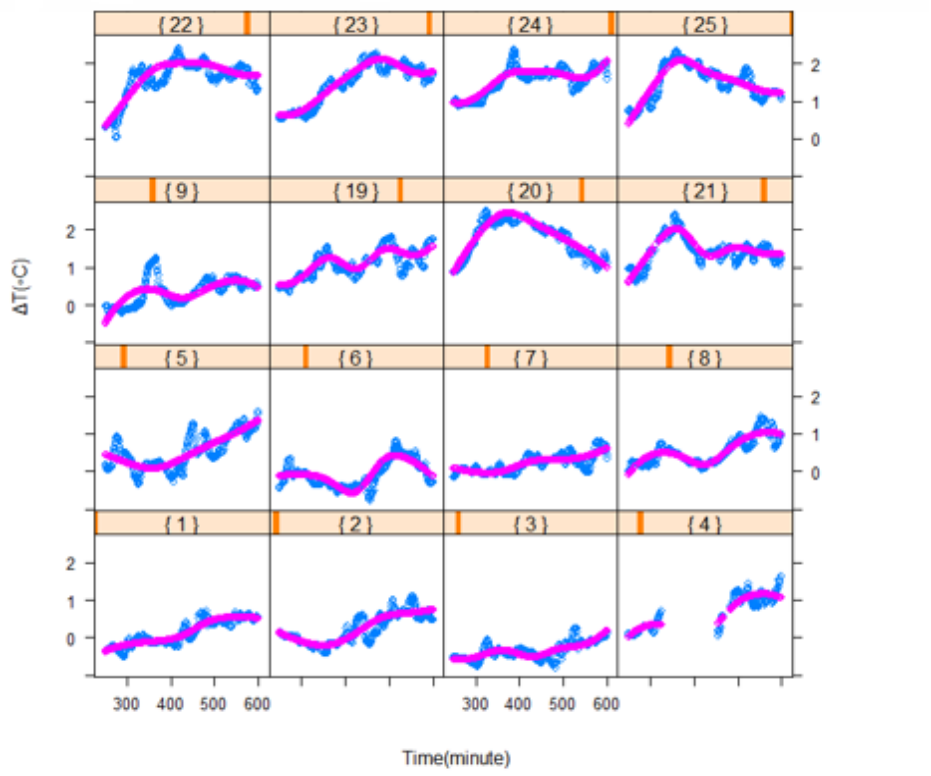

Figure A.5. Statistical model (mixed effects spline regression (low rank thin spline)) fitted to ≥ 250 minute of saline+saline (n=9) and saline+LPS O111:B4 (n=7) groups. Blue lines indicate the observed points in the experiments and pink lines indicate to what extent the fitted model captured those observed points (α= 0.05 was taken as nominal significance level per pairwise comparison).

Result: For the second time slot (≥ 250 mins), there is a statistically signficant difference between Saline+Saline and Saline+LPS groups with 95% posterior interval in terms of T_{ab} changes (Beta1= 2.415 (2.269, 2.563)). This value indicates that with 95% posterior interval, temperature change in salin+LPS O111:B4 group is approximately 2.4 fold larger compared to saline+saline group (this result is adjusted for time*; that is at any time point, ΔT of saline+LPS O111:B4 group is 2.4 fold larger compared to ΔT of saline+saline group).

A.3 Saline+ LPS O111:B4 (n=7) vs. KML29+ LPS O111:B4 (n=7)

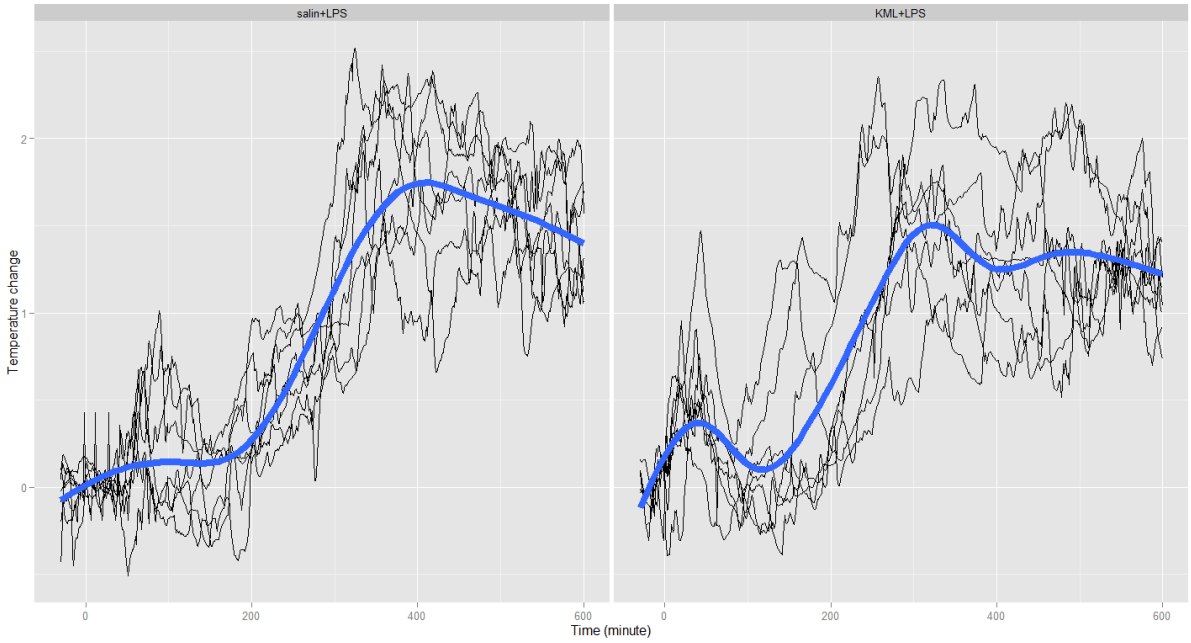

Figure A.6. Empirical graphs (Spagetthi plot and mean curve) of Saline+ LPS (on the left) and KML29+ LPS (on the right). (Mean curve is shown in blue and obtained by smoothing the mean of data at each time point. LOESS is used for smoothing).

The analysis to determine whether there is a statistically significant difference between two groups for the first time slot (≤ 250 mins) in terms of changes in $T_{ab:}$

Mixed effects quadratic regression:

$$Yij = beta0 + betas1_i\ tij + betas2_i\ tij^2 + b0_i + b1_i\ tij + beta1 * trt \quad (A.5)$$

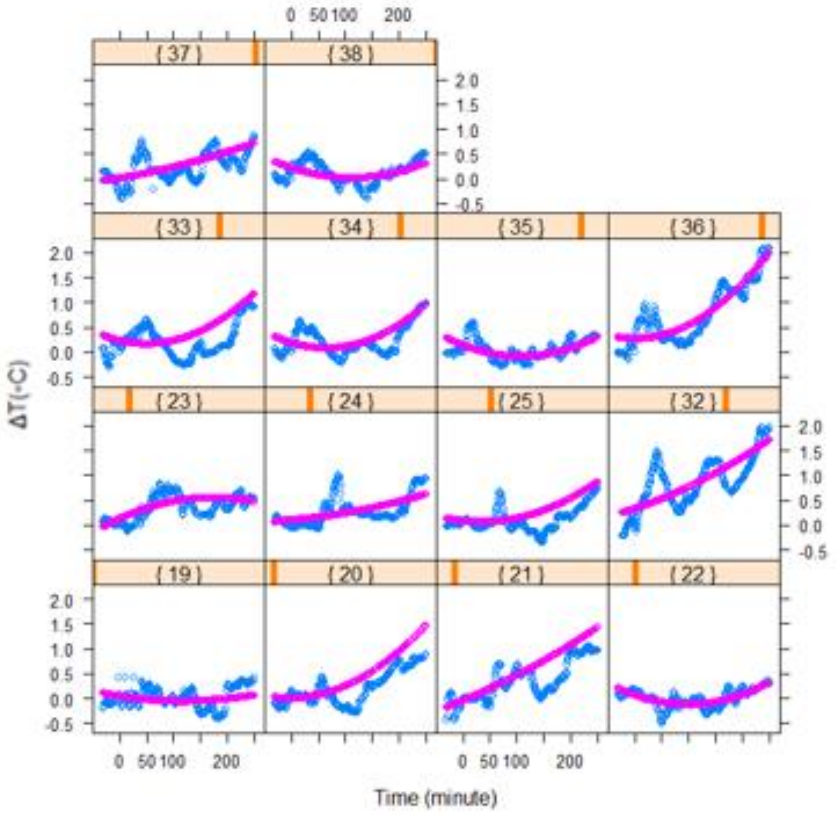

Figure A.7. Statistical model (mixed effects quadratic regression) fitted to ≤ 250 minute of Saline+LPS (n=7) and KML29+LPS (n=7) groups. Blue lines indicate the observed points in the experiments and pink lines indicate to what extent the fitted model captured those observed points (α= 0.05 was taken as nominal significance level per pairwise comparison).

Beta1 estimate = 0.1479

Standard error of Beta1 estimate = 0.002545

	2.5%	25%	50%	75%	97.5%
trt	-0.3516	-0.01471	0.1473943	0.30813	0.6394

95% posterior interval = (-0.3516, 0.6394)

Result: For the first time slot (≤ 250 mins), there is no statistically signficant difference between Saline+LPS and KML29+LPS groups with 95% posterior interval in terms of T_{ab} changes (Beta1= 0. 1479 (-0.3516, 0.6394)).

The analysis to determine whether there is a statistically significant difference between two groups for the first time slot (≥ 250 mins) in terms of changes in T_{ab}:

Mixed effects spline regression:

$$Yij = beta0 + betass1\ tij + betas1\ |tij-a1|^3 + betas2\ |tij-a2|^3 + betas3\ |tij-a3|^3 + betas4\ |tij-a4|^3 + betas5\ |tij-a5|^3 + b1i\ tij + bs1i|tij-a1|^3 + bs2i\ |tij-a2|^3 + bs3i\ |tij-a3|^3 + bs4i\ |tij-a4|^3 + bs5i\ |tij-a5|^3 + beta1 * trt \quad (A.6)$$

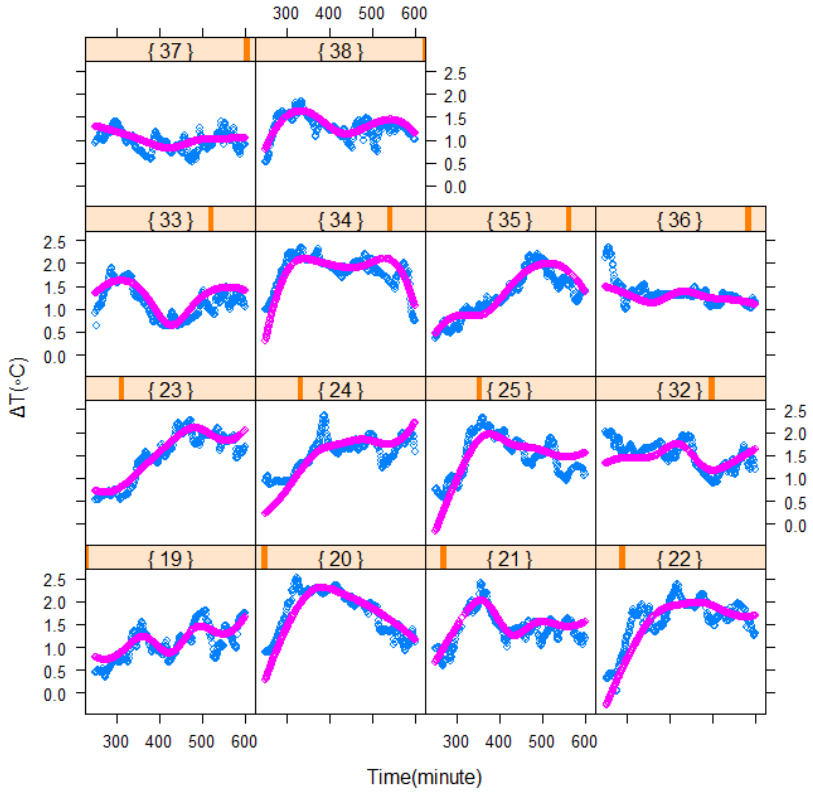

Figure A.8. Statistical model (mixed effects spline regression) fitted to ≥ 250 minute of Saline+LPS (n=7) and KML29+LPS (n=7) groups. Blue lines indicate the observed points in the experiments and pink lines indicate to what extent the fitted model captured those observed points (α= 0.05 was taken as nominal significance level per pairwise comparison).

Beta1 estimate = -1.717

Standard error of Beta1 estimate = 0.0007661

	2.5%	25%	50%	75%	97.5%
trt	-1.863	-1.768	-1.717	-1.667	-1.571

95% posterior interval = (-1.863, -1.571)

Result: For thesecond time slot (≥ 250 mins), there is a statistically signficant difference between Saline+LPS and LPS+KML29 groups with 95% posterior interval in terms of T_{ab} changes (Beta1= -1.717 (-1.863, -1.571)). This value indicates that with 95% posterior

interval the temperature change in KML29+LPS group is approximately 1.7 fold lesser compared to saline+LPS group (this result is adjusted for time*).

A.4. Salin+ LPS O111:B4 (n=7) vs. Vehicle+LPS O111:B4 (n=6)

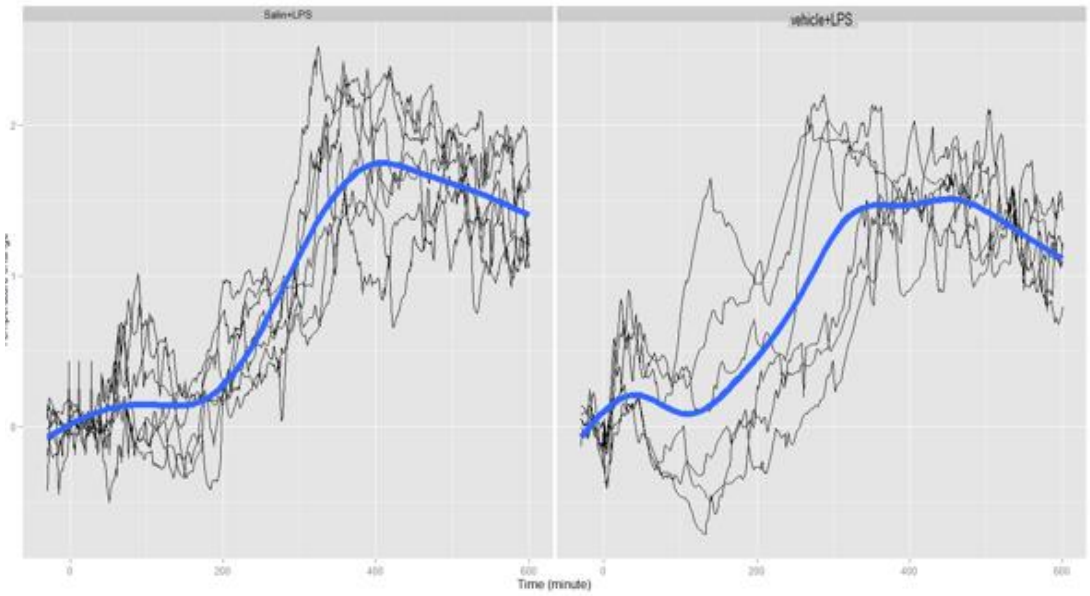

Figure A.9. Empirical graphs (Spagetthi plot and mean curve) of Saline+ LPS (on the left) and Vehicle+ LPS (on the right). (Mean curve is shown in blue and obtained by smoothing the mean of data at each time point. LOESS is used for smoothing).

The analysis to determine whether there is a statistically significant difference between two groups for the first time slot (≤ 250 mins) in terms of changes in $T_{ab:}$

Mixed effects cubic regression:

$$Yij = beta0 + beta1 * trt + betas1\ tij + betas2\ tij^2 + betas3\ tij^3 + b0_i + b1_i\ tij \qquad (A.7)$$

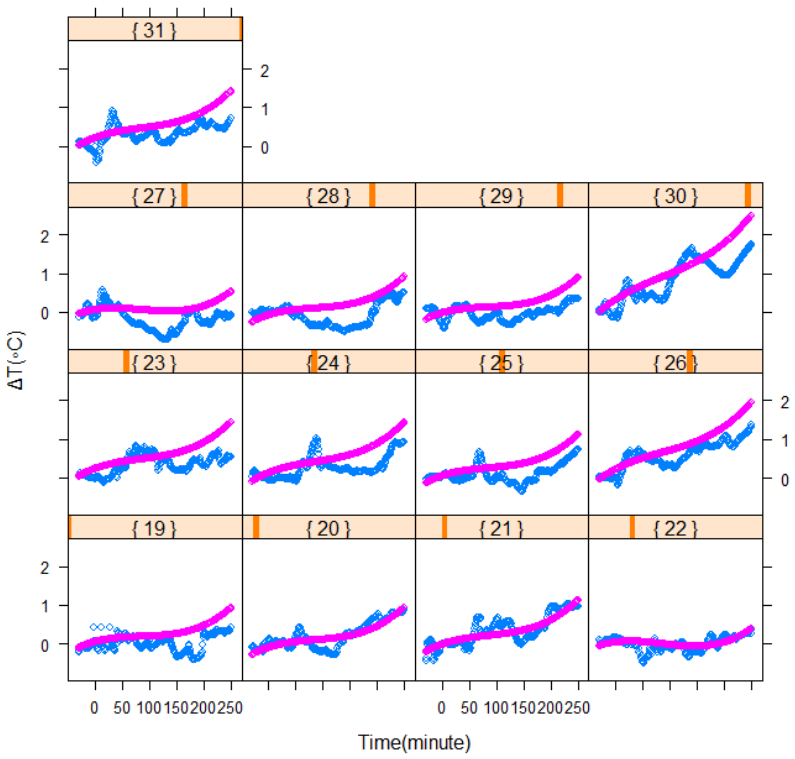

Figure A.10. Statistical model (mixed effects cubic regression) fitted to ≤ 250 minute of Saline+LPS (n=7) and Vehicle+LPS (n=6) groups. Blue lines indicate the observed points in the experiments and pink lines indicate to what extent the fitted model captured those observed points (α= 0.05 was taken as nominal significance level per pairwise comparison).

Beta1 estimate = 0.04548

Standard error of Beta1 estimate = 0.0002424

95% posterior interval = (-0.4281, 0.5147)

Result: For the first time slot (≤ 250 mins), there is no statistically signficant difference between Saline+LPS and Vehicle+LPS groups with 95% posterior interval in terms of T_{ab} changes (Beta1= 0.04548 (-0.4281, 0.5147)).

The analysis to determine whether there is a statistically significant difference between two groups for the first time slot (≥ 250 mins) in terms of changes in $T_{ab:}$

Mixed effects spline regression:

$$Yij = beta0 + betass1\ tij + betas1\ |tij-a1|^3 + betas2\ |tij-a2|^3 + betas3\ |tij-a3|^3 + betas4\ |tij-a4|^3 + betas5\ |tij-a5|^3 + b1i\ tij + bs1i|tij-a1|^3 + bs2i\ |tij-a2|^3 + bs3i\ |tij-a3|^3 + bs4i\ |tij-a4|^3 + bs5i\ |tij-a5|^3 + beta1 * trt \quad (A.8)$$

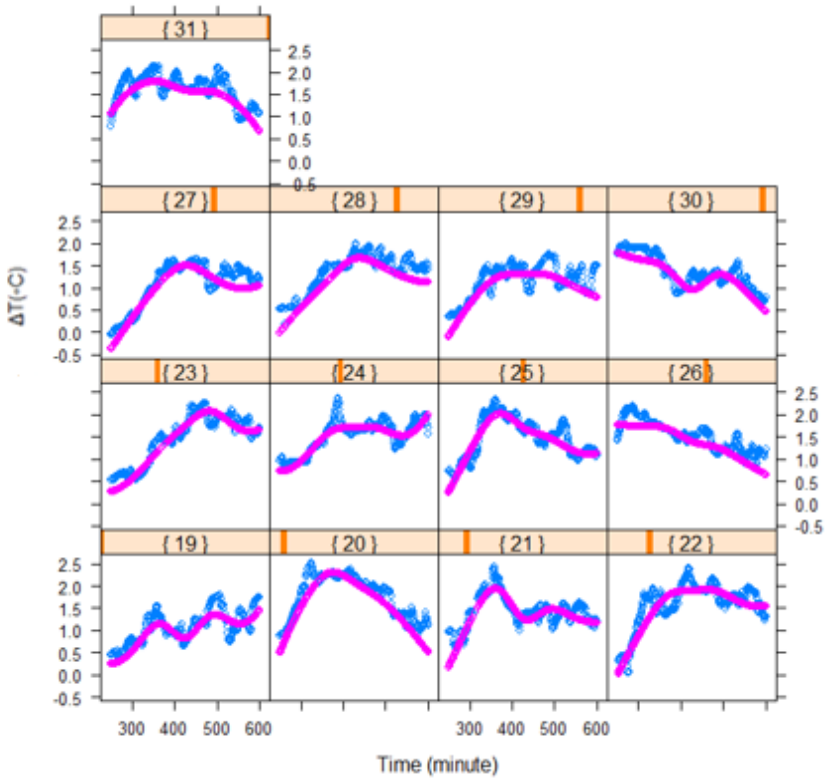

Figure A.11. Statistical model (mixed effects spline regression) fitted to ≥ 250 minute of saline+LPS (n=7) and Vehicle+LPS (n=6) groups. Blue lines indicate the observed points in the experiments and pink lines indicate to what extent the fitted model captured those observed points (α= 0.05 was taken as nominal significance level per pairwise comparison).

Beta1 estimate = -0.855

Standard error of Beta1 estimate = 7.720e-04

	2.5%	25%	50%	95%
trt	-1.006	-0.9047	-0.8547	-0.8037

95% posterior interval = (-1.006, -0.8037)

Result: For thesecond time slot (≥ 250 mins), there is a statistically signficant difference between Saline+LPS and Vehicle+LPS groups with 95% posterior interval in terms of T_{ab} changes (Beta1= -0.855 (-1.006, -0.8037)). This value indicates that with 95% posterior interval the temperature change in Vehicle+LPS group is approximately 0.8 fold lesser compared to saline+LPS group (this result is adjusted for time*).

A.5 Vehicle+LPS O111:B4 (n=6) vs. KML29+ LPS O111:B4 (n=7)

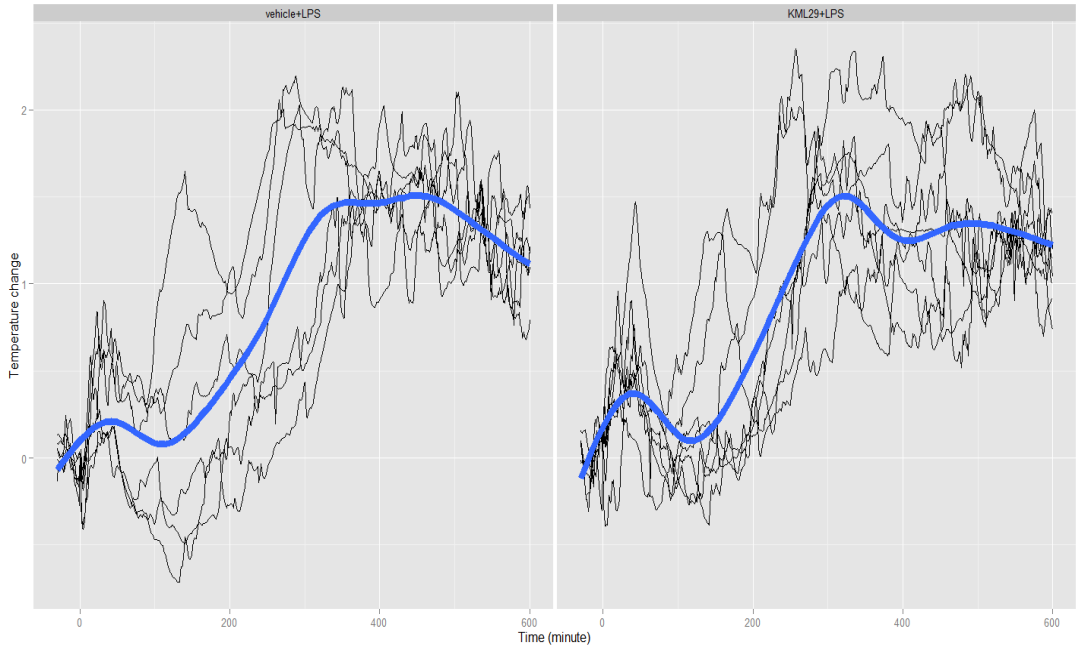

Figure A.12. Empirical graphs (Spagetthi plot and mean curve) of Vehicle+ LPS (on the left) and KML29+ LPS (on the right). (Mean curve is shown in blue and obtained by smoothing the mean of data at each time point. LOESS is used for smoothing).

The analysis to determine whether there is a statistically significant difference between two groups for the first time slot (≤ 250 mins) in terms of changes in T_{ab}:

Mixed effects quadratic regression:

$$Yij = beta0 + betas1_i\ tij + betas2_i\ tij^2 + b0_i + b1_i\ tij + beta1 * trt \quad (A.9)$$

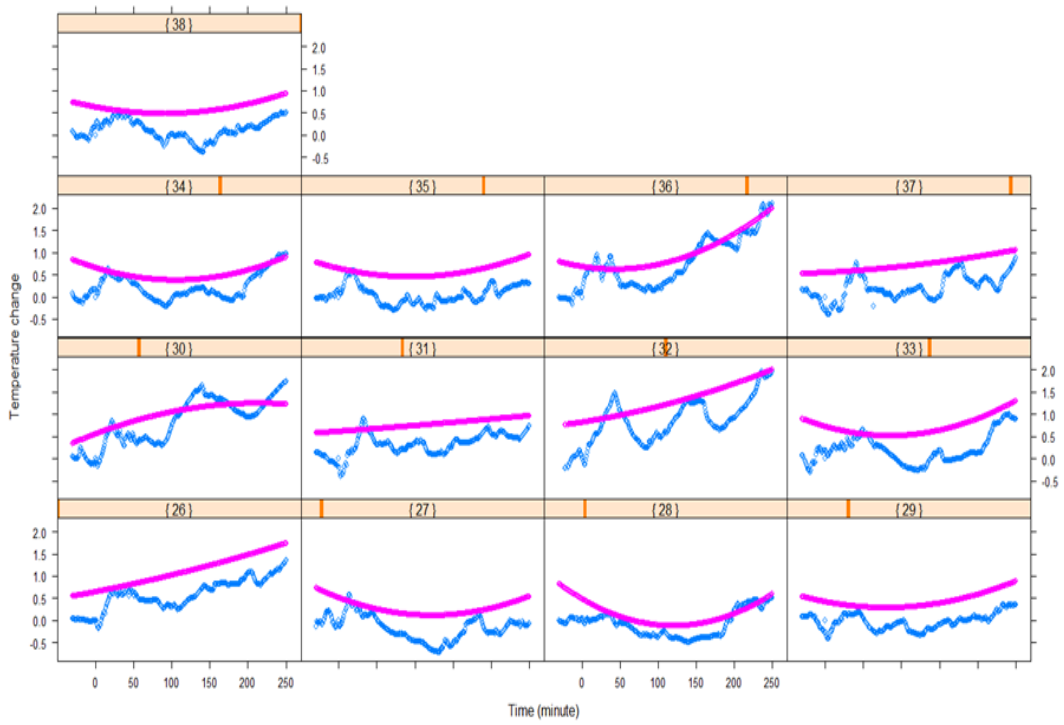

Figure A.13. Statistical model (mixed effects quadratic regression) fitted to ≤ 250 minute of Vehicle+LPS (n=6) and KML29+ LPS (n=7) groups. Blue lines indicate the observed points in the experiments and pink lines indicate to what extent the fitted model captured those observed points (α= 0.05 was taken as nominal significance level per pairwise comparison).

Beta1 estimate = 0.0917

Standard error of Beta1 estimate = 0.002653

95% posterior interval = (-0.4212, 0.5979)

Result: For the first time slot (≤ 250 mins), there is no statistically signficant difference between Vehicle+LPS and KML29+LPS groups with 95% posterior interval in terms of T_{ab} changes (Beta1= 0.0917 (-0.4212, 0.5979)).

The analysis to determine whether there is a statistically significant difference between two groups for the first time slot (≥ 250 mins) in terms of changes in T_{ab}:

Mixed effects spline regression:

$$Yij = beta0 + betass1\ tij + betas1\ |tij-a1|^3 + betas2\ |tij-a2|^3 + betas3\ |tij-a3|^3 + betas4\ |tij-a4|^3 + betas5\ |tij-a5|^3 + b1i\ tij + bs1i|tij-a1|^3 + bs2i\ |tij-a2|^3 + bs3i\ |tij-a3|^3 + bs4i\ |tij-a4|^3 + bs5i\ |tij-a5|^3 + beta1 * trt \quad (A.10)$$

Beta1 estimate = -0.7223

Standard error of Beta1 estimate = 6.851e-04

95% posterior interval = (-0.8535, -0.5917)

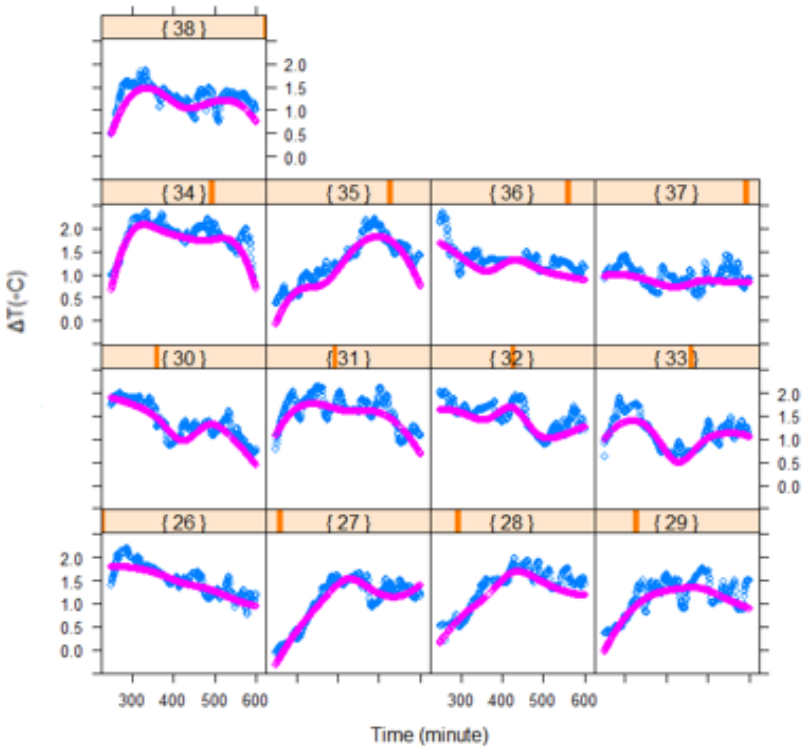

Figure A.14. Statistical model (mixed effects spline regression) fitted to ≥ 250 minute of Vehicle+LPS (n=6) and KML29+LPS (n=7) groups. Blue lines indicate the observed points in the experiments and pink lines indicate to what extent the fitted model captured those observed points (α= 0.05 was taken as nominal significance level per pairwise comparison).

Result: For the second time slot (≥ 250 mins), there is a statistically signficant difference between Vehicle+LPS and KML29+LPS groups with 95% posterior interval in terms of T_{ab} changes (Beta1= -0.7223 (-0.8535, -0.5917)). This value indicates that with 95% posterior interval the temperature change in KML29+LPS group is approximately 0.7 fold lesser compared to Vehicle+LPS group (this result is adjusted for time*).

* Due to the characteristics of fever temperature changes (ΔT_{ab}) naturally vary over time (i.e., the temperature change observed at a fixed time point may both depend on that specific time and the treatment (group)). To adjust the results for time means that time-dependent changes in ΔT_{ab} is eliminated and results only show the effects of the treatments (groups) on ΔT_{ab}.